UAH Research Report No. 174

(NASA-CR-143966) SUPERCONDUCTING COMPOUNDS AND ALLOYS RESEARCH Interim Report, 1 Jul. 1971 - 31 May 1973 (Alabama Univ., Huntsville.) 110 p HC $5.25 CSCL 11F G3/26

N75-33222

Unclas 42212

SUPERCONDUCTING COMPOUNDS AND ALLOYS RESEARCH

by

Guenther Otto

Interim Report

Prepared for

National Aeronautics and Space Administration
George C. Marshall Space Flight Center
Marshall Space Flight Center, Alabama 35812
Under Contract NAS8-27809 (Phase A)

Submitted by

The University of Alabama in Huntsville
School of Graduate Studies and Research
Huntsville, Alabama 35807

June 1975

PREFACE

This Interim Report contains the results of work performed during the period of 1 July 1971 to 31 May 1973 under Phase A of Contract NAS8-27809, entitled "Superconducting Compounds and Alloys Research." This investigation deals with the electrical and superconducting properties of Indium-Bismuth alloys and the shock-wave synthesis of the superconducting compound Nb_3Sn. Phase B of this contract investigates the properties of low-gravity processed immiscible alloys.

The research program is sponsored by the National Aeronautics and Space Administration, George C. Marshall Space Flight Center, Alabama. Dr. L. L. Lacy is the technical monitor of the contract.

ACKNOWLEDGMENTS

We would like to thank Dr. L. L. Lacy and Dr. E. W. Urban for their helpful comments and enlightening discussions during the course of this investigation. The equipment and materials for the performance of the measurements were kindly supplied by the Space Sciences Laboratory of the Marshall Space Flight Center.

ABSTRACT

Resistivity measurements as a function of temperature were performed on alloys of the binary material system $In_{1-x}Bi_x$ for x varying between 0 and 1. It was found that for all single-phase alloys (i.e. the pure elements, α-In, and the three intermetallic compounds) at temperatures sufficiently above the Debye-temperature, the resistivity ρ can be expressed as $\rho = a_o T^n$, where a_o and n are composition-dependent constants. The same exponential relationship can also be applied for the sub-system In-In_2Bi, when the two phases are in compositional equilibrium.

Due to the temperature dependent solubility of bismuth in indium, the relative composition of a eutectic material changes with temperature, giving rise to a time-dependent resistivity when quenched from one equilibrium temperature to another temperature. For such behavior, the fractional change in resistivity can be expressed as a function of time t, with the relation $\Delta\rho = 1 - \exp(-bt^m)$ where b and m are composition and temperature-dependent parameters. From these resistivity measurements, an activation energy for the diffusion of Bi in In of 0.7 eV/atom is calculated. It was established that even at -78.5 °C the eutectic material tends to achieve its equilibrium composition over a very long period of time.

The decomposition of supersaturated α-In at various temperatures was studied by the same technique. The time-dependent change in resistivity can be associated with the nucleation and growth of In_2Bi particles.

Superconductivity measurements on single and two-phase alloys can be explained with respect to the phase diagram. There occur three superconducting phases (α-In, In_2Bi, and In_5Bi_3) with different transition temperatures in the alloying system. The magnitude of the transition temperatures for the various intermetallic phases of In-Bi is such that the disappearance or occurrence of a phase in two component alloys can be demonstrated easily by means of superconductivity measurements.

The density of In-Bi alloys at room temperature was measured by the buoyancy technique. With increasing Bi-concentration in the alloys, the density increases smoothly between the values for the terminal elements. No maxima occur at any of the compositions which correspond to the intermetallic compounds. For InBi, a relative decrease in specific volume by 2.9% is found. The experimental density data for Bi-concentrations up to 50 at.% may be expressed in an additive fashion by attributing a mean atomic volume of 33.8 $\mathring{A}^3$ to the bismuth atom. This value corresponds to a density that Bi would have at room temperature in its liquid state.

TABLE OF CONTENTS

LIST OF FIGURES

LIST OF TABLES

I. INTRODUCTION

This study of indium-bismuth alloys was initiated by a request for an electrical measuring technique to characterize one of the samples obtained from the Apollo 14 Composite Casting Demonstrations [1]. The low-gravity processed material consisted of an In-Bi eutectic matrix in which small tungsten spheres were dispersed. The experiment had the objective of observing the effect of gravity on the distribution of high-density particles (tungsten) in a low-density matrix (In-Bi eutectic), when the matrix was melted and solidified under both zero-gravity [1] and one-g conditions. Significant segregation of tungsten particles was found when the matrix was melted under one-gravity; whereas in the flight sample, a more homogeneous particle distribution was observed [2].

The goal of the present investigation was to evaluate both the flight and ground sample in respect to the homogeneity of particle distribution by resistivity measurements. An optical particle count on the outer-surface of the specimens had already been undertaken. Since the samples can be considered a macroscopic composite material consisting of the two components In-Bi and W, the method of measuring the local electrical resistivity was chosen to evaluate the homogeneity (uniformity) of the particle distribution. The technique is based on the principle that a homogeneous material with uniform cross-section has a constant local electrical resistivity independent of the sampling location. Since the resistivity of W and In-Bi eutectic differ considerably, a non-uniform tungsten distribution will be represented as a change in the local resistivity. The results of these measurements are discussed in the first section of this report.

At the final stage of this investigation, the accuracy (1%) of the local resistivity measurements could not be improved any further because of the occurrence of a continuous small voltage drift. The reason for this drift was found to be in the In-Bi matrix itself, whose resistivity was changing slowly for several hours or even days after the material had experienced a sudden but small change in its environmental temperature. Such an effect had not been reported before and the behavior is quite unusual for two-phase alloys at room temperature.

A further objective was to investigate this time-dependent resistivity on wire-shaped samples and to explain the effect by assuming a temperature-dependent change in composition [3]. In order to better understand the stability of eutectic materials and to experimentally study the achievement of isothermal equilibrium compositions, an investigation of the whole In-Bi alloy system was made. The results are given in the second section of the report. The In-Bi alloys represent a model substance, with properties common to other systems. The knowledge gained can be used to characterize other low-melting alloys like Ga-Bi or Pb-Zn in respect to their compositional and homogeneity status. The electronic properties of such materials are of current active interest in the space processing program.

II. Local Resistivity Investigation

1. BACKGROUND

The sample obtained from the Apollo 14 Composite Casting Demonstration [1] had the form of a longitudinally-cut half cylinder with a length of 7.6 cm (3.0 inches) and a diameter of 1.74 cm (0.685 inches). The cross-sectional area was approximately 1.1 cm^2. The specimen consisted of 70 vol.% of low density In-Bi eutectic matrix ($d = 8.2\ g/cm^3$) in which 30 vol.% Cu-coated tungsten spheres ($d = 19.3\ g/cm^3$) were dispersed. The copper coating was used to improve the wetting conditions. The size of the spheres was 44 μm and less. This zero-gravity processed sample (NASA Code 1-F-B-00) could be compared with a ground-control sample (NASA Code 1-C-B-00) prepared under otherwise identical conditions on earth. The specimens were labelled as having a hot and a cold end which refers to the positions in which the samples solidified in the heat sink.

Generally, the resistivity of a homogeneous polycrystalline material referred to unit length and cross-section is a constant, independent of the location where the resistivity is measured. The resistivity of the two macroscopic components used for the composite material are $\rho_1 = 34.5\ \mu\Omega cm$ for In-Bi matrix [4] and $\rho_2 = 5.65\ \mu\Omega cm$ for bulk tungsten [5]. If a homogeneous and uniform dispersion of the small tungsten particles were achieved, the resistivity of the flight sample and the ground-control sample should be identical and be constant for different sections over the whole sample length. If a variation of the particle distribution occurred, the local resistivity should vary accordingly at that location.

2. EXPECTED RESISTIVITY FOR COMPOSITE MATERIALS

The actual resistivity of the composite material can be approximated by a model consideration of the following type. Assuming a homogeneous and uniform dispersion of the tungsten particles in the eutectic matrix, the composite can be synthesized from a multitude of unit cells. Each unit cell is thought to be consisting of a cube, in the center of which the W-sphere

is located. The appropriate dimensions of such a unit cell are given in Fig. 1a. If the resistivity of one unit cell were known, the resistivity for the composite would be the same as long as it is constructed by a three-dimensional electrical network of serial and parallel resistors [6].

The problem then reduces to computing the composite resistivity of a unit cell which has not yet been solved in closed form. However, a similar problem is easily accessible when transforming the sphere in a cube of equal volume [Fig. 1b]. The composite resistance of this configuration is composed of the resistance of two slices of eutectic material (R_1) having a square cross section and the resistance of the tungsten cube (R_c) with the In-Bi sleeve (R_s) which are switched in parallel. According to the switching, the following relation for the resistance (R) of a unit cell applies

$$R = 2R_1 + \frac{R_s R_c}{R_s + R_c} \qquad [0]$$

A resistivity of $\rho = 18.4\ \mu\Omega cm$ is calculated for the composite material with the cubic configuration. This value is accurate to about 10% and tends to increase slightly when the spherical conditions are approached, as we will show later. The considerations do not take into account any scattering or interface effects which may be expected for particles in the micron range [7].

3. EXPERIMENTAL RESULTS

A sample holder as shown in Fig. 2 was built which allowed measurements of the resistance of the material between two variable locations x_1 and x_2 with a sliding contact technique. The contact consisted of a brass needle (radius of the tip approximately 75 µm) which was gently pressed by gravity on the polished surface of the specimen. By this method, the contact did not dig into the soft In-Bi matrix. The location of the needle could be accurately measured with an attached micrometer which had a sensitivity of 0.02 mm (0.001 inches).

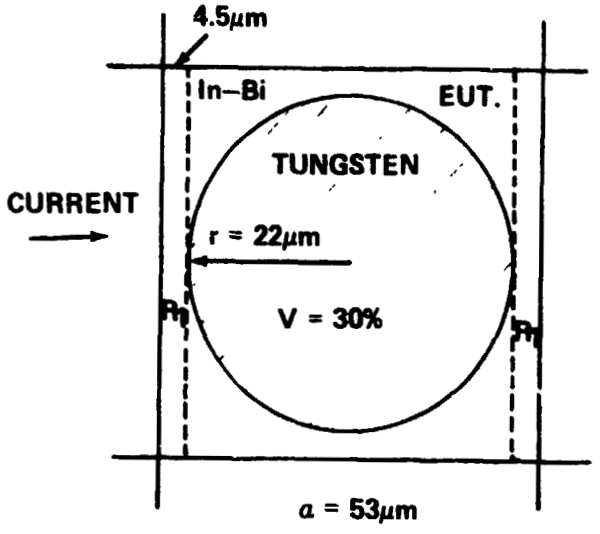

P (EUT.) = 34.5 μΩcm

P (W) = 5.65 μΩcm

P (UC) = ?

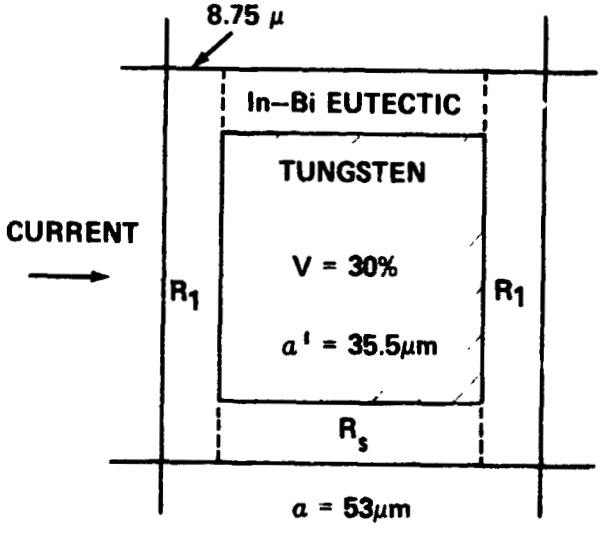

P (EUT.) = 34.5 μΩcm

P (W) = 5.65 μΩcm

P (UC) =18.4μΩcm

Fig. 1. Schematic representation of a composite unit cell for resistivity calculations.

a.) With spherical particle of 30 vol.%.

b.) With cubic particle of 30 vol.%.

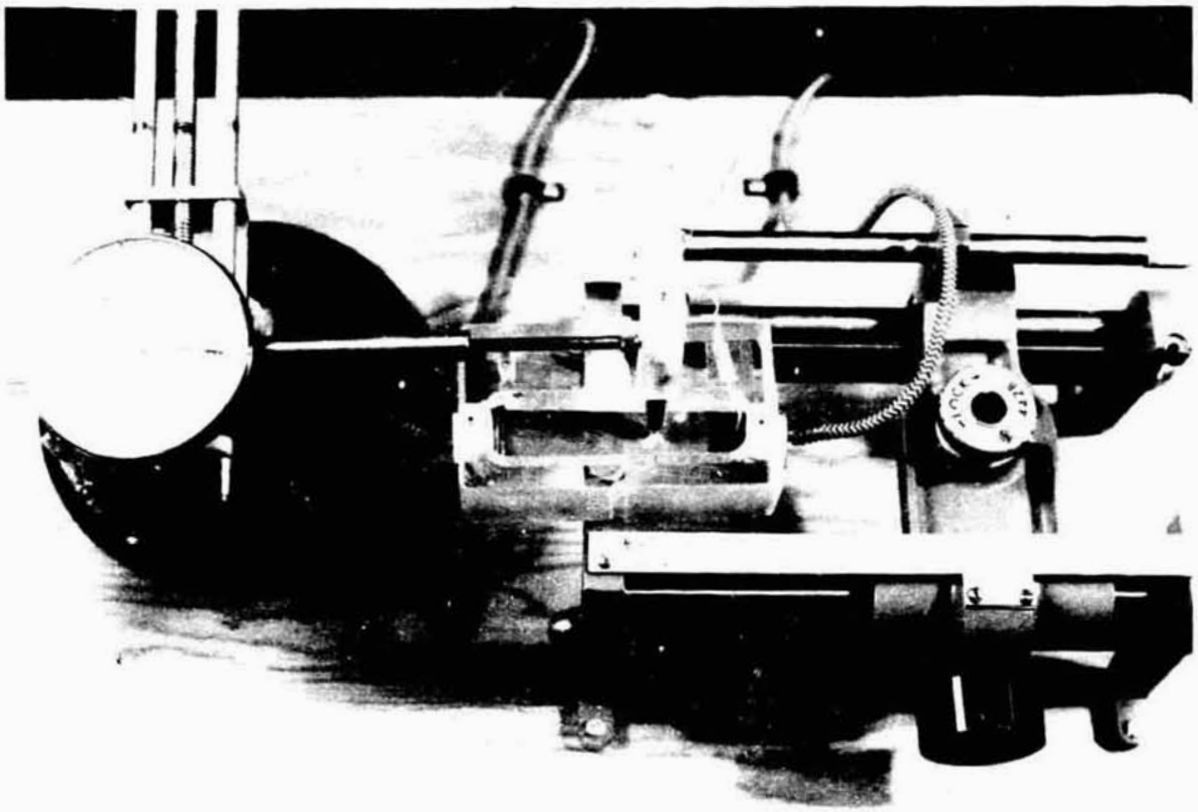

Fig. 2. Device for measuring the local resistivity of a split-cylindrical sample with a sliding contact. The relative changes in position can be measured with the attached micrometer.

A constant current of 10.00 amperes regulated to 0.1% was passed through the material. In order to reduce disturbance of the current distribution at the contact area, the Cu-current leads had the shape of the sample and were fixed with silver conductive paint on both ends of the specimen. The contact resistance ranged from 0.2 to 0.7 mΩ.

The voltage drop between a fixed point on the sample and variable locations, usually 0.75 cm (0.3 inches) apart, was measured directly with a digital millivoltmeter of 0.5 μV resolution. An interval of $\Delta x = 0.75$ cm normally gave a change in voltage of 250 μV. The uncertainty in location caused by the finite extension of the needle contact resulted in a misreading of a maximum 2.5 μV. In order to reduce this error, ten repeated measurements at the same locations were made and the average value taken so that the error of the absolute resistivity could be reduced to $\pm$ 0.5%. An apparent reduction of the size of the measuring interval was obtained by offsetting the starting points of the intervals by a certain length so that intercalating spatials of 0.75 cm were obtained.

The apparatus was tested with a piece of flawless brass having the same dimensions as the samples. The results of the local resistivity measurements are plotted in the lower part of Fig. 3. The spatial resolution for every measured point was 0.3 inches and the average of 10 measurements is plotted. The figure shows that the resistivity of the brass sample within an error of 1%, is constant and independent of the measuring position. An exception has to be made at both sample ends where, due to a current distortion, a deviation occurs. These end-effects disturb the measurement up to 0.4 inches into the sample and, therefore, only data beyond this area are considered significant. The resistivities at the left end of the sample close to the zero location could not be measured because of a restraint in the construction of the equipment.

The local resistivities for the flight and ground-control sample as well as for the In-Bi matrix itself are plotted in the upper part of Fig. 3. The zero location refers to the cold end of both materials. It may be noticed that the resistivities of the two samples are quite different

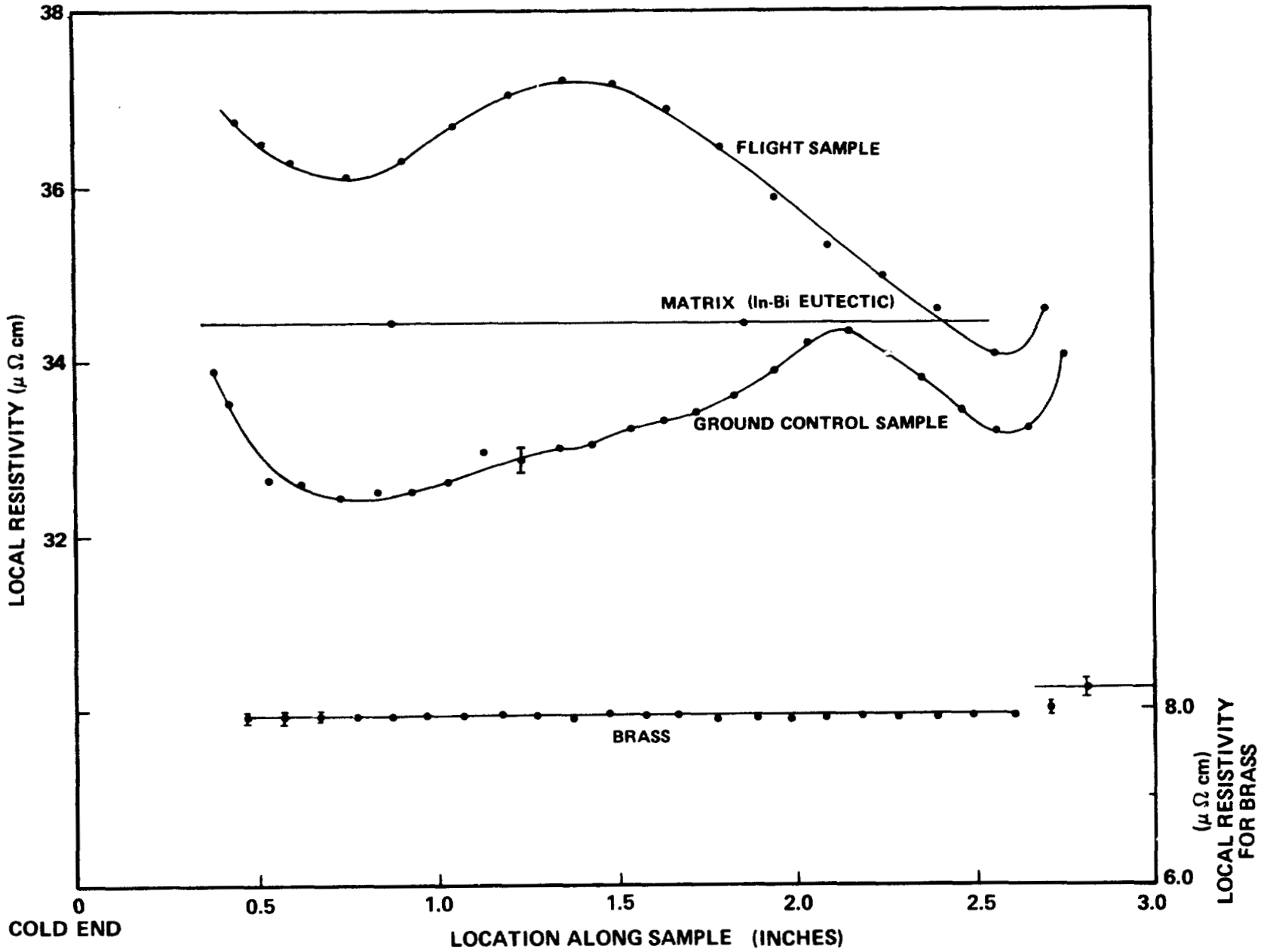

Fig. 3. Local resistivities for the Apollo 14 composite materials. Test results for brass are given in the lower part of the figure.

from each other and are not constant over the length of the samples. Essentially the same results were obtained when the direction of the current flow was reversed. Measurements were also made with the positions of the sample ends in the holder reversed and showed no effect on the shape of the curves.

The interpretation of the experimental results in terms of a change in the distribution of the tungsten particles can be excluded because the resistivity curves for the two samplesare much higher than the expected value of 18.4 μΩcm. The average resistivity for the flight sample is even higher than that of the ground-control sample, and larger than the resistivity of the pure matrix itself. The fact that the resistivity is close to the resistivity of the pure eutectic leads to the conclusion that part of the current is shielded from penetrating the highly conducting tungsten particles. This effect could, for example, be caused by an oxide layer on the spheres or by partially nonwetting conditions during the melting process of the eutectic. If the W-particles were completely insulated from the matrix by an oxide layer, the expected resistivity of the composite would be 53.3 μΩcm.

After discussion of these results, we, indeed, learned of the existence of oxide layers on the copper-coated tungsten spheres, and from the existence of approximately 2 vol.% of voids in the flight sample. The presence of voids in the flight sample explains the higher resistivity when compared with the ground-control sample. For these reasons, a quantitative analysis of the particle distribution with the resistivity technique was not possible.

III. Resistivity of In-Bi Alloys

1. BACKGROUND

The accuracy of the local resisitivity measurements could not be increased beyond 1% because of a drift in the voltage signal during the 30 min measuring cycle. The changing signal was obviously caused by changes in the sample temperature. However, there was no phase correlation between the resistivity and the sample temperature as usually is the case for metals. An example of the time-dependent resistivity of eutectic material (66.3 W.% In and 33.7 W.% Bi) when suddenly cooled from 35.6 °C to 23 °C is shown in Fig. 4. The steep decrease of the resistance at t = 0 is due to the temperature change. However, the long tail section which is still not constant even after 30 hrs is usually not observed for metals. During this period of time, the eutectic material is obviously approaching its new thermodynamic equilibrium composition for the lower temperature. According to the phase diagram (Fig. 5), the relative composition of the eutectic should change such that α-In transforms into the compound In_2Bi, which transformation can be monitored by resistance measurements.

In the following section, we will report about the resistivity measurements made on the individual components which form the eutectic material. No previous data were available and, therefore, the measurements represent a rather complete information about the electrical properties of single and two-phase In-Bi alloys.

The phase diagram of In-Bi has been investigated by several authors [8,9] and a composite of the results is given in Fig. 5. It is generally well established [10,11] that the three stable intermetallic phases (In_2Bi, In_5Bi_3 and InBi) occur in the system at room temperature. In addition, it has been shown that metastable phases can be prepared by quenching [10] or high-pressure [12,13] techniques. Our results will be correlated with the presently-known phase diagram and, in certain areas, will supplement the hitherto available data about phase boundaries.

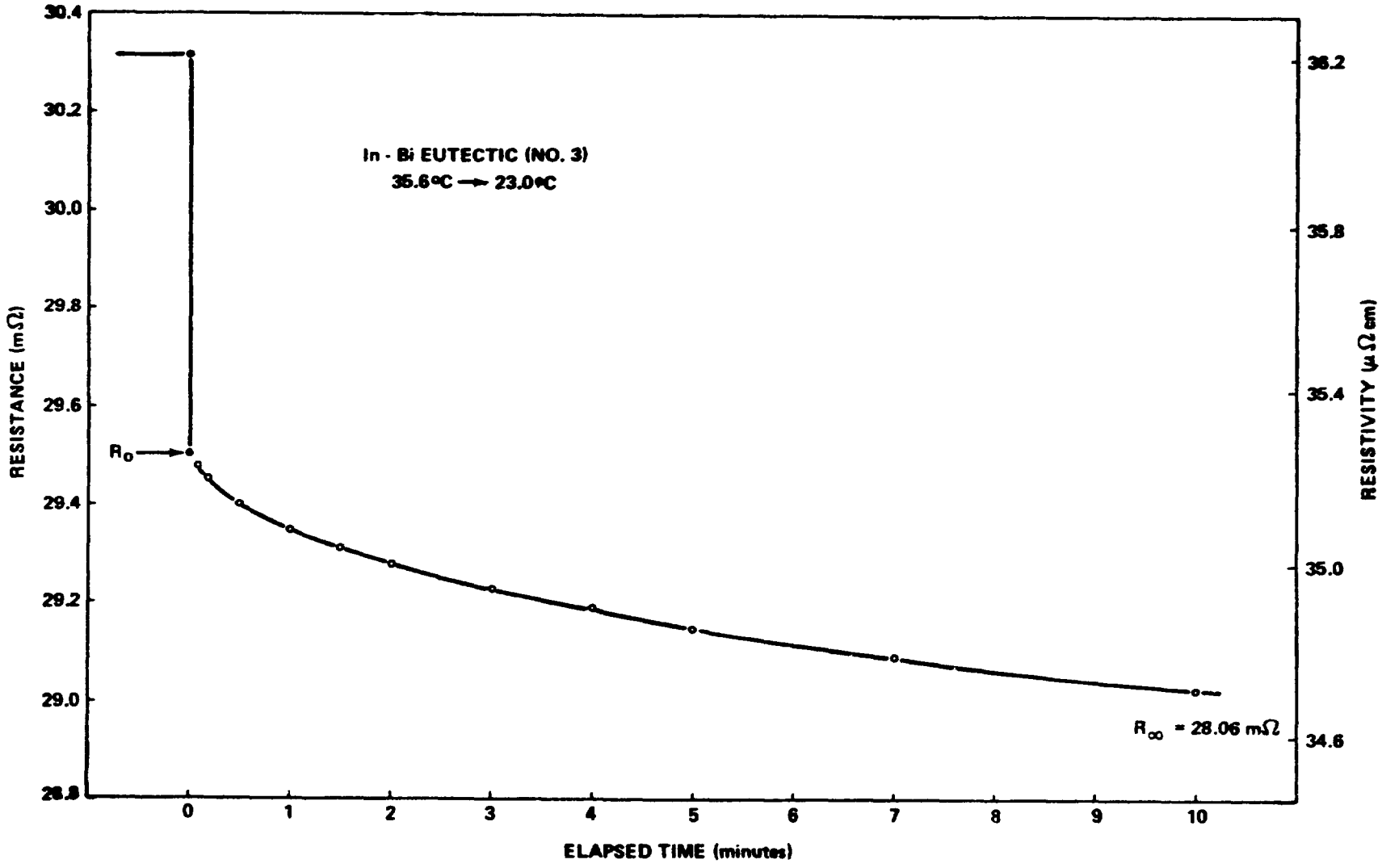

Fig. 4. Time-dependent resistivity of an In-Bi eutectic alloy when cooled from 35.6 to 23 °C.

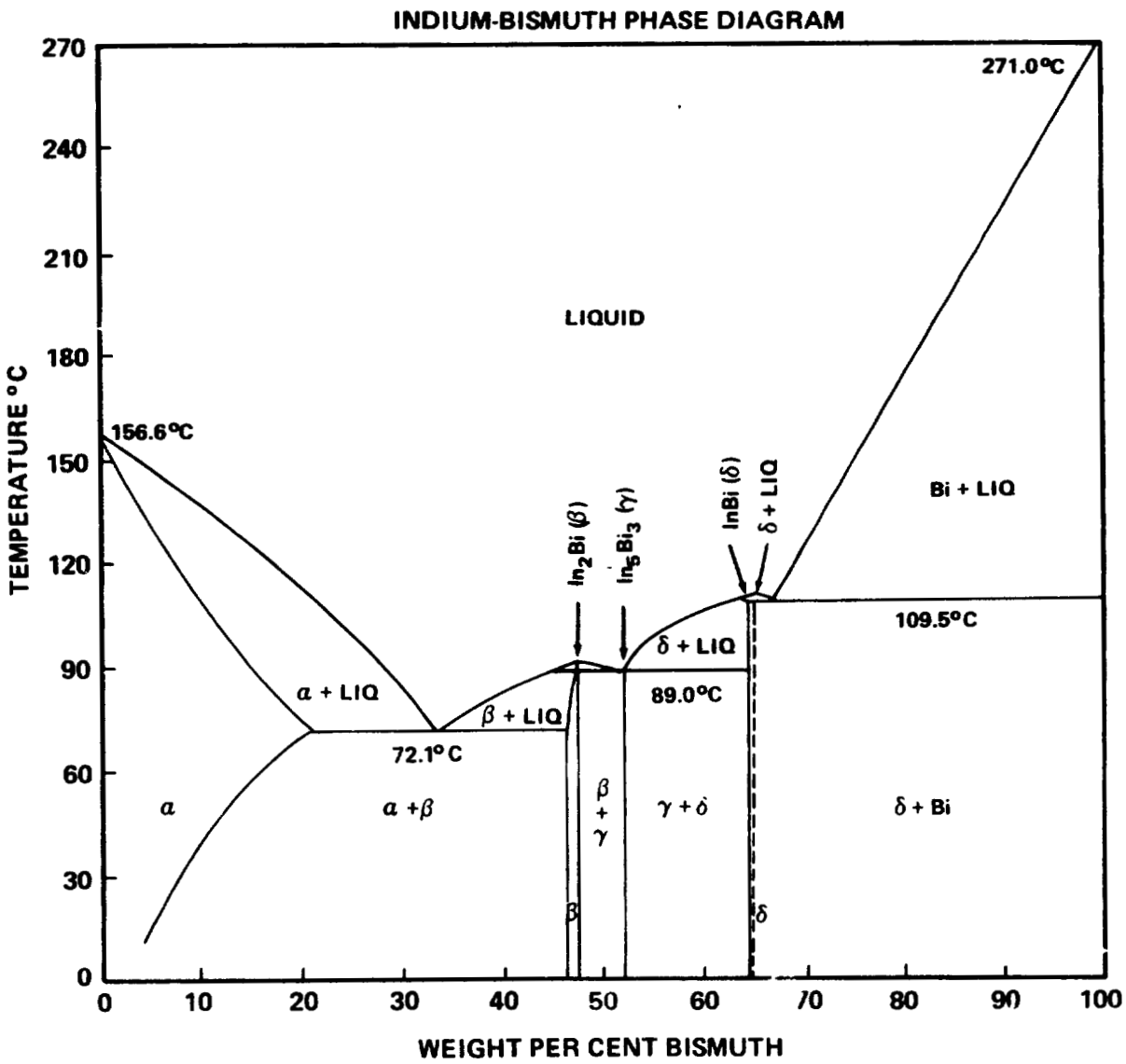

Fig. 5. Composite phase diagram of the system Indium-Bismuth (after Henry and Badwick [8], Peretti and Carapella [9], Giessen, Morris and Grant [10]).

2. SAMPLE PREPARATION

Polycrystalline ingots of the composition $In_{1-x}Bi_x$ were cast from high purity (99.999%) indium and bismuth pellets. The corresponding composition was weighed and melted on a hot plate in a clean pyrex beaker in air or under silicone oil. Samples were cast in a cylindrically-shaped graphite mold. From the ingots, a cylindrical piece of 7 mm length and 7 mm diameter was cut and used for superconductivity as well as density [14] measurements.

The remaining material was used to fabricate short pieces of wire with a diameter of 0.55 mm for the resistivity measurements. For this purpose, a suitable amount of material was again remelted and then sucked into a pre-heated teflon capillary of 0.55 mm diameter. An approximately 2 cm long flawless piece of the filled capillary was then selected and four potential leads were attached with solder having the same chemical composition as the specimen. This precaution was taken to avoid contamination of the samples by Sn or Pb from the common solder. All electrical connections were protected by a water resistant coating.

3. ELECTRICAL MEASUREMENTS

To determine the resistance of the wire, normally in the range of 10^{-2} Ohms, a current of 200 mA (stabilized to within 1 part in 10^{+5}) was passed through the sample and the resulting potential was measured with a sensitive digital millivoltmeter. The relative potential determinations were accurate to within 0.2 μV corresponding to an accuracy of 10^{-6} Ohm in resistance. With this experimental setup, changes in the resistance as a function of temperature or time of 1 part in 10^4 could be detected. However, the absolute values of the resistivities for the different materials are accurate to 2% due to uncertainties in the wire diameter and distance of potential leads.

The wire resistance was either measured as a function of temperature or as a function of time, when the sample was plunged directly from one constant temperature water bath into another one of different temperature. Due to thermal lag, the first good voltage reading was obtained after about 10 sec. Temperature measurements were made with a calibrated platinum thermometer with an accuracy at room-temperature of 0.2 °C.

For the superconductivity measurements, the cylindrical samples were placed in the center of a symmetrical pick-up coil and the a-c inductance of the coil at 1 kHz was recorded during cool down or heating [15]. The inductance was measured in a bridge circuit with a lock-in amplifier as a detector. A calibrated Ge-resistor attached to one face of the sample served as a thermometer for the low temperature investigations.

4. RESISTIVITY OF PURE IN AND BI

The resistance R of pure metals with a periodic lattice is due to the interaction of electrons with phonons or lattice imperfections. On the basis of Bloch's theory that the electron waves move in an electrostatic field having the periodicy of the crystal lattice, Grüneissen [16] calculated the temperature dependence of the resistivity ρ (T). In the integer expression obtained by Grüneissen, two extreme temperature ranges will have a simple temperature-dependent resistivity:

$$\rho \propto T^5 \qquad (T \ll \Theta) \tag{1}$$

$$\rho \propto T \qquad (T \gg \Theta). \tag{2a}$$

Here, Θ is a characteristic temperature for the particular metal which is close to the Debye temperature of the specific heat. Whereas, at low temperatures, the quantization of the different modes of the lattice vibration is important and leads to a T^5 behavior; it is possible at high temperatures to neglect this quantization and treat the vibrations classically [17]. Then, the probability of a collision of an electron with the lattice is proportional to the mean square amplitude of the lattice displacement, $(x^2)_{ave}$, which, in turn, is again linearly dependent on the absolute temperature,

the atomic mass M, and the Debye temperature Θ as given:

$$\rho \sim (x^2)_{ave.} \sim T/M\Theta^2. \qquad (2b)$$

The theory, applied to real metals gives very good agreement in some cases [18] (Cu, Au, Al, Na, Pb), however, deviations are common in other metals (Ni, W) [18,19].

The extent to which the pure materials In and Bi and the compounds of the system In-Bi fit into this relationship is demonstrated below.

Fig. 6 contains the high temperature resistivity (Θ > 109 K) measured on a 99.99% pure In-wire. The value of the resistivity at 0 °C (8.14 μΩcm) agrees very well with the data (8.19 μΩcm) published elsewhere [20]. The ratio of the resistance at room temperature (RT) to the resistance at 4.2 K for this sample was 5100, reflecting the high purity of the material used. It may be seen from Fig. 6 that the shape of the resistivity curve shows a slight deviation from linearity, not accounted for by Equation 2b. To demonstrate this deviation and to compare our results for In with materials showing a linear relationship (Cu, Au, Pb, Bi), a plot of the temperature dependence of the resistivity in reduced coordinates T/Θ is shown in Fig. 7. We recognize that at about 200 K ($T/\Theta = 2$) deviations from Equation 2b occur. The Debye temperature Θ for In was taken from Ref. 20. Measurements on pure bismuth and specific characteristic data are listed in Table 1.

Deviations from the proportionality of the resistance with absolute temperature at temperatures below the melting point have been explained by Mott [21] as caused by changes in the Debye temperature as a result of thermal expansion. As the metal expands, Θ decreases, leading to an increase in the resistivity according to (2b). Indeed, the thermal expansion coefficient of In at room temperature is three times that of copper or gold [20].

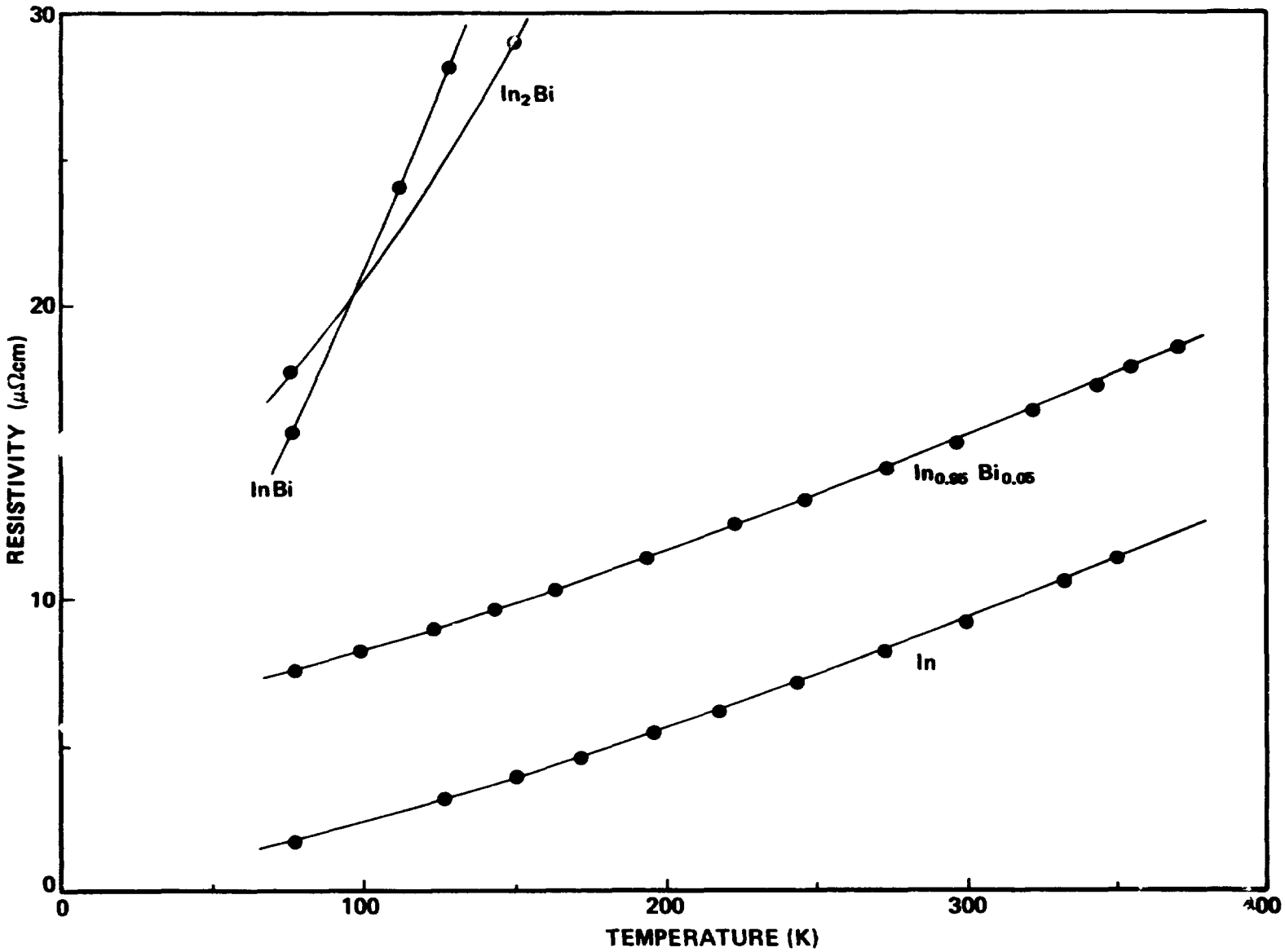

Fig. 6. Temperature dependence of the resistivity for the single-phase alloys In, α-In, In_2Bi and InBi.

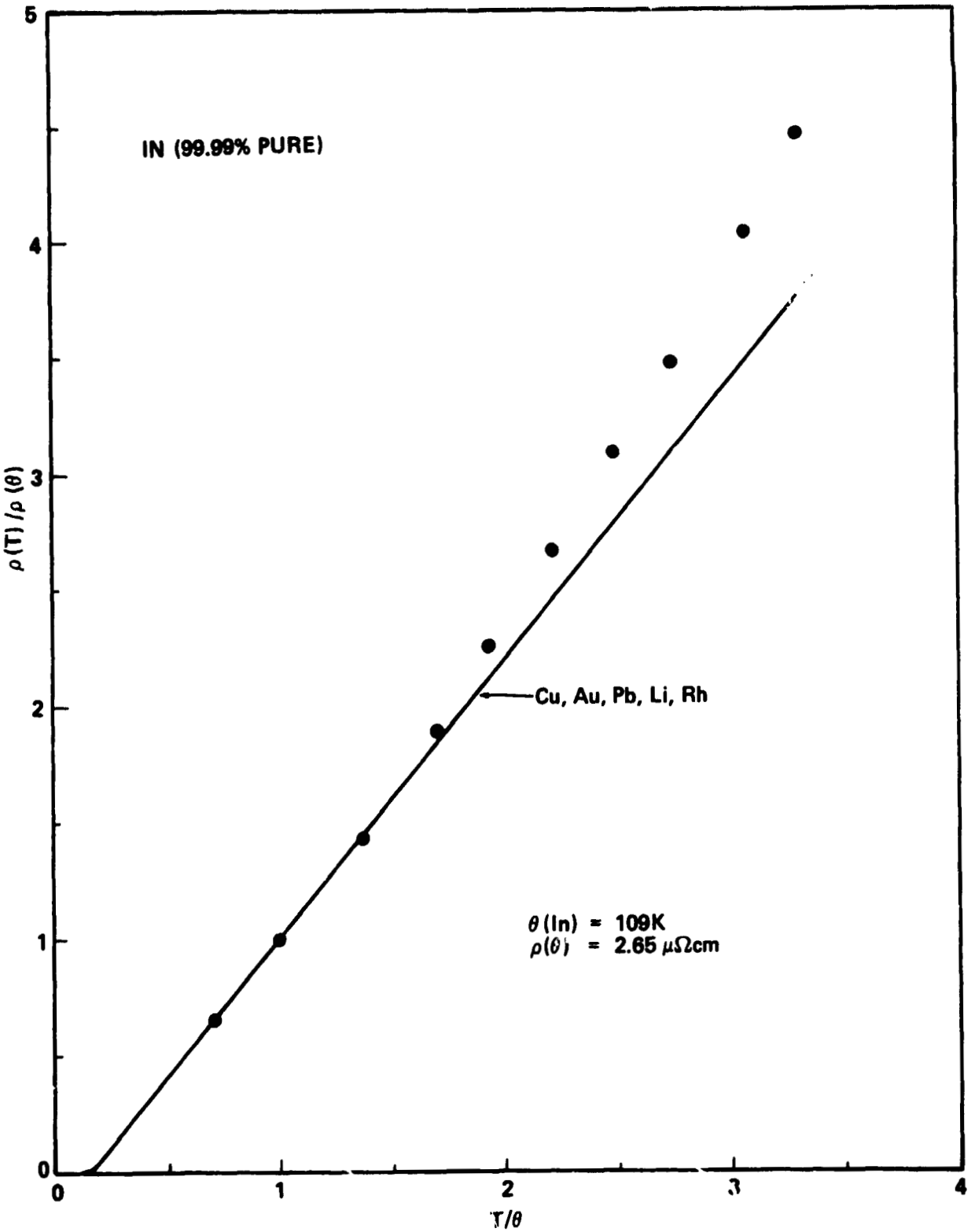

Fig. 7. Temperature dependence of the resistivity for In in reduced coordinates in comparison with other metals [18].

TABLE 1

EXPERIMENTAL RESISTIVITIES AND CURVE FITTING PARAMETERS FOR SINGLE-PHASE ALLOYS

Composition	ρ(77 K) ($\mu\Omega$cm)	ρ(298 K) ($\mu\Omega$cm)	ρ(333 K) ($\mu\Omega$cm)	n	$\alpha(25\ ^\circ C) = \frac{n}{T}$ (K^{-1})	a_o ($\mu\Omega cm\ K^{-1}$)	$\left(\frac{d\rho}{dT}\right)_{60\ ^\circ C} = \frac{n\rho}{T}$ ($\mu\Omega cm\ K^{-1}$)
In	1.76	9.15	10.58	1.27	0.00426	0.00656	0.0400
$In_{0.95}Bi_{0.05}$	(7.52)*	15.41	16.83	0.83	0.00279	0.136	0.0421
$In_{0.90}Bi_{0.10}$	(13.48)*	(21.20)	22.62	0.63	0.00211	0.583	0.0428
$In_{0.85}Bi_{0.15}$ (1)	(17.54)*	(25.90)	27.16	0.55	0.00185	1.113	0.0449
$In_{0.85}Bi_{0.15}$ (2)	-	(25.60)	26.87	0.56	0.00188	1.039	0.0452
$In_{0.80}Bi_{0.20}$	(20.04)*	(29.44)	30.99	0.49	0.00164	1.800	0.0456
In_2Bi	17.71	53.80	59.01	0.815	0.00273	0.518	0.144
In_5Bi_3	43.48	90.72	92.82	0.20	0.00067	29.02	0.0587
InBi	15.59	82.28	93.71	1.324	0.00444	0.0436	0.379
Bi	-	120	133.5	0.97	0.00326	0.477	0.389

Values in brackets refer to a metastable composition
*Data obtained on quenched samples
(1) Sample #1
(2) Sample #2

The variation of the resistivity for $T > 0$ can be expressed more adequately for indium by the empirical relationship

$$\rho = \rho_o + a_o T^n \qquad (3)$$

with $a_o = 0.00737\ \mu\Omega cm\ K^{-1}$ and $n = 1.27$. The material constants a_o and n can be taken from Fig. 8 which is a plot of the experimentally obtained resistivities as a function of temperature using a logarithmic scale. Equation 3 holds in a temperature region from 140 to 335 K with an accuracy of better than 1%. Since this relationship can be applied only for $T > \Theta$, the value of ρ_o, which is very small, will be neglected in our considerations. The data for pure Bi had to be omitted from Fig. 8, but the corresponding values are: $a_o = 0.477\ \mu\Omega cm\ K^{-1}$ and $n = 0.97$ (Table 1), demonstrating a nearly linear resistivity behavior. The constant a_o is a factor which depends upon the detailed nature of the band structure, the Debye temperature, and the atomic mass of the sample. It was found during the course of this investigation that this exponential relationship does not only hold for In and Bi but also for the α-phase and the intermetallic compounds of In and Bi. Therefore, with this relationship, the resistivities of the different In-Bi phases can be uniformly compared with each other.

Using Equation 3, the temperature coefficient of the resistivity α becomes

$$\alpha \equiv \frac{1}{\rho}\frac{d\rho}{dT} = \frac{n}{T} \qquad (4)$$

For most metals, a value of $\alpha \tilde{=} 0.004\ K^{-1}$ is generally found at RT, as can be seen from published data [20] and from Table 1.

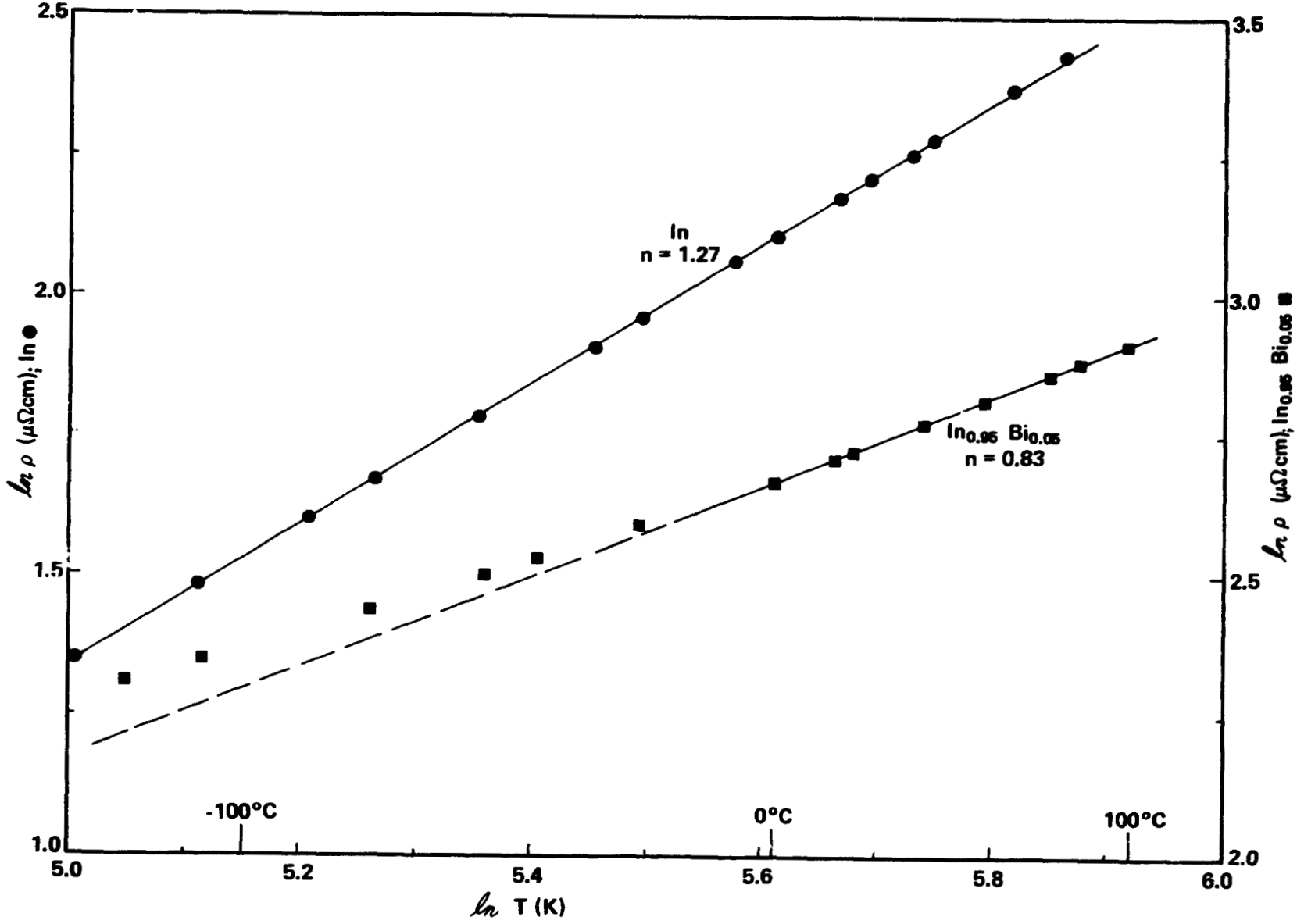

Fig. 8. Logarithmic plot of the resistivity for In and $In_{0.95}Bi_{0.05}$ as a function of temperature.

5. RESISTIVITY OF THE INTERMETALLIC COMPOUNDS, In_2Bi, In_5Bi_3, InBi

In alloy systems with intermediate phases, the variation of the resistivity with composition is very complex. Each phase has its own electrical behavior, depending on composition, lattice structure and band structure [22]. Since a new lattice periodicy is existing which may not be the one of the pure constituents, the resistivity normally will vary within the limits of the elementary constituents.

The temperature dependence of the resistivity for the three intermetallic compounds, In_2Bi (hexagonal), In_5Bi_3 (tetragonal), and InBi (tetragonal), has been measured and the results are shown in a logarithmic plot in Fig. 9. The data in a certain temperature region for $T > \theta$ can indeed be fitted with Equation 3 and small deviations occur close to the melting temperatures. From this graph, the values of n and a_o were determined and are given in Tables 1 and 2, together with the temperature range for which exponential fit is useful. With the exception of In_5Bi_3, the resistivities at room temperature increase nearly proportionally with the Bi content in the compounds and vary over the wide range from 9.1 to 120 $\mu\Omega$cm. In_5Bi_3 does not fit in this pattern because of its very high RT value of the resistivity, the narrow temperature range of the exponential fit, and the very small exponent of $n = 0.2$. With the exponent n being an indicator for the conducting mechanism, In_5Bi_3 seems to be closer to semiconducting behavior than the III-V compound InBi, where semiconducting properties could be expected [23]. It must be noted, however, that the results on In_5Bi_3 are preliminary and were obtained on a single sample. A confirmation of these measurements on more than one sample is desirable.

6. RESISTIVITY OF α-PHASE (α-In)

Thermal analysis data indicate [9] that the face centered tetragonal (fct) indium lattice can dissolve up to 7.1 W.% (4.0 At.%) Bi at 25 °C, forming the α-phase. The solubility is temperature dependent

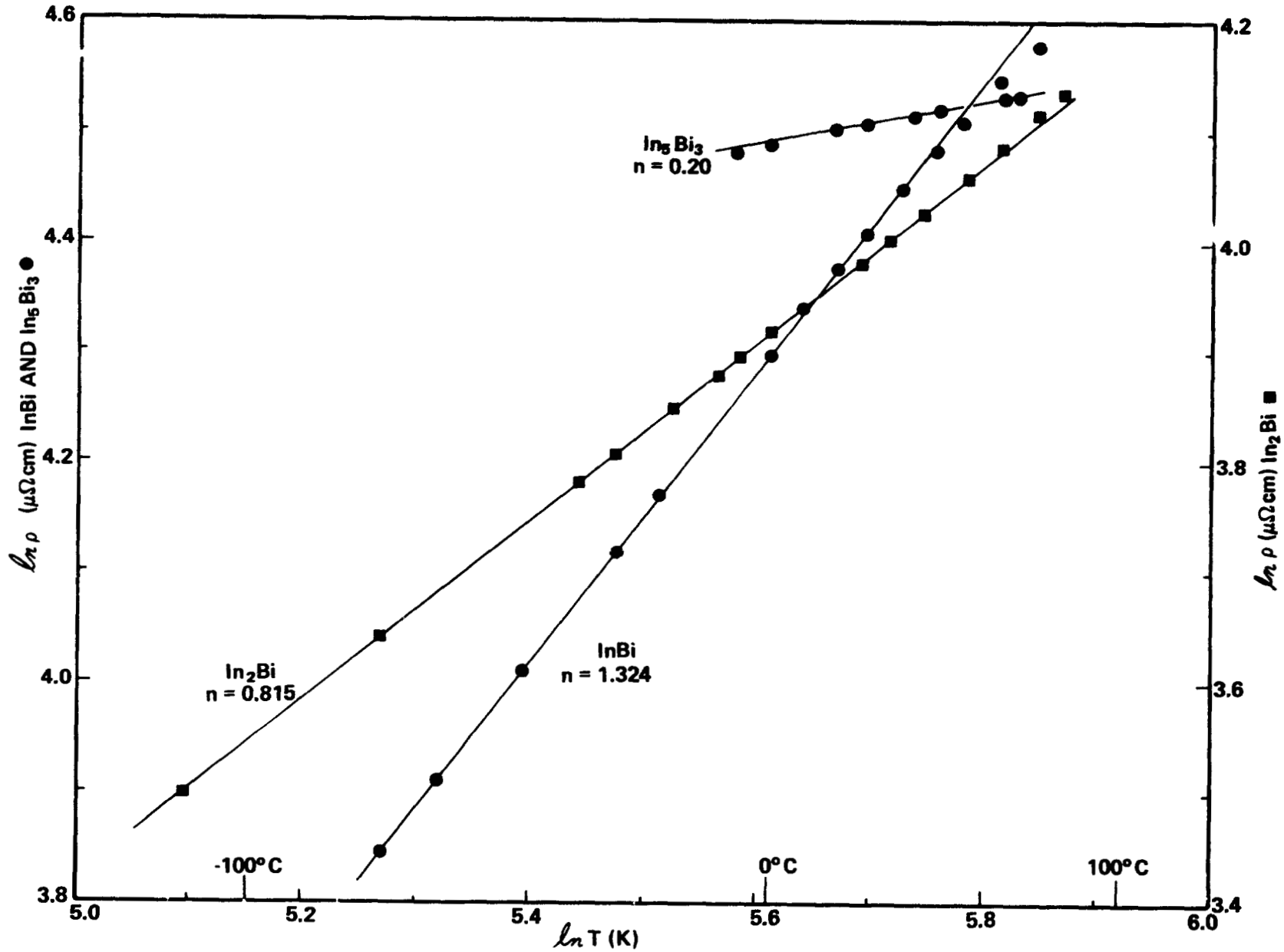

Fig. 9. Logarithmic plot of the temperature dependence of the resistivity for the intermetallic compounds

and at 72 °C, the maximum amount of In atoms which can be substituted by Bi atoms is 20.5 W.% at.% (see Fig. 5). This high solubility implies that of every eight In atoms, there is one randomly substituted by a larger Bi atom. Such a configuration is unstable below 72 °C, and, therefore, the α-phase precipitates the phase In_2Bi upon cooling [24]. The effect of supercooling of the α-phase by a few degrees is observed. The stability range of α-In from the phase diagram for various Bi concentrations, not considering the effect of supercooling, is given in Table 2.

We have measured on four samples with Bi concentrations (5, 10, 15, 20 W.%) the temperature dependence of the electrical resistivity. The results are given in Figs. 8 and 10. Two different samples of the composition $In_{0.85}Bi_{0.15}$ were available and the individual data, which agree to within 1%, are plotted in the same Fig. 10. It is interesting to note the steady increase of ρ with increasing Bi concentration. In the temperature range of stability, the resistance curves can again be represented by Eq.(3) with the concentration-dependent constants a_o and n listed in Table 1. Noticeable deviations from Eq. (3) occur outside the temperature range of stability, as demonstrated on the the sample $In_{0.95}Bi_{0.05}$ (W.%) in Fig. 8. Due to superheating and supercooling effects, the range of stability extends by several degrees K into the metastable region before decomposition and deviation from linearity occur.

On adding Bi to In, the axial ratio c/a of the fct lattice is increased [9] from 1.077 for pure In up to 1.122 for $In_{0.795}Bi_{0.205}$ (W.%). The Bi atoms can be considered as impurity atoms in the In lattice which act as additional scatter centers for the electrons (R_i) to the already present scatter at lattice vibrations (R_l).

For small impurity concentrations, Matthiessen's rule [25] states that these two contributions to the resistance are additive and the total resistance R is then composed of the two terms,

$$R = R_i + R_l(T) \quad \text{or} \quad \rho = \rho_i + \rho_l(T). \tag{5}$$

TABLE 2

TEMPERATURE RANGE OF STABILITY FOR α-PHASE AND ACCURACY OF EXPONENTIAL FIT (EQ. 3)

Designation	Bismuth Concentr. at.%	vol.%	w.%	Range of Stability** From K	To K	Temp. Range for Exponential Fit From (K)	To (K)	Accuracy of Exp. Fit (%)
In	0	0	0	<429*		335 to 140 280 to 170		1 0.1
$In_{0.95}Bi_{0.05}$	2.81	3.77	5	404	285	370 370	273 290	1 0.1
$In_{0.90}Bi_{0.10}$	5.75	7.64	10	382	314	363	310	0.1
$In_{0.85}Bi_{0.15}$	8.84	11.62	15	365	331	357	320	0.1
$In_{0.80}Bi_{0.20}$	12.08	15.7	20	352	343	346	328	0.03
In_2Bi	33.33	40.41	47.66	<362*		345 330	77 180	1 0.1
In_5Bi_3	37.50	44.86	52.23	<362*		345	273	0.2
InBi	50	57.55	64.54	<283.5*		325 300	160 205	1 0.1
Bi	100	100	100	<544*		330	180	1

* Melting temperatures

** From Phase Diagram

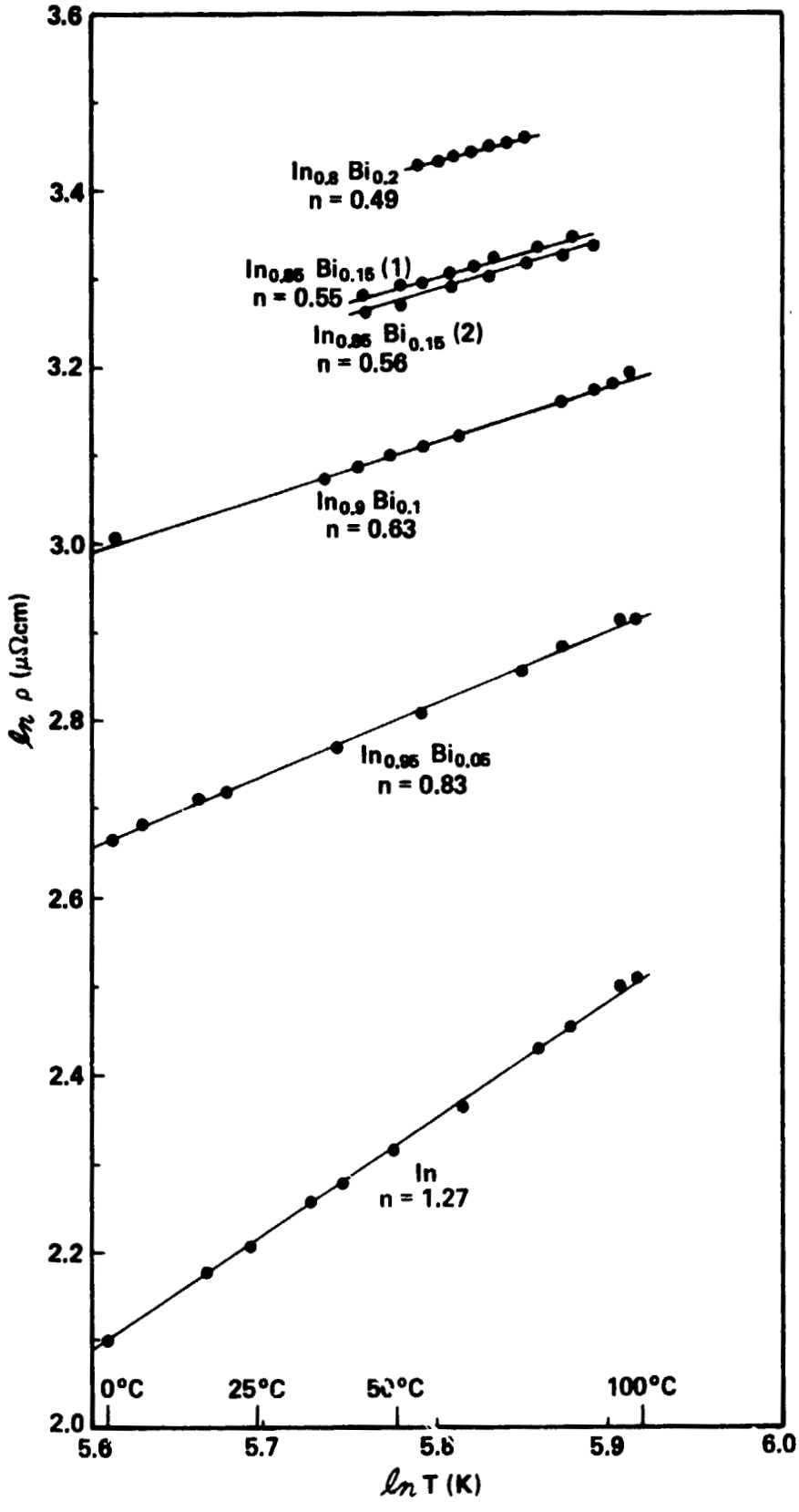

Fig. 10. Logarithmic plot of the temperature-dependent resistivity for the resistivity for the α-phase.

The term (R_1) introduced by the lattice vibrations is temperature dependent, whereas, the impurity term (R_i) is independent of temperature and should be proportional to the impurity concentration for small concentrations. To check the extent to which Matthiessen's rule applies for the experimentally obtained resistivities of the α-phase, the following consideration is useful. When the temperature dependent term ρ_1 is independent of the impurity concentration, then the following relation can be derived from Eq. (5).

$$\left(\frac{d\rho}{dT}\right)_{In} = \left(\frac{d\rho}{dT}\right)_{\alpha\text{-In}} \qquad (6)$$

Slope values for all samples in the single-phase region are available for T=60° and are listed in Table 1. We see that at 333 K (60 °C) the slope of the resistivity curves for In is changed by only 6% when up to 20 W.% Bi is dissolved. Although there is a weak coupling of the impurity atoms and the phonons, Matthiessen's rule is applicable to α-In with the accuracy stated. We note that $d\rho/dT$ for In_5Bi_3 is close to the values for the α-phase whereas the slopes for In_2Bi, InBi and Bi are nearly a magnitude larger.

Combining Eq. (6) and (3), we find the useful relationship

$$n(\alpha)\rho(\alpha) = n(In)\rho(In) \quad \text{or} \quad n(\alpha) = \rho(In)\, n(In)\, \frac{1}{\rho(\alpha)}$$

$$(T = \text{constant}) \qquad (7)$$

which correlates the exponent and the resistivity for In with those for the α-phase. Plotting the exponents obtained for the α-phase as a function of $1/\rho_\alpha$ should result in a straight line with $\rho(In)n(In)$ as the slope value. This relation is demonstrated in Fig. 11 for a temperature of 60 °C. The slope of the continuous line was chosen as 13.31 μΩcm according to the experimental data for In and, therefore, the offset of data points from this line is a quantitative measure for the deviation from Matthiessen's rule. Fig. 11 also contains the measurements for the compound In_5Bi_3 which fit surprisingly well with these data. It may be concluded from this behavior that In_5Bi_3 (tetr.) in its electrical properties is similar to the isostructural α-phase and may be considered a stabilized continuation of the solid solution phase.

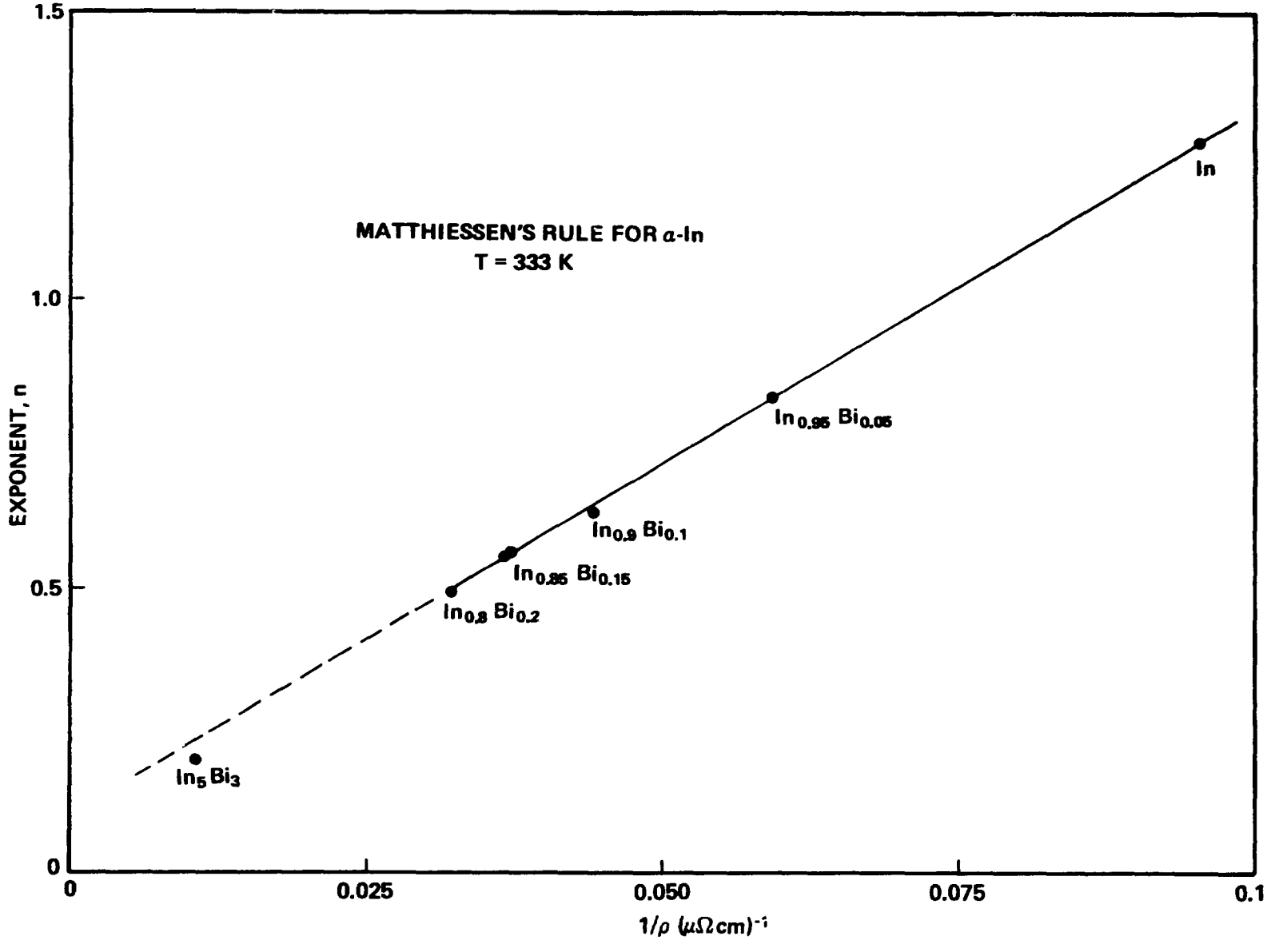

Fig. 11. Matthiessen's rule applied to the resistivity of the α-phase and In_5Bi_3 with Eq. (7).

Above, we have related the resistivity of the α-phase with the exponent n, using Matthiessen's rule. A correlation of the resistivity with the concentration of Bi is possible on the basis of considerations by Nordheim [26]. He finds that, at a constant temperature, the resistivity $\rho(\alpha)$ is proportional to the concentration product of the two partners. If x is the concentration of Bi in W.% and (1-x) the concentration of In, then the resistivity should follow as:

$$\rho_\alpha = \rho_{In} + bx(1-x) \qquad (8)$$

where the constant b has the value 123 μΩ cm at 60 °C.

The α-phase, up to the solubility limit of 20.5 W.%, follows the proposed relationship as we can see from Fig. 12, where $(\rho_\alpha - \rho_{In})/(1-x)$ is plotted as a function of concentration at 60 °C. The experimentally obtained resistivities are compared with the expected resistivities from Eq. 8 in Table 4. It may be noted that the linear fit of the data is best when the Bi concentration on both axes is expressed in weight %. The resistivity increase for indium by the solution of small bismuth concentrations is found to be 2.22 μΩcm/at.%.

7. RESISTIVITY OF TWO-PHASE ALLOYS (α-In + In_2Bi)

According to the In-Bi phase diagram, there are four concentration regions at 25 °C in which two different phases co-exist with each other:

| α-In + In_2Bi | In_2Bi + In_5Bi_3 | In_5Bi_3 + InBi | InBi + Bi |

The most interesting phase combination, considering the electric properties, is the region α-In + In_2Bi because of the temperature-dependent solubility of In_2Bi in the α-phase. A temperature-dependent solubility causes the relative amount of the two phases to change with temperature, whereas, in the remaining three concentration ranges, this is not the case. In the following, we will discuss the results obtained on alloys, including the eutectic composition, consisting of α-In and In_2Bi.

TABLE 3

EQUILIBRIUM RESISTIVITIES FOR TWO-PHASE ALLOYS AND CURVE-FITTING PARAMETERS

Designation* (w.%)	ρ(25 °C) ($\mu\Omega$cm)	$d\rho/dT$ ($\mu\Omega$cm K^{-1})	$\alpha \times 10^{-3}$ (K^{-1})	$n = \alpha T$	a_o ($\mu\Omega$cm K^{-1})	Calc. ρ T = 273 K ($\mu\Omega$cm)	Exp. ρ T = 273 K ($\mu\Omega$cm)
$In_{0.90}Bi_{0.10}$	18.6	0.17	9.21	2.74	3.091×10^{-6}	14.63	14.79
$In_{0.85}Bi_{0.15}$	21.3	0.174	8.1	2.41	2.320×10^{-5}	17.24	17.18
$In_{0.80}Bi_{0.20}$	22.6	0.165	7.3	2.18	9.127×10^{-5}	18.67	18.60
$In_{0.75}Bi_{0.25}$	26.4	0.187	7.0	2.09	1.780×10^{-4}	21.98	21.93
$In_{0.66}Bi_{0.34}$	33.9	0.19	5.7	1.70	2.109×10^{-3}	29.21	29.10
$In_{0.55}Bi_{0.45}$	49.2	0.17	3.5	1.04	1.314×10^{-1}	44.90	45.05
In_2Bi	53.8	0.15	2.7	0.815	5.180×10^{-1}	50.10	50.23

* These compositions are nominal and are derived from the weights of the constituents.

TABLE 4

CONCENTRATION DEPENDENT RESISTIVITY OF α-In AT T = 333K

Bi Concentr., x (w.%)	Calc. Resistivity* (μΩcm)	Calc. Resistivity** (μΩcm)	Experimental Resistivity (μΩcm)
0	10.58	10.58	10.58
5	16.42	16.66	16.83
10	21.65	22.10	22.62
15	26.26	26.90	27.16
15	26.26	26.90	26.87
20	30.26	31.06	30.99
52.2 (In_5Bi_3)	41.15	42.52	92.82

* for b = 123 μΩcm [ρ(Bi) = 133.3 μΩcm]

** for b = 128 μΩcm [ρ(Bi) = 138.6 μΩcm]

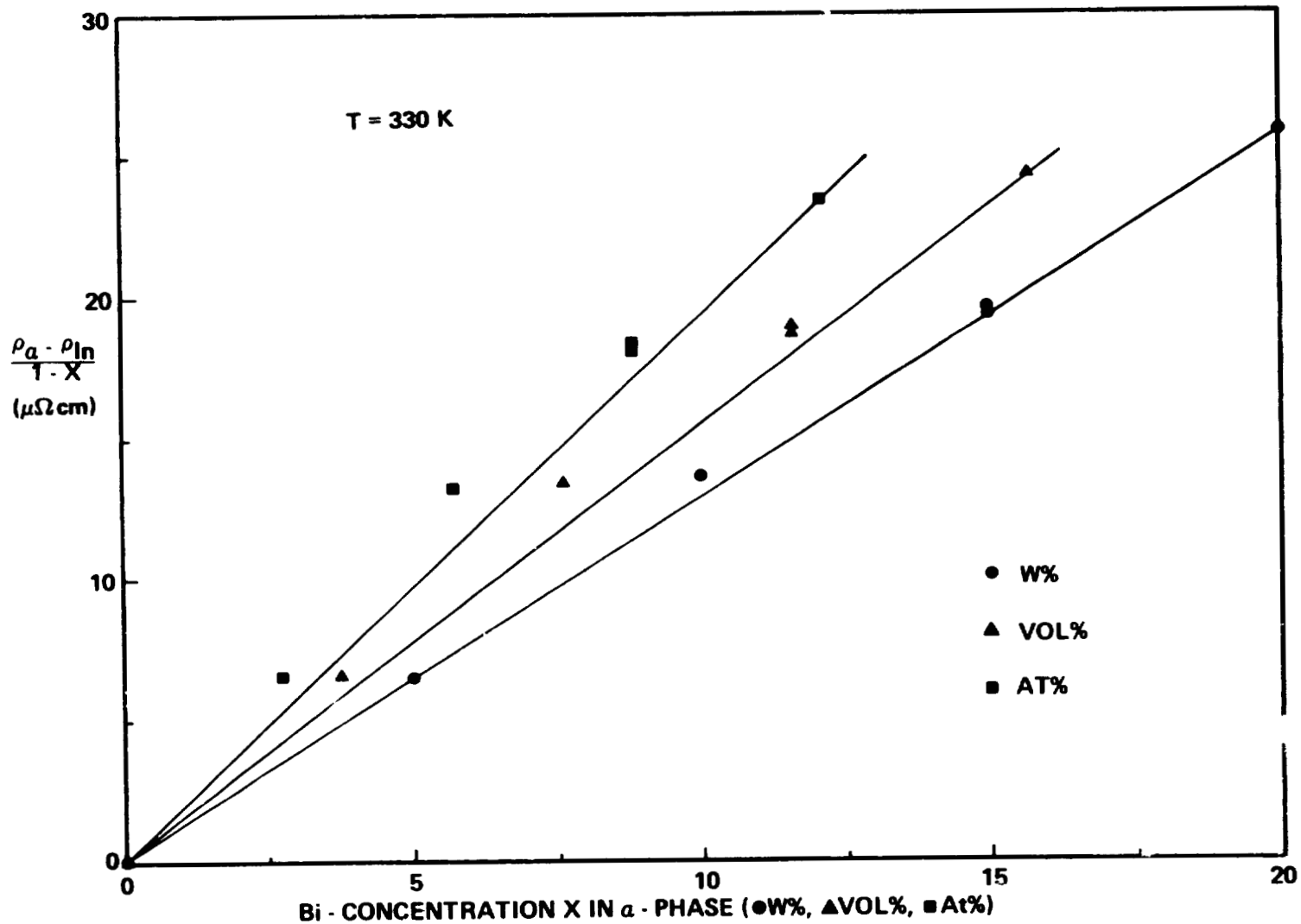

Fig. 12. Concentration dependence of the scaled resistivity for α-In.

In order to get reliable data for those materials, the two phases have to be in thermodynamic equilibrium with each other and the achievement of this condition is a function of time. We were able to follow the approach to equilibrium conditions by measuring the time dependence of the resistance and, after gaining knowledge of the analytical function for this behavior, could extrapolate the resistivity to $t = \infty$. These studies are further explained in a later chapter (IV). Such extrapolated equilibrium values are used in Fig. 13 which contains the resistivities at T = 25 °C for the two-phase alloys as a function of the overall Bi concentration. The data of Fig. 13 are also listed in the first column of Table 3. Since the two-phase region is terminated by the single-phase alloys α-In and In_2Bi, all properties of the two-phase region have to start and to end with the properties of each single-phase material. Therefore, the cusp in the curve at 7.2 W.% Bi reflects the phase boundary for the α-phase at 25 °C.

Fig. 13 also contains a dashed line representing the resistivities for metastable (supersaturated) α-phase. These resistivities can be obtained either from Eq. (3) when the extension in the metastable range is made, or from experimental readings when the α-phase is quenched from a high temperature to 25 °C where it is stable for some seconds before the precipitation of In_2Bi occurs. It may be seen from this figure that of two samples with the same Bi concentration, the resistivity of the two-phase alloy is always lower than that of the single-phase material although the resistivity of the precipitated compound is appreciably higher than that of the α-phase. Measurements of this kind could be useful in determining the electrical switching (parallel or series) of the precipitated phase. Similar curves to the ones in Fig. 13 are obtained when different equilibrium temperatures are chosen.

With the Bi concentration left constant, the equilibrium resistivity has been measured at several temperatures, usually between 0 °C and 60 °C. The temperature could not be chosen too low because then the adjustment to the equilibrium composition becomes increasingly slow. For example, consider the eutectic material (33.7 W.% Bi and 66.3 W.% In) where it will take

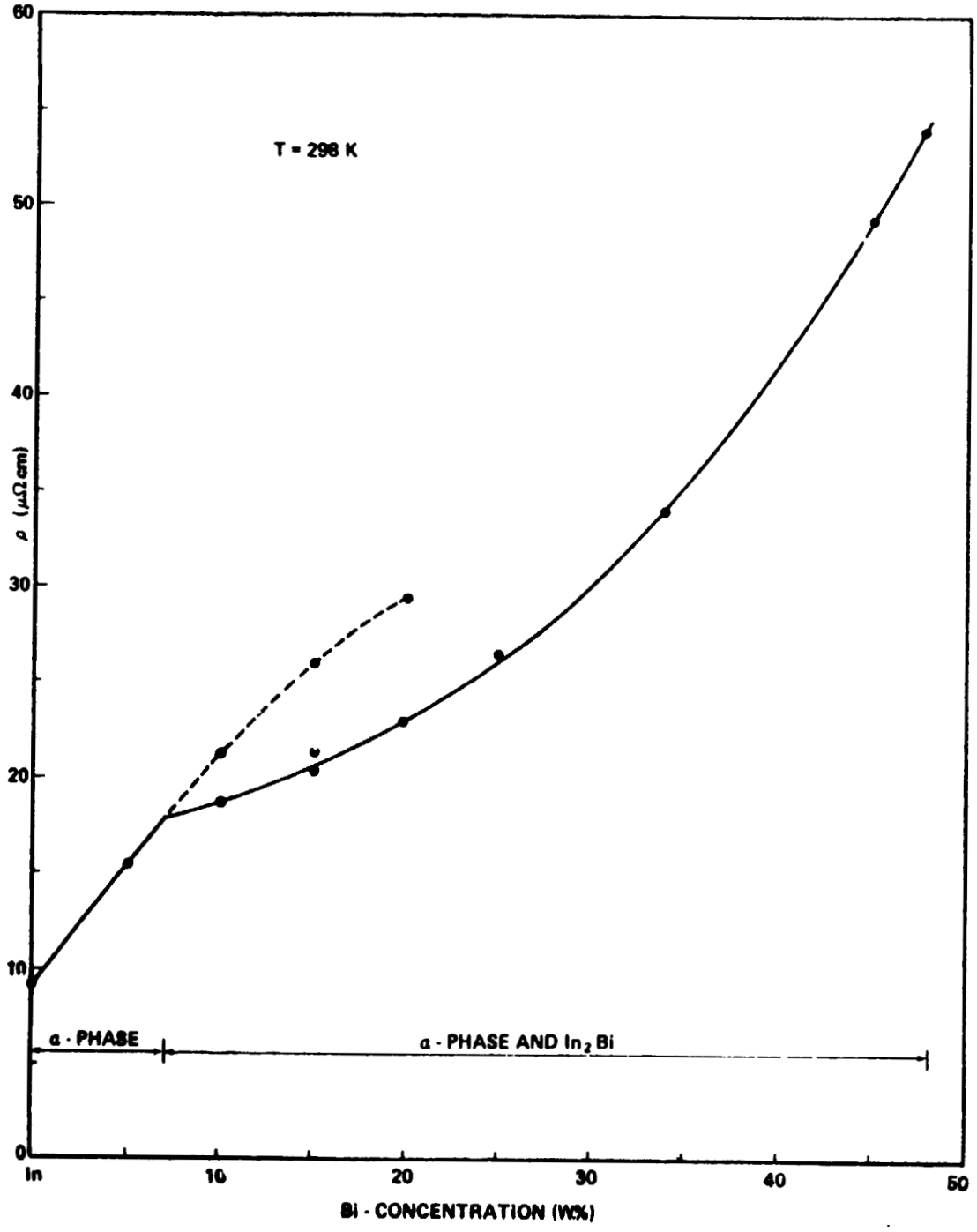

Fig. 13. Concentration dependence of the resistivity for the two-phase alloys (α-In/In_2Bi) at 25°C. The dashed line is for the metastable α-phase at this temperature.

approximately 90 hrs. at 0 °C to achieve 95% of the equilibrium composition, whereas at 24 °C, equilibrium (95%) will be achieved in only 9 hrs.

The equilibrium resistivities were used to determine graphically the values of $d\rho/dT$ at 25 °C which are listed in the second column of Table 3. It is remarkable that the slope for these two-phase materials - because of the temperature-dependent solubility - are four to five times larger than those for single-phase materials, listed in Table 1. This increased temperature sensitivity of the sample resistance makes an accurate potential measurement difficult for very long elapsed times and requires a high degree of temperature stability of the water bath. Typically, the RT resistivity changes by 0.5 to 1% of the measured resistivity for every degree change in temperature.

Multiplication of the slope values with $1/\rho$ gives the temperature coefficient α for the two-phase material. Also listed in Table 3 are the "hypothetical" values for the exponents n and the constants a_o derived from knowledge of α and with Eq. (3). Although there is no obvious justification available for doing so, the agreement of the results obtained is quite encouraging. Using RT data to compute the constants for Eq. (3), the calculated and measured values for ρ at 0 °C can be compared, which is done in the last two columns of Table 3. The agreement of the resistivities is better than 1%.

8. ELECTRIC MODELING OF TWO-PHASE ALLOYS

Very often it is desirable to estimate the resistivity of a two-phase alloy when the resistivities of the individual components are known. As a first approximation, the weighed average of the resistivities on a volume basis is recommended [27]. The difficulty in obtaining a better approximation lies in the fact that the switching characteristics of the second phase (percentage of parallel and series connection) is not known. The extreme cases would be that all the particles of the second phase are connected either in series or in parallel. The true value for the resistivity will lie somewhere in between.

A better approach to this problem will be the application of the composite resistivity model obtained in Chapter II, 2. Since the equilibrium resistivities of the two phases are available, we can demonstrate the quality of the model by the degree of agreement we obtain with the experimental data. These resistivities are listed in Table 5 for several two-phase In-Bi alloys. Also given are the extreme values for serial and parallel connection of the second phase. The data of Table 5 are illustrated in Fig. 14. Considering the small amount of data put into the model, the agreement with the experimental resistivities is good and is within the scatter of the data obtained.

9. THE DETERMINATION OF THE α-PHASE LINE BY RESISTIVITY MEASUREMENTS

The α-phase line in the phase diagram (Fig. 1) can be determined with resistance measurements by cooling a sample of α-In with fixed composition slowly through that critical temperature region. When the phase line is crossed, precipitation of In_2Bi occurs which is associated with a change in slope of the resistance temperature curve. However, the supercooling of the α-phase delays precipitation of In_2Bi. This effect can be eliminated by cooling the sample sufficiently below the supercooling temperature and subsequently performing equilibrium measurements at increasing temperatures.

A series of such measurements on the sample $In_{0.9}Bi_{0.1}$ is shown in Fig. 15. The decomposition temperature of 312 K (39 °C) can be derived from the data. Similar curves are obtained for α-In with 15 and 20 w.% Bi, leading to critical temperatures of 325 K (52 °C) and 341 K (68 °C), respectively.

Here is another opportunity to check if Eq. (3) is applicable for two-phase materials. For α-In, the temperature dependence of the resistivity in the single-phase region is given by Eq. (3) with the constants listed in Table 1. The resistivities in the two-phase region may be expressed by the same equation but with different constants listed in Table 3. The temperature at which the two resistivity curves intercept will be the critical

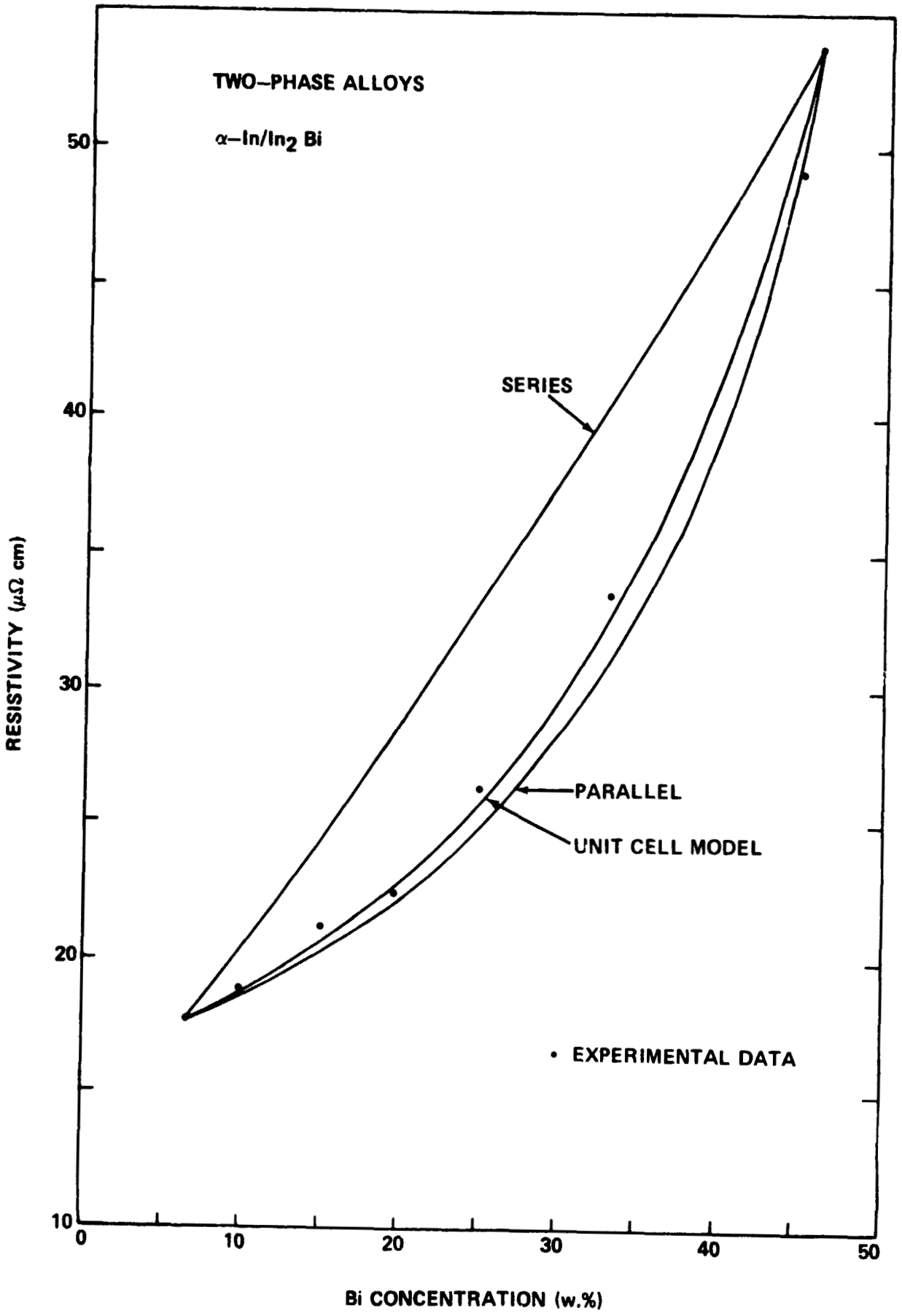

Fig. 14. The calculated resistivity of two-phase alloys according to different models.

TABLE 5

THE ELECTRICAL RESISTIVITY OF TWO-PHASE ALLOYS OBTAINED FROM DIFFERENT MODELS

(T = 25 °C)

Designation (w.%)	Conc. of α-In (vol.%)	Serial Connect. (μΩ cm)	Parallel Connect.† (μΩ cm)	Cubic Unit Cell* (μΩ cm)	Exp. Equil. Resistivity** (μΩ cm)
$In_{0.928}Bi_{0.072}$	100	17.79	17.79	17.79	17.79
$In_{0.90}Bi_{0.10}$	93.68	20.06	18.58	18.63	18.6
$In_{0.85}Bi_{0.15}$	82.12	24.23	20.21	20.48	21.3
$In_{0.80}Bi_{0.20}$	70.19	28.52	22.22	22.85	22.6
$In_{0.75}Bi_{0.25}$	57.87	32.96	24.78	25.82	26.4
$In_{0.663}Bi_{0.337}$	35.41	41.05	31.34	34.68	33.9
$In_{0.55}Bi_{0.45}$	4.32	52.24	49.47	50.04	49.2
$In_{0.535}Bi_{0.465}$	0	53.80	53.80	53.80	53.80

† Also referred to in literature as "weighed average."

* The second phase is assumed to be dispersed in cubic form.

** Experimental data obtained by extrapolation to $t = \infty$.

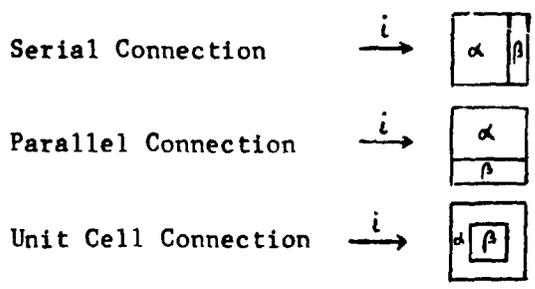

temperature for decomposition. The following temperatures are then calculated: 316 K, 328.5 K and 348 K for the three Bi-concentrations mentioned above. The agreement is good regarding the accuracy of 1% with which the exponents n are determined.

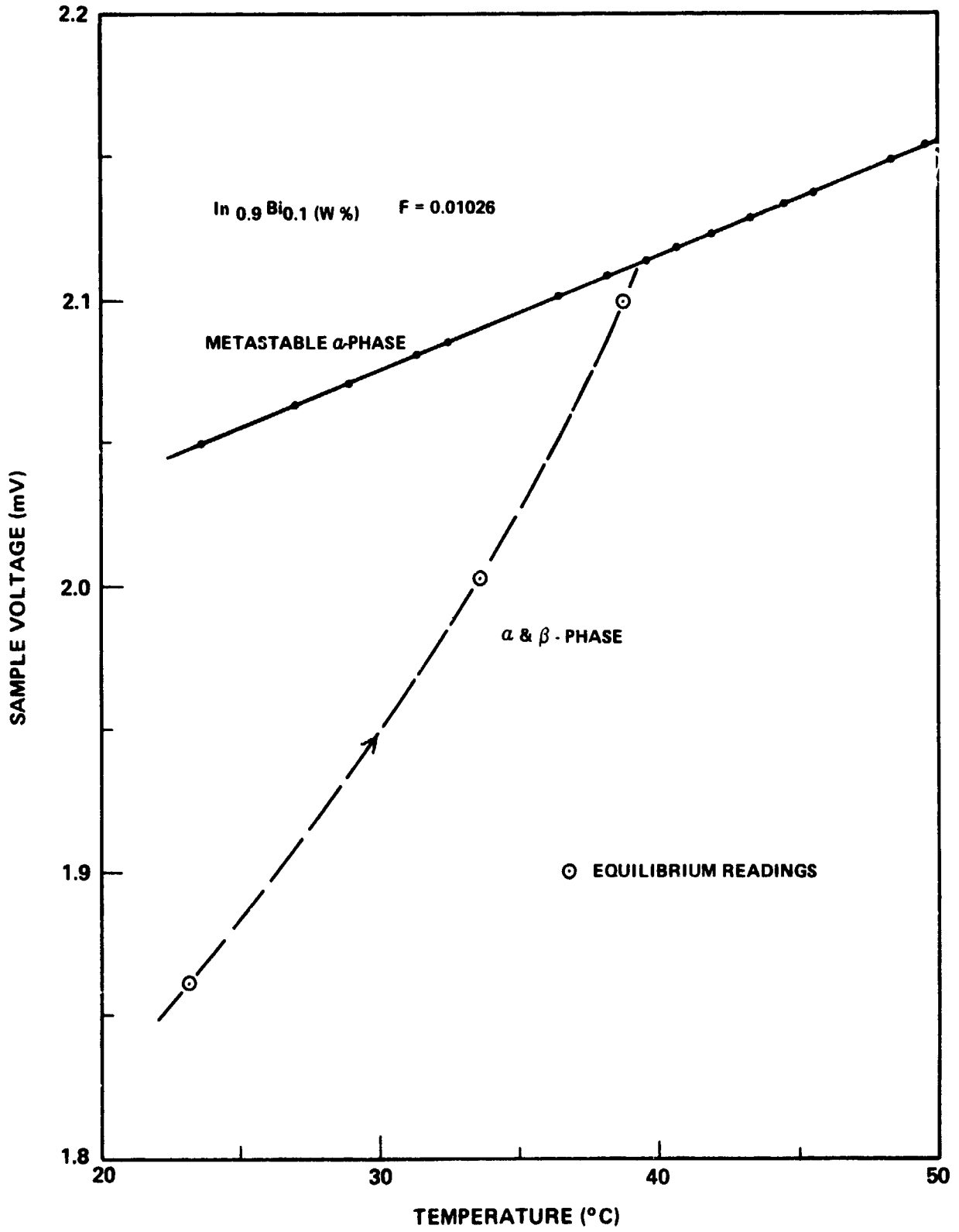

Fig. 15. The determination of the α-phase boundary by resistivity measurements.

IV. Adjustment to Thermodynamic Equilibrium in Two-Phase In-Bi Alloys

1. EUTECTIC ALLOYS

The eutectic alloy is a two-phase material composed of α-In and In_2Bi. Since the α-phase has a temperature-dependent solubility limit for bismuth or In_2Bi, the relative composition of the two phases in the alloy is dependent on temperature. For some common temperatures used in this investigation, the concentrations of both phases are listed in Table 6, along with the solubility limit for α-In. These quantities are calculated from the phase diagram.

TABLE 6

TEMPERATURE DEPENDENT COMPOSITION OF In-Bi EUTECTIC MATERIAL
(66.3 w.% In - 33.7 w.% Bi)

Temperature		Bi-conc. in α-phase	Relative Amount of α-phase	In_2Bi
(K)	(°C)	(w.%)	(w.%)	(w.%)
322.3	49.3	12.8	38.0	62.0
308.6	35.6	9.7	35.2	64.8
297.0	24.0	6.9	32.4	67.6
273.0	0.0	3.4	29.7	70.3

Upon cooling of an eutectic alloy from 35.6 °C to 24.0 °C, the relative composition of the sample should change according to the values listed in Table 6. This compositional change implies that 2.8 w.% of the phase In_2Bi will be formed from α-In at 24 °C. The compound formation is a thermally activated process and requires a certain time for its completion. Since the resistivities for the two phases differ by a considerable amount, it is possible to follow the adjustment to the new equilibrium composition by resistivity measurements.

If no time-dependent change in composition occurs, the sample may be in a "frozen" state and behaves electrically like a single-phase material.

The change in resistance as a function of time for the first 10 minutes of an experiment in which a sample was rapidly cooled from 35.6 °C to 23 °C is shown in Fig. 4. It can be recognized that the cooling curve consists of two parts. First, there is a rapid drop in resistance caused by the sudden change in temperature. It was determined that the time required for the sample to adopt the new temperature was 5 to 10 seconds, depending on the temperature difference. Secondly, there is a gradual decrease in the resistance with time after the material achieved the constant temperature of the bath. This effect can be attributed to the adjustment towards the new equilibrium composition at 23 °C. The decrease in the resistivity can be observed for days or even weeks until the sensitivity limit of the instrumentation is reached.

In the following, we will describe analytically the time dependence of the resistivity. The changes in resistivity caused by the growth of a second phase may be expressed by the Avrami equation [28]. Adjusted to our needs, the following relation can be applied:

$$\Delta\rho \equiv \frac{\rho_o-\rho}{\rho_o-\rho_\infty} = 1 - \exp(-bt^m) \qquad (9)$$

where

t = time

ρ = resistivity at $t = 0$

ρ_∞ = resistivity at $t = \infty$

b = a reaction constant

m = a constant which depends on the nucleation and the geometry of the growing particles

For $t = 0$, we obtain $\Delta\rho = 0$ and for $t = \infty$, $\Delta\rho = 1$ results. The extreme conditions show that only relative changes in the resistivity are considered.

The limiting resistivities were determined as follows: ρ_o can be obtained by extrapolating the first readings after 10, 15, 20 and 30 seconds to $t = 0$. At room temperature (small reaction rates), this could be achieved by a linear extrapolation. For higher reaction rates, the linear extrapolation proved not to be sufficient and a best curve was then drawn through the data points. The value for ρ_∞ was estimated by a logarithmic extrapolation of the readings obtained after several days into the experiment. By this method four to five decades in elapsed time were covered.

Knowledge of ρ_o and ρ_∞ after completion of the isothermal reaction gave the $\Delta\rho$ as a function of time. Plotting log ln $\frac{1}{1-\Delta_\rho}$ as a function of log t satisfies Eq. (9), and a straight line will result with the slope m when the Avrami equation is applicable to the process.

Fig.16a shows the experimental readings for the isothermal reaction at 23 °C, when plotted in the reduced coordinates. It may be noticed that the precipitation of In_2Bi occurs immediately with no induction time required. The first reading (35.30 μΩcm) obtained at $t = 10$ sec is located on the straight line and differs from the extrapolated ρ_o by only 0.07 μΩcm. The linear relationship with $m = 0.57$ is followed within three decades of time, until 70% of the equilibrium resistivity reading is reached after approximately 100 min. Then, a marked deviation from Avrami's relationship occurs. This deviation has been observed on many samples and the reason for this effect is not yet known. The change in slope occurs when the sample is about 70 to 80% close to ρ_∞ and indicates a much slower reaction rate. Measurements after such long elapsed times, where only an additional 10% change in resistivity can be expected, are very difficult to make because of the required long time stability of the instrumentation. Therefore, we will be mainly concerned with the first 50% change in the resistivity.

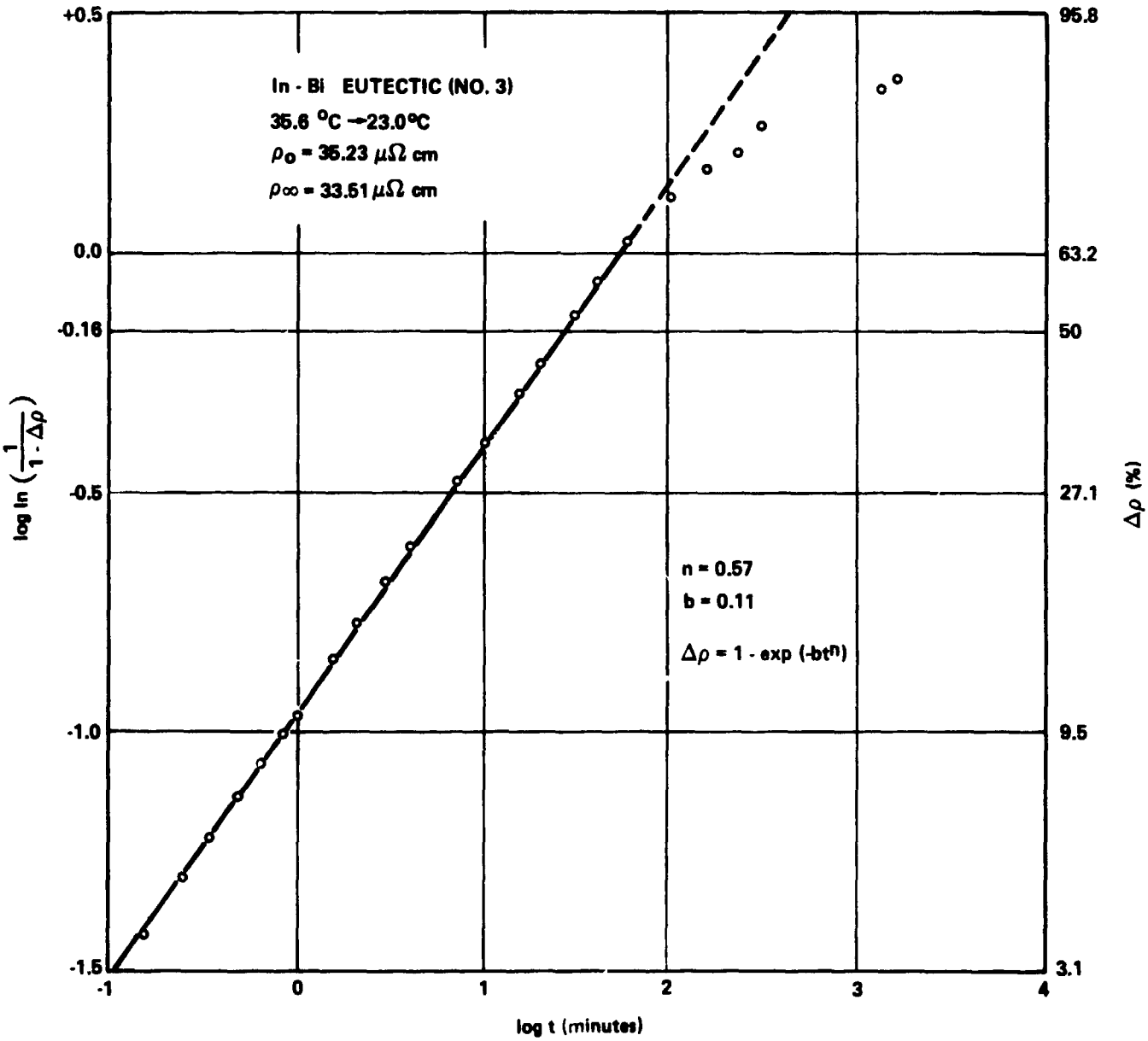

Fig. 16a. Temperature and time-dependent resistivity of an In-Bi eutectic alloy when quenched from 35.6 to 23.0 °C.

The adjustment to the equilibrium compositon may be studied at several temperatures and then the curves shown in Fig. 17 are obtained. Heating or cooling the eutectic alloy to a new equilibrium temperature can be expressed by the same formalism. The slope of the lines is approximately the same with a value of $m = 0.59$ and a mean deviation of 8%. The time at which the relative resistivity $\Delta\rho$ passes 50% will be called $t_{1/2}$. This time is a measure for the temperature-dependent rate of the precipitation. Reaction rates are markedly slower at 0 °C than at higher temperatures. Since the precipitation is a thermally activated process, $t_{1/2}$ will be connected with the temperature by the Arrhenius-type equation [28]:

$$t_{1/2} = C \exp(-q/kT) \qquad (10)$$

where C is a constant, containing explicitly the frequency of the lattice vibrations and q is the activation energy for the volume diffusion of bismuth in indium. From Fig. 18, an activation energy of 0.73 eV/atom or 17 kcal/mole can be calculated from the averaged slope. There is considerable scatter in these data for the narrow temperature range available and, therefore, the error in the activation energy is in the order of 20%.

An experiment was performed to investigate the adjustment to the equilibrium composition at -78.5 °C, the temperature of dry ice. When at equilibrium at this low temperature the α-phase will contain only approximately 0.06 at.% Bi dissolved and could be considered as pure indium. On the other hand, the precipitation rate is expected to be very small, making the determination of the half time practically impossible.

Two eutectic samples were used: one, brought from room temperature equilibrium and the other from 0 °C equilibrium to -78.5 °C. In both cases, a change in resistivity with time was observed over a period of one week, indicating the formation of In_2Bi even at this low temperature. The evaluation of the data, however, presented difficulties because of the unknown value for ρ_∞. This parameter is needed for the plot of the relative resistivity with the Avrami equation. When we estimate ρ_∞ being

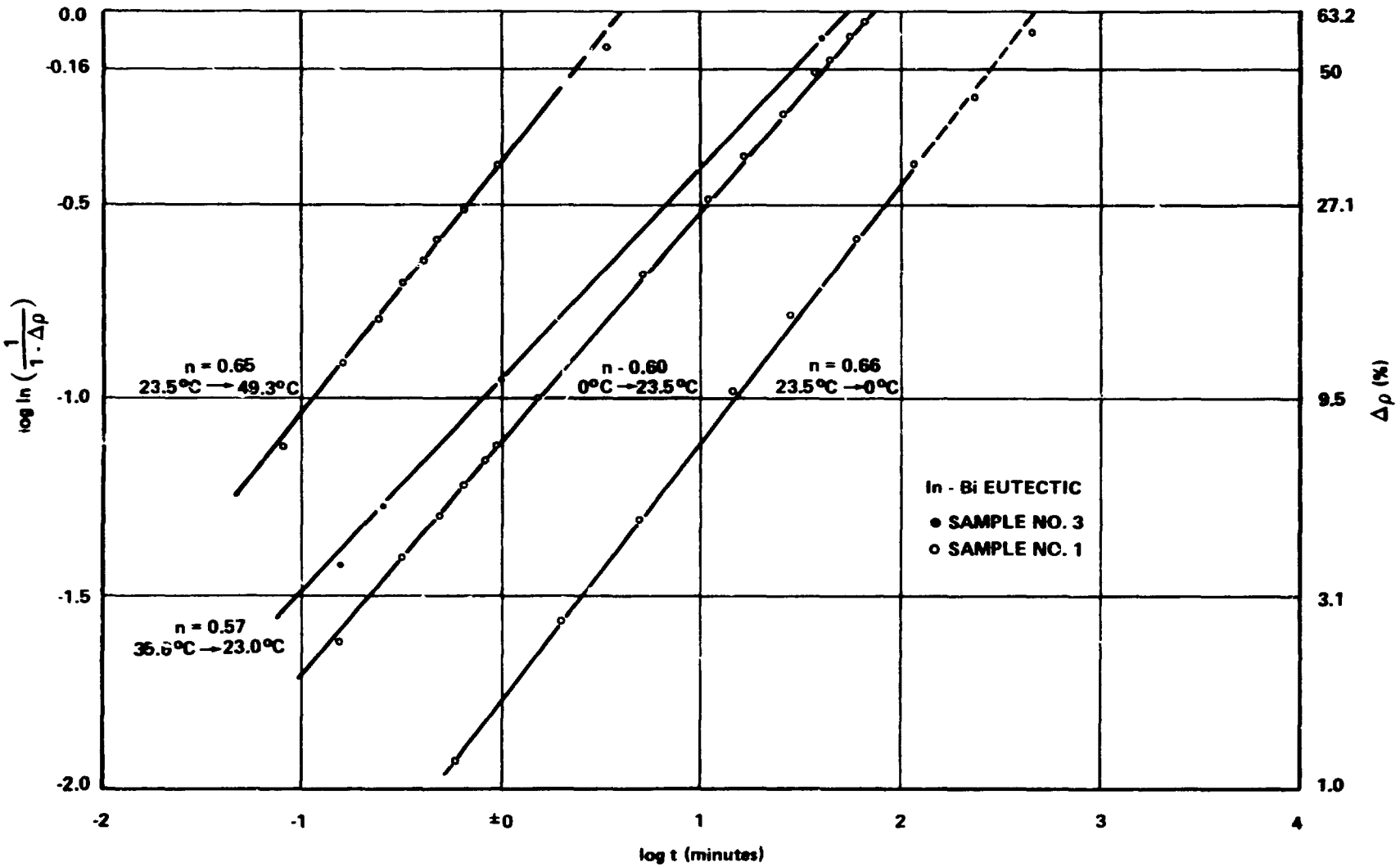

Fig. 17. Time dependence of the scaled resistivity for eutectic alloys at various quenching temperatures.

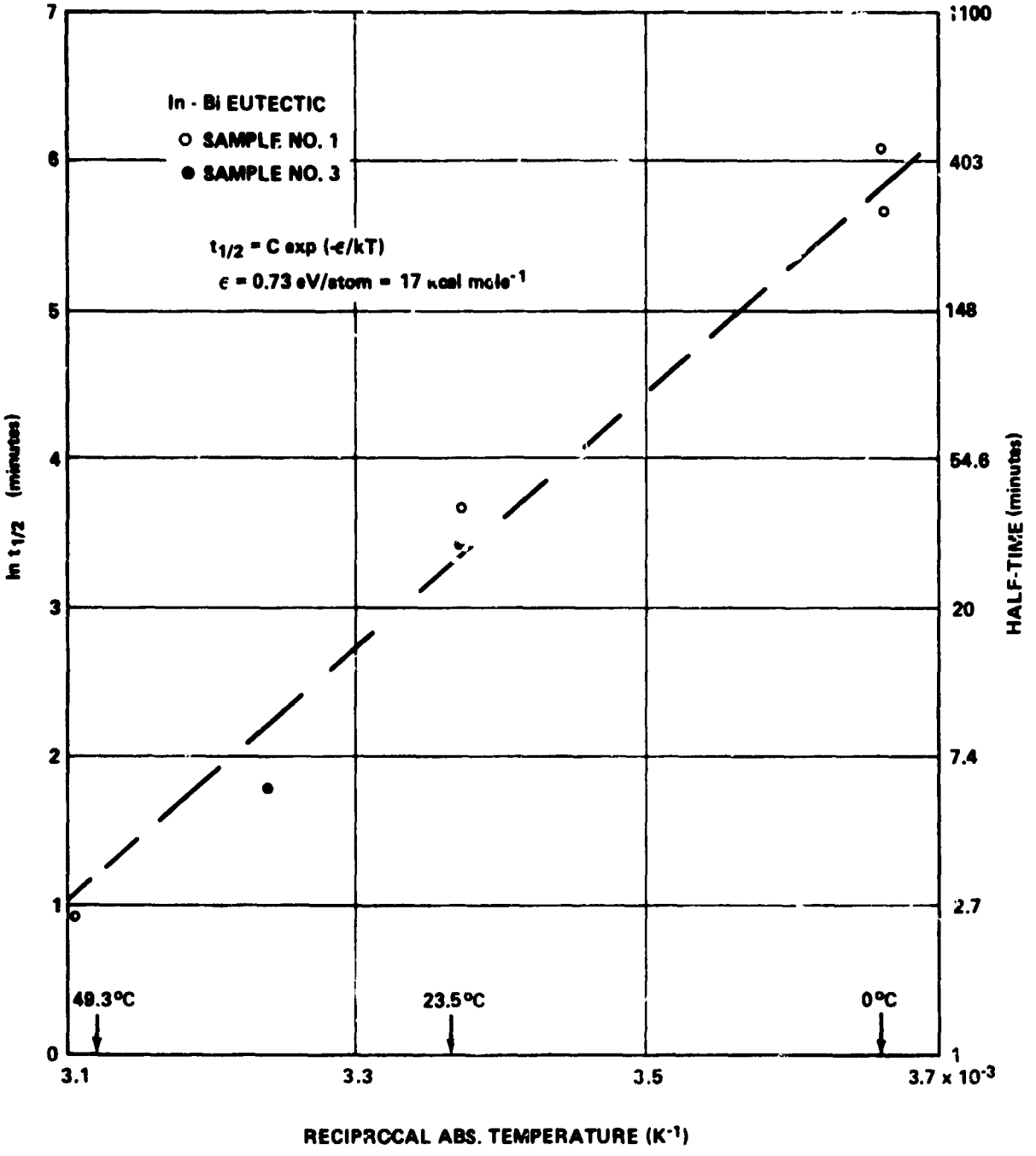

Fig. 18. Plot of the half-times of Eq. (10) vs. 1/T for In-Bi eutectic alloys.

16.4 μΩcm using Eq. (3), a slope value of m = 0.35 and a half time of 47.8 years will be obtained.

No adjustment to thermodynamic equilibrium was found at 77 K, the temperature of liquid nitrogen.

2. OFF-EUTECTIC ALLOYS

The eutectic material is distinguished from other binary alloys by having the lowest melting temperature. This fact is represented in the microstructure of these alloys. Whereas a eutectic structure contains only systematically alternating regions of the two solid phases, an off-eutectic structure contains additional islands of either α-phase or In_2Bi (Fig.16b,c). This structural difference may very well have an influence on the precipitation behavior of In_2Bi.

We have cooled various off-eutectic alloys, the thermal history of which is schematically shown in Fig. 19, from room temperature to 0 °C and followed the adjustment to the new equilibrium composition at 0 °C by resistivity measurements. The Avrami-type equation could again be applied to the data and the results are plotted in reduced coordinates in Fig. 20. It can be seen that the materials with different Bi-concentrations behave uniformly and that the slope value (m=0.43) seems to be independent of the bismuth concentration. The half-times are very much the same, the only exception being the alloy $In_{0.9}Bi_{0.1}$.

After this set of samples had been kept and data had been taken at 0 °C for five weeks, they were quenched into room temperature water of 24 °C and the change in resistivity was followed again as a function of time. The characteristic values for the slope m as well as the half-time $t_{1/2}$ are listed in Table 7. The data for a repeated cooling to 0 °C (3 weeks) with a subsequent quench to room temperature for a check of reproducibility are also contained in this table.

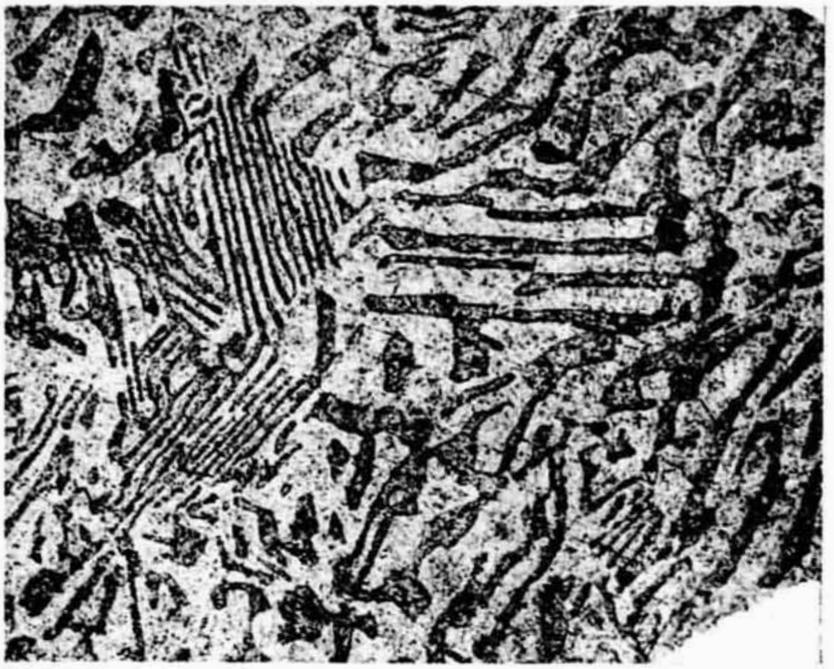

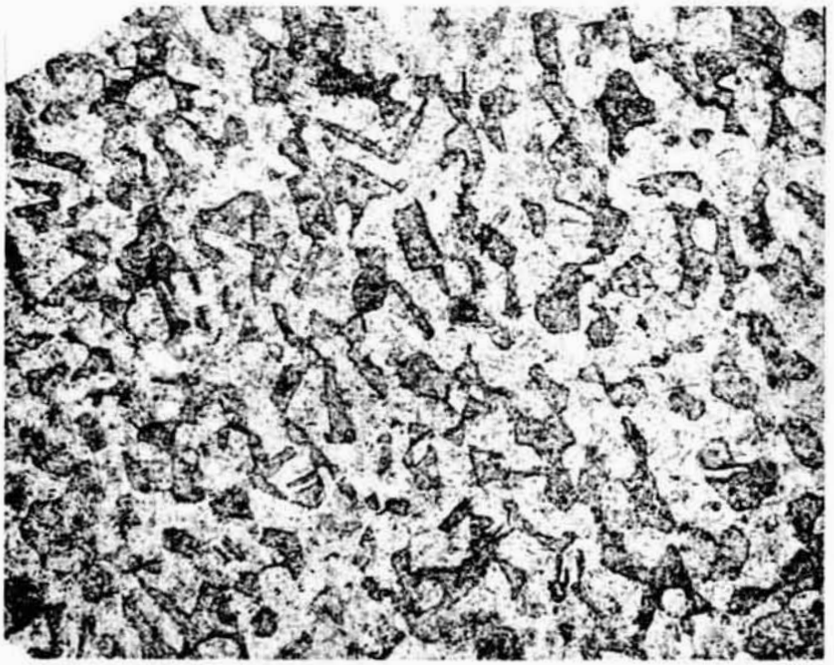

Fig. 16b,c. Microstructures of In-Bi alloys a) Eutectic composition. b) $In_{0.75}Bi_{0.25}$ (w.%) 250X.

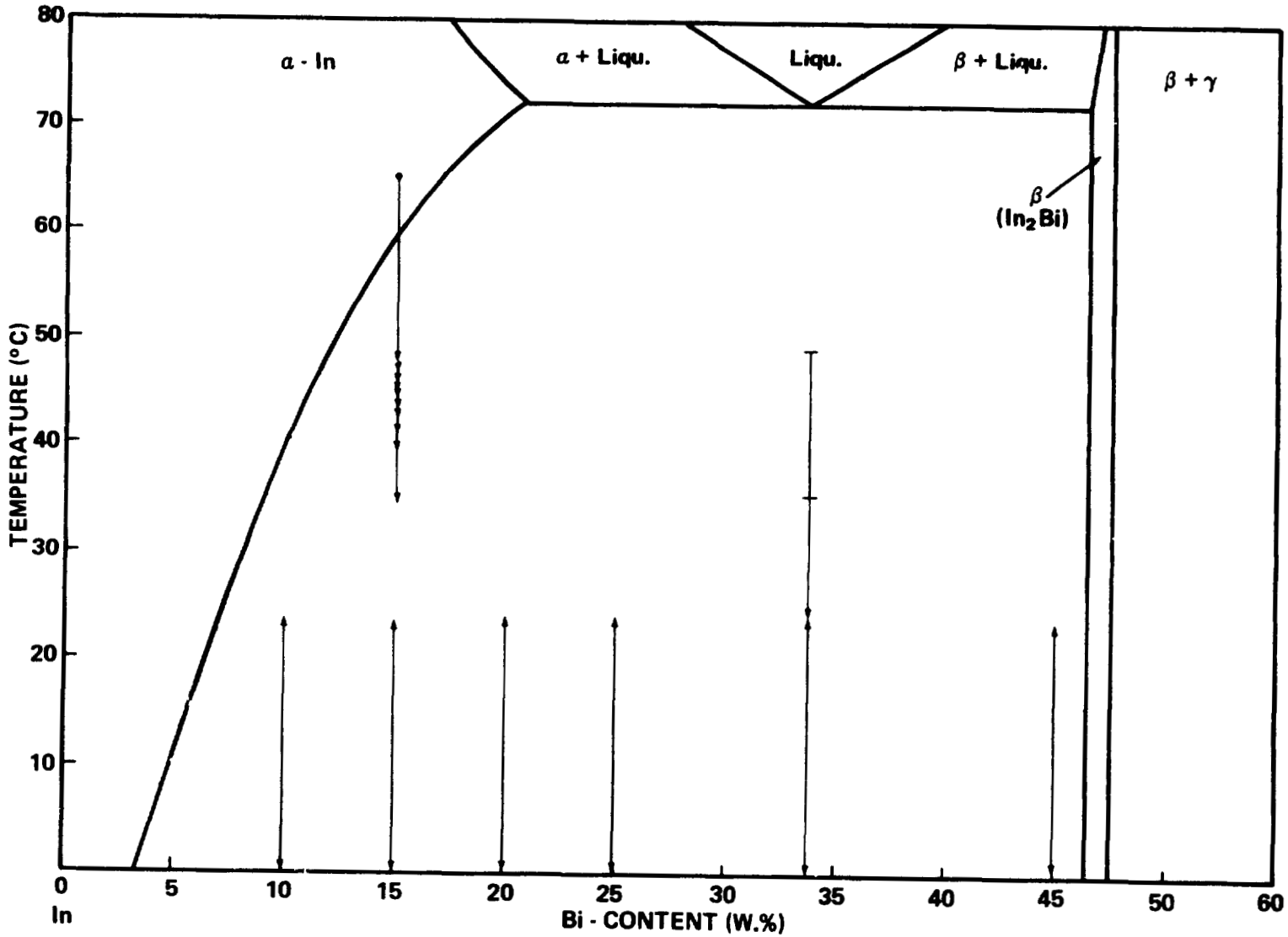

Fig. 19. Schematic drawing for the cooling and heating cycles performed on samples with various Bi concentrations of the subsystem In-In_2Bi.

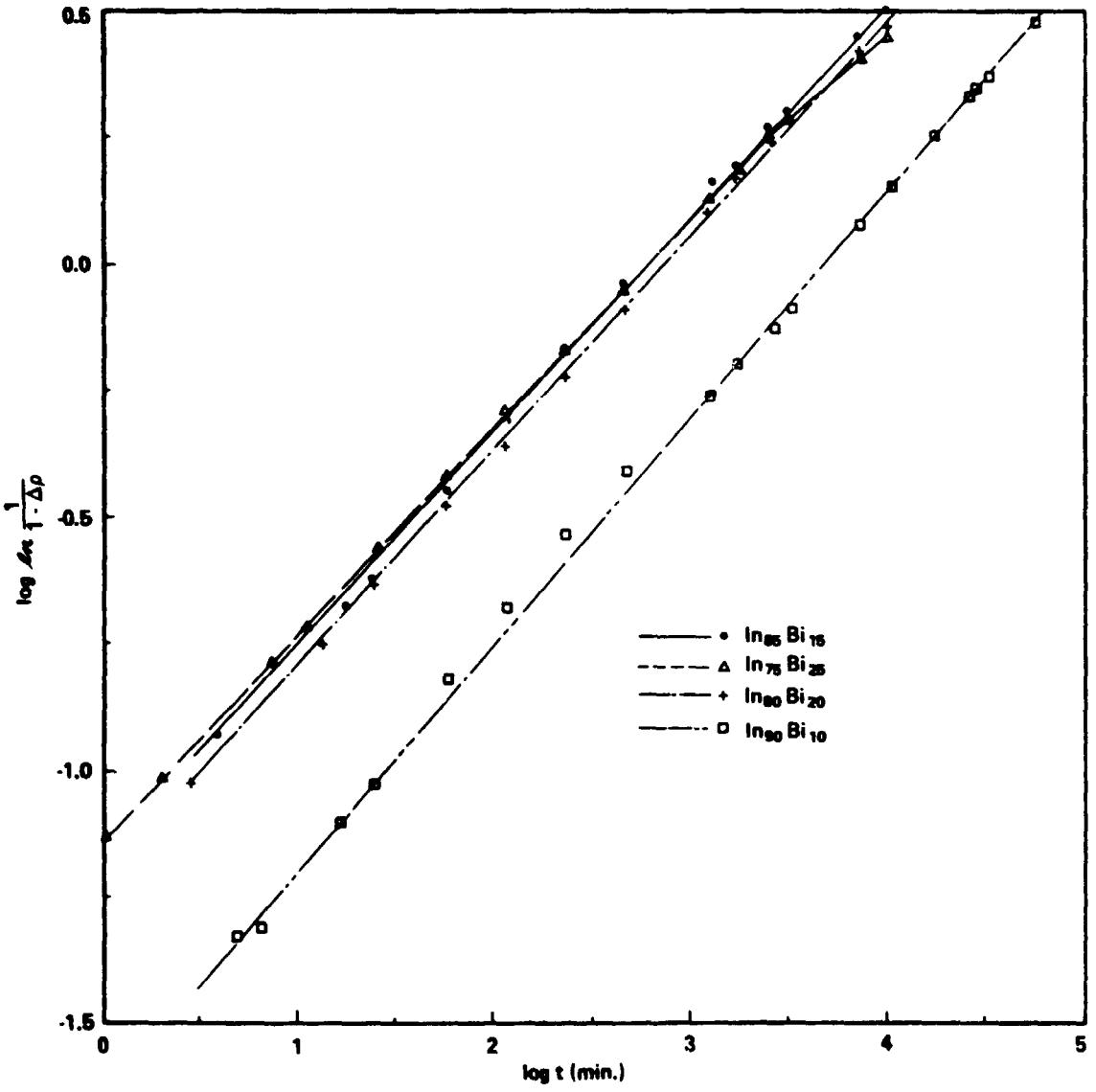

Fig. 20. Time dependence of the scaled resistivity for two-phase alloys of the In-In_2Bi subsystem, when quenched from room temperature to 0 °C.

TABLE 7

SLOPE VALUES, HALF-TIMES AND RESISTIVITIES OF TWO-PHASE ALLOYS, CYCLED BETWEEN 24 AND 0 °C

Sample Composition (W.%)	$In_{0.90}Bi_{0.10}$	$In_{0.85}Bi_{0.15}$	$In_{0.80}Bi_{0.20}$	$In_{0.75}Bi_{0.25}$	$In_{0.663}Bi_{0.337}$	$In_{0.55}Bi_{0.45}$
24 → 0 °C						
m	0.45	0.43	0.425	0.425	0.68	0.67
$t_{1/2}$ (min.)	2200	270	330	270	270	160
(μΩcm)	14.80	17.10	18.59	21.80	28.95	45.00
0 → 24 °C						
m	0.58	0.49	0.48	0.47	0.61	0.47
$t_{1/2}$ (min.)	200	71	46	50	40	28
(μΩcm)	18.15	20.76	22.48	26.20	33.68	49.15
24 → 0 °C						
m	0.51	0.46	0.44	0.47	0.53	contacts
$t_{1/2}$ (min.)	1300	400	280	330	500	defect
(μΩcm)	15.03	17.10	18.65	21.91	29.05	
0 → 24 °C						
m	0.58	0.52	0.59	0.57	0.59	0.54
$t_{1/2}$ (min.)	150	56	140?	25	40	20
(μΩcm)	18.10	20.68	22.2	25.85	33.50	49.59

From all the isothermal measurements, the following conclusions can be drawn:

1. The Avrami equation can be applied to the data up to at least $\Delta\rho = 95\%$. However, a deviation from linearity is noticed for eutectic samples. The reason for this behavior should lie in the different microstructure of the eutectic alloy.

2. The observed slope values of m range from 0.68 to 0.42. The slopes larger than 0.59 (3 cases) are always associated with eutectic or trans-eutectic ($In_{0.55}Bi_{0.45}$) materials. For off-eutectic compositions between 10 and 25 w.% Bi, the slopes are found between 0.59 and 0.42 (17 cases) with a probable dependence on temperature but not on Bi-concentration.

3. The reproducibility of the data is not too good as can be seen from Table 7 and is most likely caused by microstructural changes in the samples due to thermal cycling. There is only a fair reproducibility of ρ_∞. Since the precipitation and disappearance of In_2Bi is a dynamic effect, it may well be that the obtained results weakly depend on the thermal history of the material.

We have shown the feasibility of following the isothermal precipitation of In_2Bi from alloys by means of resistivity measurements. It is established that even at -78.5 °C the two-phase alloys are not in a "frozen" state. The precipitation proved to be a thermally activated process and the activation energy could be determined with those experiments. The precipitation of a phase always involves the process of nucleation and growth by diffusion. Since, in all cooling or heating experiments, the phase precipitating was already present in the microstructure of the alloy, the effect of nucleation seemed obviously less dominant than the mechanism of growth. It is known [28] that the time dependence of the resistivity can be used to draw conclusions about the geometry of the growing particles. However, since microscopic studies of the two phase structure of the alloys have not been undertaken, the discussion of this topic will be reviewed.

3. THE DECOMPOSITION OF SUPERSATURATED α-PHASE

The decomposition of supersaturated α-phase as an example for a solid state reaction is demonstrated on a sample containing 85 w.% In. According to the phase diagram, the α-phase for this composition is stable between 92 and 58 °C, and its temperature-dependent resistivity has already been discussed. Below 58 °C, the material decomposes in α-phase and In_2Bi. The sample used had a sligltly lower critical temperature of decomposition (52 °C).

We have quenched this sample from the single-phase region (65 °C) repeatedly to various temperatures below the solvus line into the two-phase region as indicated in Fig. 19. The precipitation of In_2Bi was monitored by resistivity measurements. Unlike the off-eutectic samples described earlier, this sample contained no second phase at the starting temperature and, therefore, the formation of critical size nuclei and their isothermal growth will be observed with the changing resistivity.

The measured voltage drop as a function of time for different decomposition temperatures is plotted in Fig. 21. It may be noticed that after a temperature-dependent induction (holding) period, the resistivity decreases faster than linear. The induction period exceeded 3 hrs. for the temperature of 47.0 and 47.9 °C. It is assumed that during this holding period, the nucleation of In_2Bi clusters occurs, whereas for higher values, the growth of the particles is reflected. The number of clusters (nuclei) formed per unit time increases with the temperature difference ΔT, the amount of supercooling.

It is indeed surprising that all the resistivity readings could again be fitted to the Avrami equation at least up to $\Delta\rho = 50\%$. The results are shown in Fig. 22. We can see from this graph that a ΔT of only 17.6 °C induces a very high reaction rate and causes that at 34.4 °C after only 1 min, 50% of the eventual change in resistivity has already occurred. It can be stated from these data that after 10 min, the sample is essentially (99%) in its equilibrium state. For even larger ΔT values, the reaction rate will eventually decrease again but we were not able, due to the thermal lag of the sample, to demonstrate this behavior. What cannot be seen from the plain data (Fig. 21) is the fact that the exponent m shows a strong dependence on the temperature difference ΔT. This temperature dependence of m is separately demonstrated in Fig. 23. It is very likely that the maximum value of the exponent at 44.9 °C may be associated with the locus of the spinodal curve for this binary system. The spinodal defines for any composition a temperature below which a quenched alloy will decompose by segregation without the necessity of thermal activation. Above this temperature, segregation requires an activation energy which should increase with the temperature, according to an hypothesis by Borelius [29].

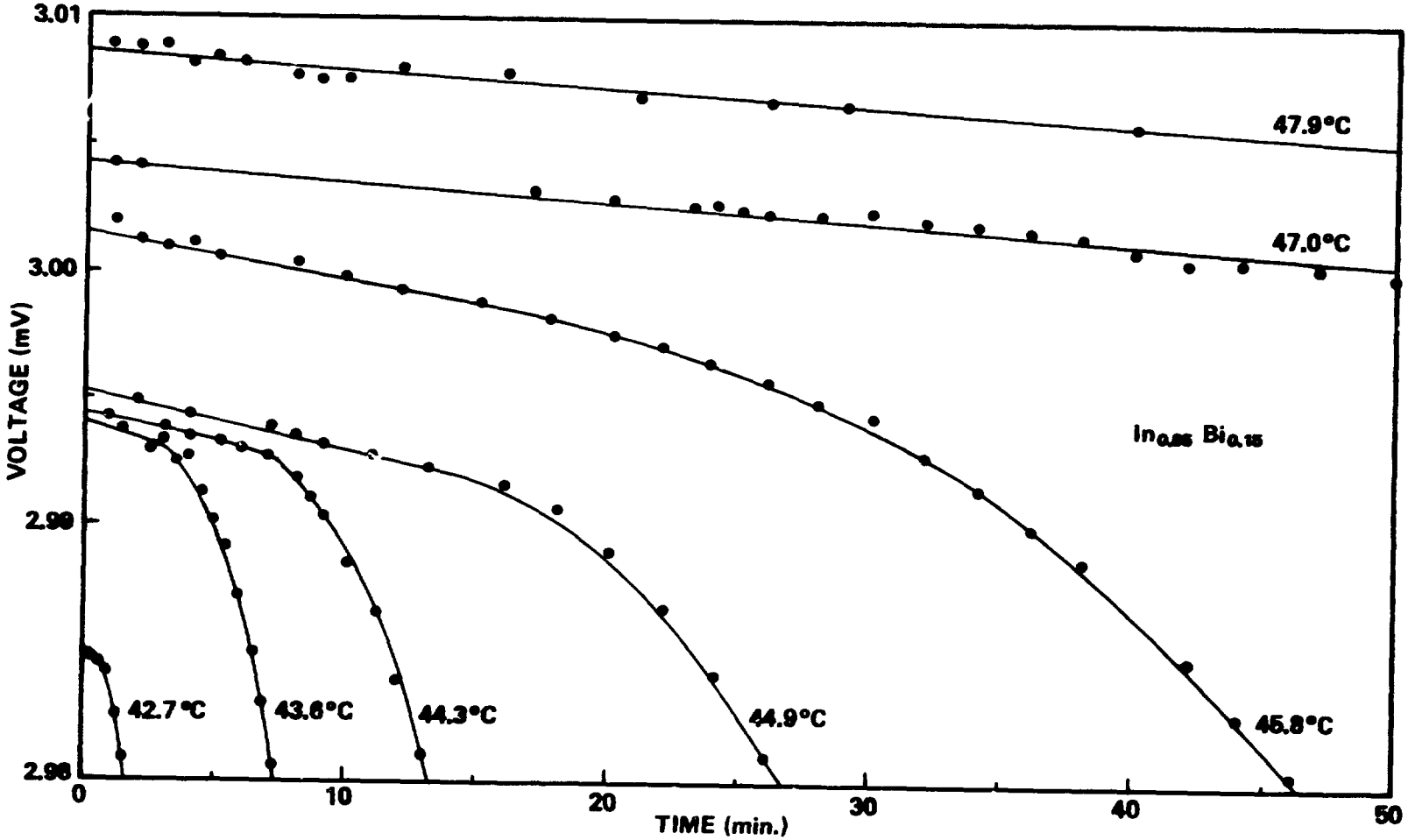

Fig. 21. The change of the voltage signal (resistance) with time after quenching of α-In from the single-phase region to various decompos. tion temperatures.

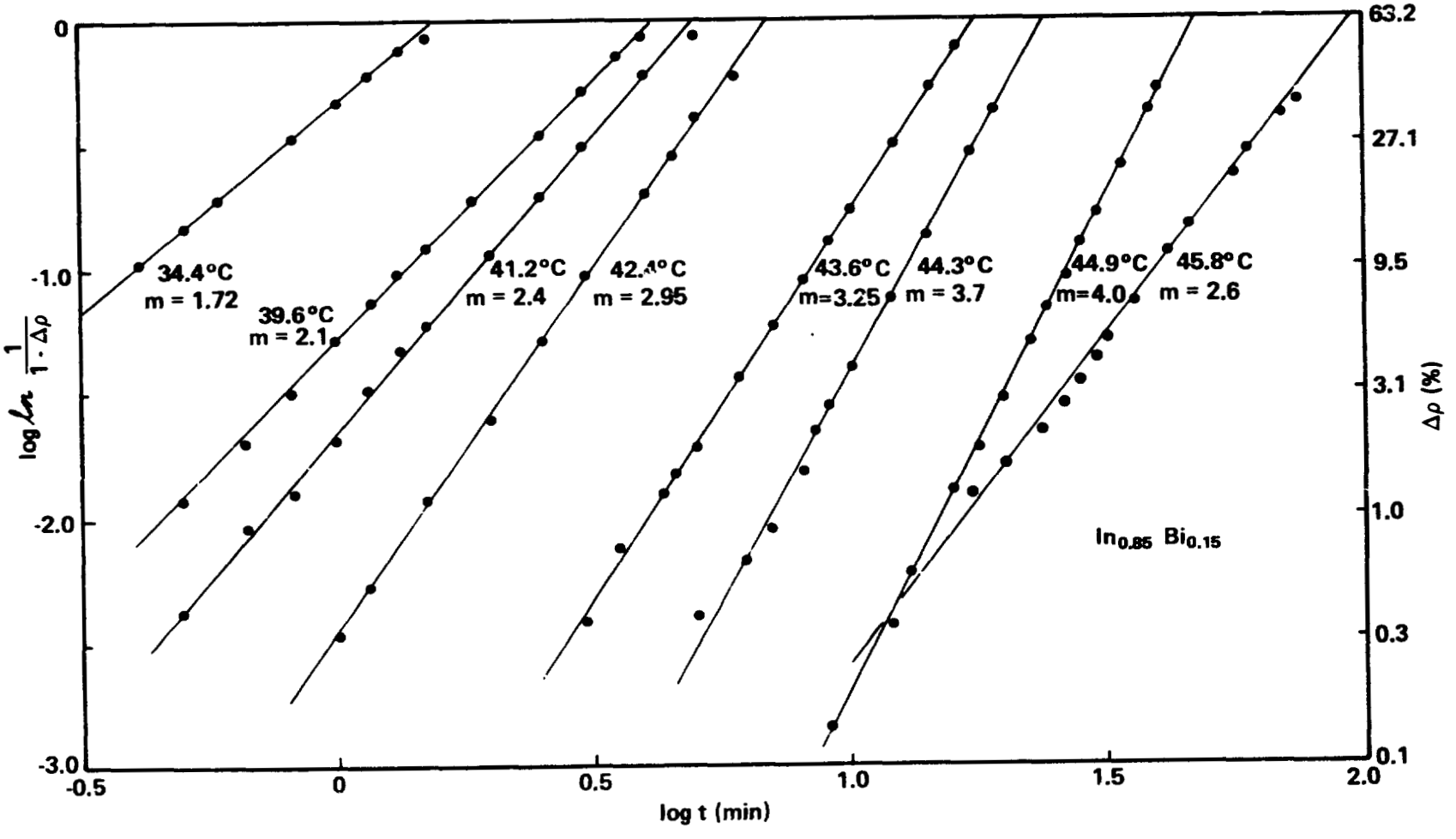

Fig. 22. The precipitation of In_2Bi from α-In at different temperatures shown by the time dependence of the scaled resistivity.

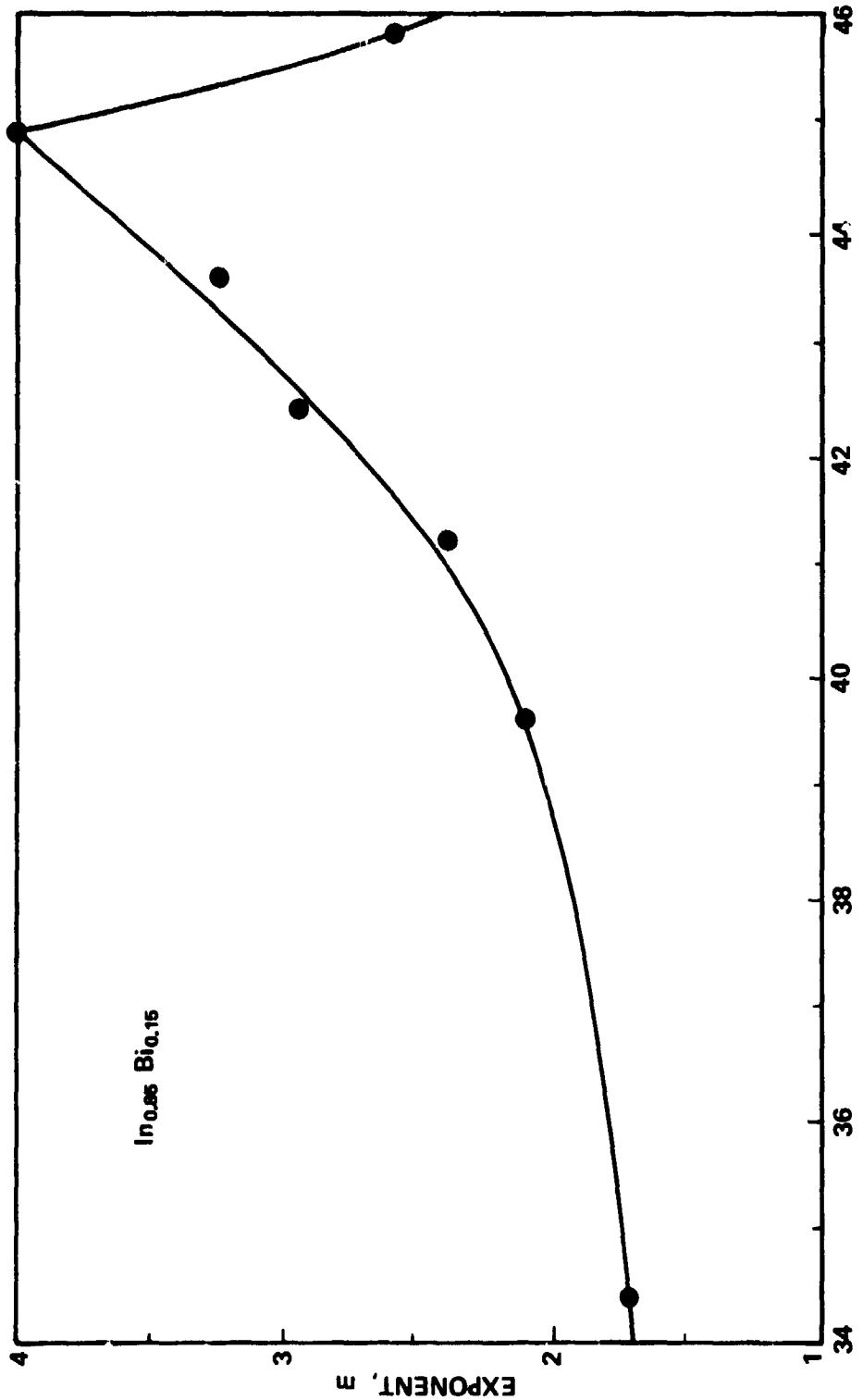

Fig. 23. Temperature dependence of the exponent m for the sample $In_{0.85}Bi_{0.15}$ (w.%).

In contrast to the results obtained for the two-phase alloys (eutectic and off-eutectic structures), the half-time for the α-phase decreases with the amount of supercooling ΔT as well as with temperature. Further investigation of this behavior is needed on samples with 5, 10, and 20 w.% Bi to integrate these results with existing nucleation and growth theories.

V. Superconducting Transition Temperatures of In-Bi Alloys

1. SINGLE-PHASE ALLOYS

The transition temperatures of various In-Bi alloys were measured in order to correlate the superconducting properties of the materials with their phase status and electrical behavior. This procedure is applicable because the single-phase materials are either superconductors with different transition temperatures (see Table 8) or nonsuperconductors down to 1.5 K, the lowest temperature obtainable by us.

TABLE 8

TRANSITION TEMPERATURES OF SINGLE-PHASE In-Bi ALLOYS

Composition	Midpoint of Transition (K)	Reference
In	3.41	E. A. Lynton [30]
	3.40	This investigation
In_2Bi	5.6	R. E. Jones [31]
	5.7	J. V. Hutcherson [32]
	5.46 - 5.76	This investigation
In_5Bi_3	4.1	J. V. Hutcherson [32]
	4.2	E. Cruceanu [33]
	4.2	This investigation
InBi	< 0.5	J. V. Hutcherson [32]
	< 1.5	This investigation
Bi	< 0.005	N. Kurti [34]

Using the a-c inductance technique [35] for measuring the superconducting transition, a single transition curve is obtained for a single-phase superconductor, with the change in inductance being proportional

to the volume of the superconducting material. The a-c inductance technique makes use of the Meissner effect where a superconductor expels magnetic flux from its interior by establishing superconducting eddy currents on its surface. If the sample is composed of two superconducting phases with different transition temperatures, two transitions are picked up, provided that the volume fraction of the higher T_c phase is small. If the portion of the phase with the higher transition temperature exceeds a certain critical value, superconducting surface currents in this phase can cover the whole sample and thus shield the transition of the second phase. The transition curve for such a sample then is like the one obtained on a single-phase material [36].

2. TWO-PHASE ALLOYS

Fig. 24 contains the measured transition temperatures of single and two-phase alloys with the phase boundaries taken from reference [8,9,10]. The bars indicate the onset and the end of the transition, whereas a circle marks its half point, called transition temperature T_c. There are concentration regions in which the T_c of the samples is either sensitively dependent or independent of the Bi concentration.

The transition temperature of α-In up to the solubility limit of 7.1 w.% at room temperature increases nearly linearly with the amount of Bi dissolved. It should be noted, however, that Chanin et al. [36] reported an initial drop in T_c of 16mK for very small Bi impurities up to 0.5 w.% before the transition temperature shows the increasing trend. This behavior can be explained with the valency effect [37,38] and will be discussed later.

Samples containing more than 7.1 and less than 46.5 w.% Bi are two-phase and composed of α-In and In_2Bi. Due to the higher T_c of In_2Bi compared with that of the saturated α-phase, the appearance of In_2Bi can be monitored by measuring the transition temperature of alloys with increasing Bi concentration. This fact is demonstrated on the material $In_{0.9}Bi_{0.1}$ (w.%) which is composed mostly of α-In (92 Vol.%) and a smaller amount of In_2Bi (8 Vol.%). As expected, the transition is clearly split up into the transition

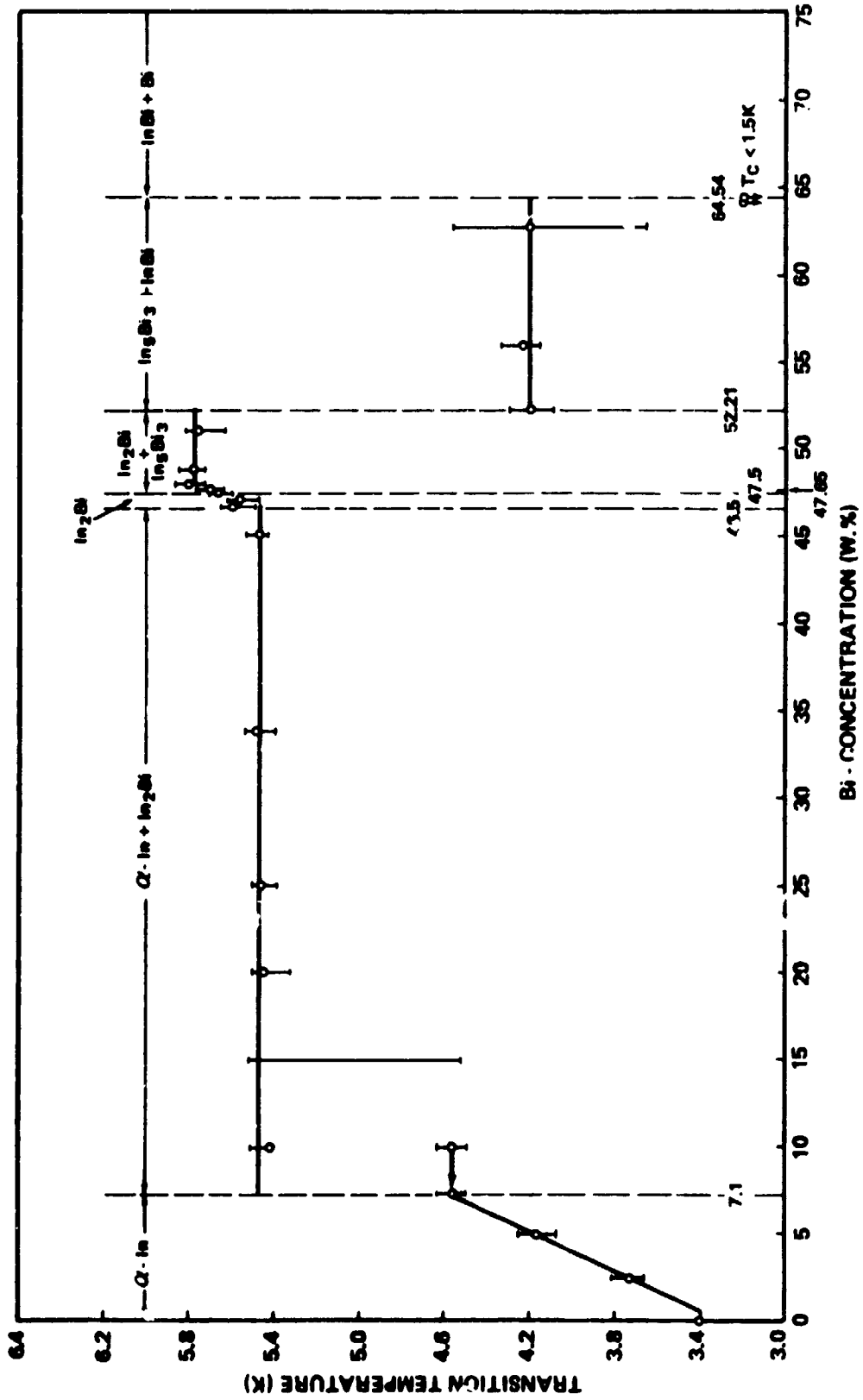

Fig. 24. The superconducting transition temperatures of In-Bi alloys and compounds.

for In_2Bi at 5.41 K and α-In occurring at 4.56 K, according to Fig. 25. The portion of the measured transition due to In_2Bi is approximately 10%. The same effect is true for the material $In_{0.85}Bi_{0.15}$ (w.%) containing 20 vol.% In_2Bi. For the 15 w.% Bi case, the transition to superconductivity is extended over the same temperature range, and the two transitions are no longer clearly resolved as indicated by the larger bar of Fig. 24. The T_c only of In_2Bi is observed on the sample $In_{0.8}Bi_{0.2}$ (w.%), although the alloy still contains both phases. The In_2Bi phase which constitutes approximately 35 vol.% of the alloy now obvicusly forms a continuous surface layer and is able to shield the transition of the α-phase which would occur at 4.56 K. Now, regardless of composition up to a Bi-concentration of 46.5 w.%, all samples exhibit the transition of the In_2Bi phase only. As can be taken from Fig. 24, the T_c of In_2Bi as part of the two-phase alloy is 5.45 ± 0.05 K, the uncertainty being caused by the limited temperature stability. The T_c of the α-phase, if not shielded by eddy currents would be accordingly constant at 4.56 K.

Peretti and Carapella [9] have determined the homogeneity range for the intermetallic compound In_2Bi to lie between 46.5 and 47.5 w.% Bi. This region of single-phase status does not, however, include the stoichiometric composition which would occur at 47.65 w.% Bi. We have cast five samples in the concentration range from 46.6 to 47.9 w.% Bi with a 0.4 w.% increment and measured their transition temperature. The T_c values for these alloys increases with increasing Bi content and reaches its maximum of 5.8 K at 47.9 w.% Bi. This 0.3 K increase in T_c is most likely due to improved atomic ordering in the compound, with the stoichiometric composition having the maximum T_c. The effect of ordering at the stoichiometric composition has been observed and investigated on many compounds. We have not checked the order parameter in our materials nor their homogeneity or phase status; however, the T_c measurements can only be explained when the homogeneity range of the In_2Bi phase is extended. No further investigations concerning this problem have been made.

According to the phase diagram, alloys in the concentration range between 47.65 and 52.21 w.% Bi have again a two-phase status with In_2Bi and the line compound In_5Bi_3 in coexistence. This fact necessitates

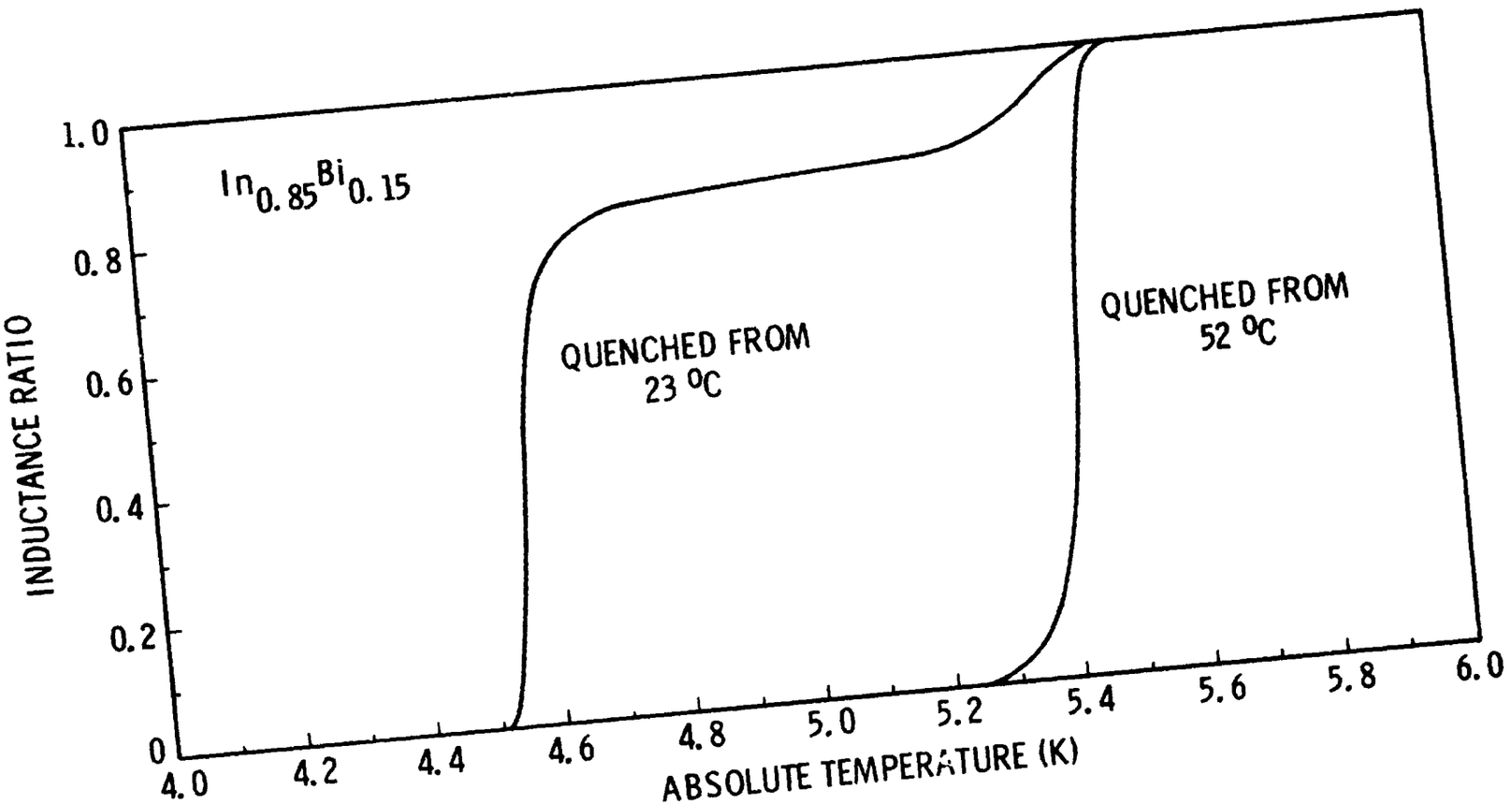

Fig. 25. Superconducting transition curves for $In_{0.85}Bi_{0.5}$ (w.%) when quenched from different temperatures and phase conditions.

that, in such samples, two transitions should be observed. Since the effect of shielding occurs again, the higher T_c of only In_2Bi is measured (Fig. 24).

In the concentration range between 52.25 and 64.54 w.% Bi, the compounds In_5Bi_3 and InBi coexist. Whereas, the compound In_5Bi_3 is a superconductor with a T_c of 4.2 K (Fig. 24), the compound InBi is not a superconductor down to 1.5 K [4]. Alloys in this concentration region show, accordingly, only one transition at 4.2 K with the inductance signal being proportional to the amount of In_5Bi_3 phase present in the alloy. The sample with the stoichiometric composition In_5Bi_3 became superconducting at 4.2 K and did not show any indication of superconductivity at 5.8 K which would have indicated the presence of a small amount of In_2Bi phase. On the other hand, a sample with 64.08 w.% Bi whose composition is very close to InBi, showed no superconductivity down to 1.5 K, indicating that InBi is not a line compound as published in the phase diagram but has at least a homogeneity range of 0.5 w.%. No compounds other than InBi and the element bismuth itself occur at ambient pressure in the concentration range from 64.54 to 100 w.% Bi. A superconducting transition for InBi, if it should be found, would occur at less than 0.5 K [32].

The semimetal Bi, with the rhombohedral structure, is a rather poor conductor which is not superconducting down to 0.005 K [34]. However, several modifications of Bi under hydrostatic pressure are known to have a pronounced metallic character and exhibit superconducting behavior [39]. Abrupt changes in the superconducting transition temperature occur for Bi at 25.2 kbar (T_c = 3.9 K), at 27.0 kbar (T_c = 7.25 K), and at 80 kbar (T_c = 8.3 K). These variations in the critical temperature appear to correspond to rearrangements in the electronic structure of the crystal at the phase transition. Determination of this structure has not yet been successful [12].

3. THE TRANSITION TEMPERATURE OF METASTABLE α-PHASE

The solubility limit for α-In at room temperature is 7.1 w.% Bi as stated in the previous section, whereas, at 72 °C, a maximum of 20.5 w.% Bi can be randomly dissolved in the In lattice [9]. α-In with 20.5 w.% Bi is metastable below 72 °C and we were able to retain a certain amount of this metastable phase by quenching small pieces of material (approximately 0.5 g) in liquid nitrogen. Prior to the quenching, the material was annealed and homogenized for several hours at 72 °C.

The transition temperatures for both the stable and metastable α-phase, up to 20 w.% Bi, are shown in Fig. 26. The increase of the T_c values with Bi concentration proceeds smoothly between the stable and metastable samples. In addition, the following observations should be noted.

The sample containing 10 w.% Bi in its equilibrium state at room temperature showed two transitions, whereas, in the quenched state, it had only one transition with a halfpoint at 4.86 K. The superconductivity measurements exclude the presence of In_2Bi phase (with a portion of more than 0.2 vol.%) and, therefore, that quenched sample appears to be single phase.

The sample containing 15 w.% Bi in its quenched state became superconducting at 5.43 K with only a single transition observable. So far, the t_c value does not exclude the formation of In_2Bi (T_c 5.46 K) during the quenching process. However, the transition width in the quenched alloy when compared with the equilibrium sample was reduced considerably and it can be concluded that it is the T_c of the α-phase which was increased to 5.34 K.

Two transitions were observed in the quenched sample of the composition $In_{0.8}Bi_{0.2}$ (w.%). The first transition occurred at 5.76 K where 10% of the material became superconducting and the main transition was found at 5.44 K, caused by the superconductivity of In_2Bi. This sample was annealed for 20 hrs at room temperature and when remeasured, the transition at 5.76 K had disappeared.

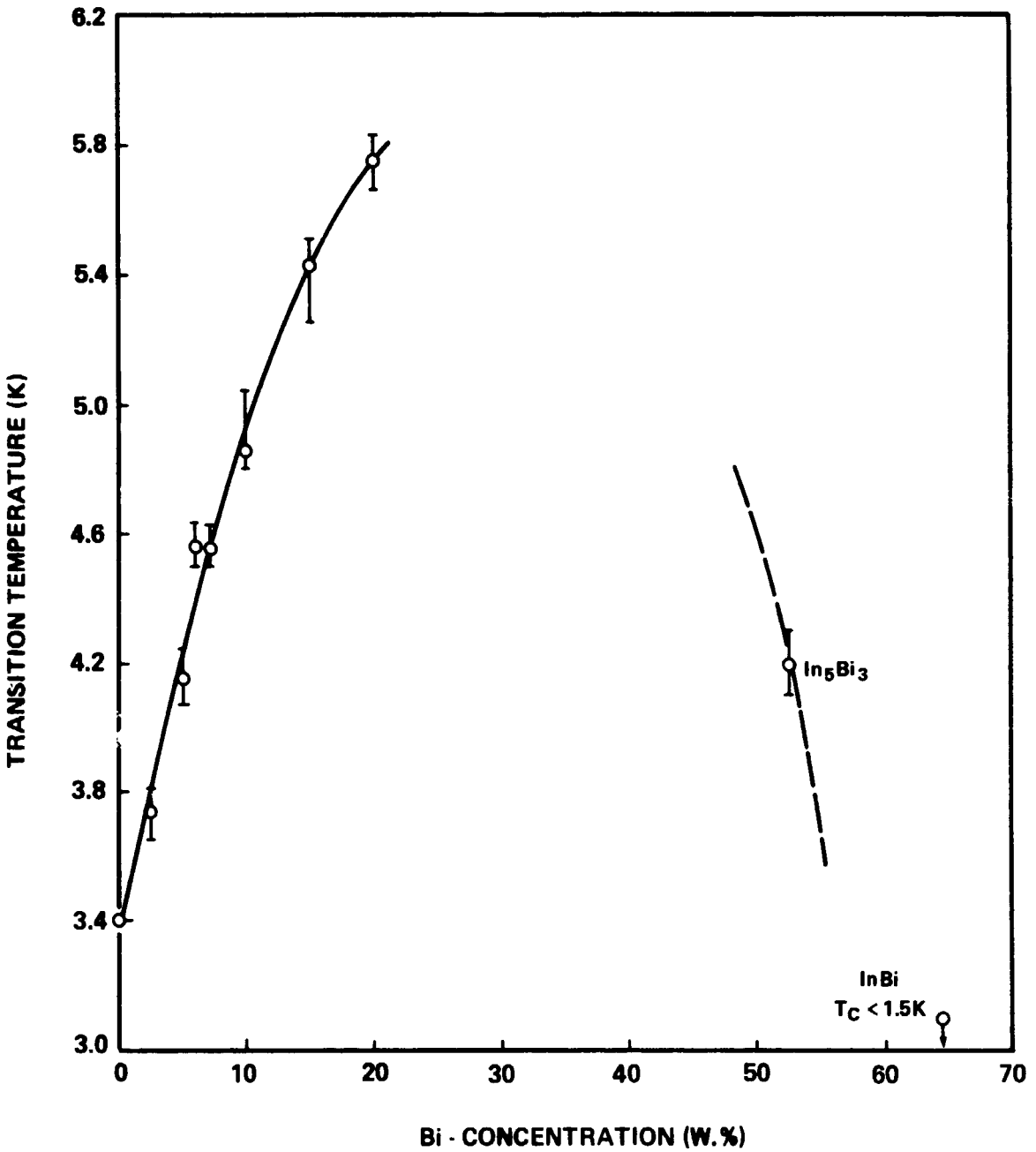

Fig. 16. The transition temperature for stable and metastable α-In phase. The value for the isostructural compound In_5Bi_3 has been included and a dashed curve with the corresponding slope has been drawn through the data point.

More than 20.5 w.% Bi cannot be dissolved in the face-centered tetragonal lattice of indium without the structure becoming instable. However, it is expected, according to Fig. 26, that the transition temperature of these samples would increase further if, by some means, the solubility could be increased further. Also, plotted in Fig.26 is the transition temperature of the isostructural compound In_5Bi_3. We have stated earlier, on the basis of resistivity measurements, that In_5Bi_3 seems to be a stablized combination of the α-phase. We have, therefore, drawn a curve with the same slope through this data point as it is evident on the rising side of the curve. With this premise, it is reasonable to assume that the α-phase with 30 w.% Bi would have a maximum transition temperature if it could be synthesized.

We will now discuss the variation of the transition temperature of the α-phase with increasing bismuth concentration using the theory of Markowitz and Kadanoff [40]. According to their considerations, the change in transition temperature, caused by a nonmagnetic solute, is the sum of two terms, the mean-free path effect and the valence effect. As an impurity is added to the pure element in the concentrations of a few tenths of an atomic percent, the mean-free path of the electrons is shortened and the transition temperature of the material is simultaneously lowered. When the normal state electronic mean-free path is reduced to a value somewhat smaller than the superconducting coherence length in the pure element, the valence effect becomes dominant. The valence effect depends on the valence difference of the solvent in relation to the solute, and on the mean-free path reduction. Whereas the shortening of the mean-free path always results in a decrease in T_c, the valence effect can have either sign and is the most difficult to represent in a simple formalism.

The change in T_c can be fit in a number of solid solutions based on Sn, Al, and In [37, 38] with an expression of the form

$$\Delta T_c = k_1 x + k_2 x \ln x \qquad (10)$$

where x is the atomic concentration of the solute and k_1 and k_2 are material dependent constants. In this equation, the second term describes the mean-free-path effect, whereas, both mean-free-path and valence effects are contained in k_1 of the first term. For sufficiently small x, the second term should dominate.

A plot of $\Delta T_c/x$ versus $\ln x$, as undertaken in Fig. 27, should yield a straight line when above considerations are applicable to the α-In phase. For small Bi concentrations up to 1.4 at.% (25 w.%) and using mostly the data of Ref. [37,41], the observed increase in transition temperature is in accordance with Eq. (10). However, a marked deviation from the linearity occurs for Bi concentrations higher than 1.4 at.%, and the measured increase of T_c is smaller than the theoretically expected value. The deviation from Eq.(10) may be caused by several additional effects. For example, at high Bi concentrations, the impurity atoms do not act independently of each other and their contribution to T_c is no longer a simple additive effect. Another influence may be that the average velocity of the electrons at the Fermi surface changes stronger by alloying than is accounted for in the reduction of the mean-free path [42].

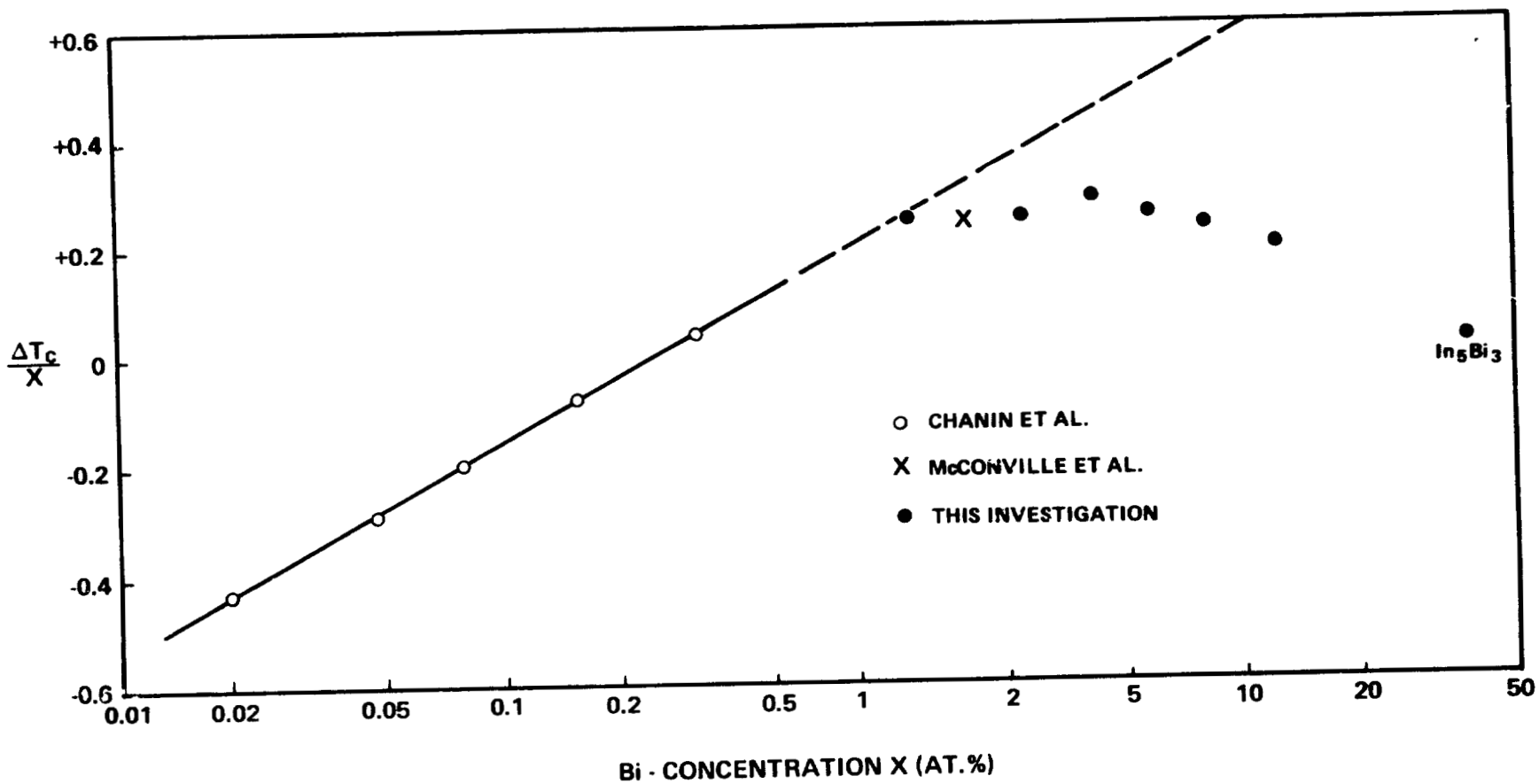

Fig. 27. The reduced transition temperatures for α-In and isostructural In_5Bi_3.

VI. REFERENCES

1. I. C. Yates: "Apollo 14 Composite Casting Demonstration." Interim Report, NASA-MSFC S&E-PT-IN-71-1, July 1971.

2. I. C. Yates: "Apollo 14 Composite Casting Demonstration." Final Report, NASA TM X-64641, October 1971.

3. G. H. Otto: "Time Dependent Resistivity of In-Bi Eutectic Alloy," Bull. Am. Phys. Soc., Series II, 18, 253 (1973).

4. This investigation.

5. "Handbook for Applied Engineering Science," 1st Edition. The Chemical Rubber Co., Cleveland, Ohio, 1970.

6. D. Hardin: Thesis, The University of Alabama in Huntsville. In preparation.

7. V. N. Lutskii: Phys. Stat. Sol. (a) 1, 199 (1970).
   L. I. Maissel: "Handbook of Thin Film Technology," McGraw-Hill, New York, 1970, p. 13-1.

8. O. H. Henry and E. L. Badwick: Trans. AIME 171, 389 (1947).

9. E. A. Peretti and S. C. Carapella: Trans. Am. Soc. Metals 41, 947 (1949).

10. B. C. Giessen, M. Morris, and N. J. Grant: Trans. Met. Soc. AIME 239, 883 (1967).

11. W. P. Binnie: Acta Cryst. 9, 686 (1956).

12. D. E. Gordon and B. C. Deaton: Phys. Rev. B6, 2982 (1972).

13. V. N. Laukhin, V. K. Matyushchenkov, and A. G. Rabin'kin: Sov. Phys. Solid State 16, 183 (1974).

14. G. H. Otto: J. of Less-Common Metals, to be published.

15. G. H. Otto, U. Roy and O. Y. Reece: J. of Less-Common Metals 32, 355 (1973).

16. E. Grüneissen: Ann. der Physik 16, 530 (1933)

17. See for example: C. Kittel: "Introduction to Solid State Physics," 3rd Ed. J. Wiley & Sons, New York, 1966.

18. A. N. Gerritsen: "Handbuch der Physik," Springer-Verlag, Berlin 1956, Vol. XIX, p. 170.

19. G. Grüneissen: "Handbuch der Physik," Springer-Verlag, Berlin 1928, Vol. XIII, p. 13.

20. "Handbook of Chemistry and Physics," The Chemical Rubber Publ. Co., Cleveland, Ohio, 42nd ed. 1961.

21. N. F. Mott: Proc. Roy. Soc. A153, 699 (1936).

22. J. Bardeen: J. of Appl. Physics 11, 88 (1940).

23. N. N. Sirota in "Semiconductors and Semimetals" (R. K. Willardson and A. C. Beer, eds.), Academic Press, New York, 1968, p. 127.

24. G. H. Otto: J. Ala. Acad. of Sciences 44, 200 (1973).

25. A. H. Wilson: "The Theory of Metals," 2nd ed., Cambridge University Press, New York, 1965.

26. L. Nordheim: Ann. Phys., Lpz. 9, 607 (1931).

27. L. M. Rose, L. A. Shepard, and J. Wulf, "Electronic Properties," John Wiley and Sons, New York, 1966, Vol. 4, p. 87.

28. M. Avrami: J. Chem. Phys. 7, 1103 (1940). See also J. W. Christian: "The Theory of Transformations in Metals and Alloys,: Pergamon Press, Oxford, 1965, p. 471.

29. G. Borelius: "Defects in Crystalline Solids," Physical Society, London, 1954.

30. E. A. Lynton and D. McLachlan, Phys. Rev. 126, 40 (1962).

31. R. E. Jones and W. B. Ittner, Phys. Rev. 113, 1520 (1959).

32. J. V. Hutcherson, R. L. Guay, and J. S. Herold, J. Less-Common Metals 11, 296 (1966).

33. E. Cruceanu, E. Hering, and H. Schwarz, Phys. Letters 32A, 295 (1970).

34. N. Kurti and F. Simon, Proc. Roy. Soc. 151, 6 (1935).

35. M. F. Merriam, Phys. Rev. 144, 300 (1966).

36. M. F. Merriam, J. Hagen, and H. L. Luo, Phys. Rev. 154, 424 (1967).

37. G. Chanin, E. A. Lynton, and B. Serin Phys. Rev. 114, 719 (1959).

38. D. Seraphim, C. Chiou and D. Quinn, Acta Met. 9, 861 (1961).

39. N. B. Brandt and N. I. Ginzburg, Scientific American 224, 83, April 1971 and Soviet Physics USPEKHI, 8, 202 (1965).

40. D. Markowitz and L. P. Kadanoff, Phys. Rev. 131, 563 (1963).

41. T. McConville and B. Serin, Phys. Rev. Lett. 13, 365 (1964).

42. T. Kinsel, E. A. Lynton, and B. Serin, Phys. Lett. 3, 30 (1962).

APPENDICES

APPENDIX A

THE DENSITY OF INDIUM-BISMUTH ALLOYS*

Guenther H. Otto
The University of Alabama in Huntsville, Physics Department
Huntsville, Alabama 35807 (U.S.A.)

ABSTRACT

The density of various In-Bi alloys at room temperature was measured by the buoyancy technique. With increasing Bi-concentration in the alloys, the density increases smoothly between the values for the terminal elements In and Bi. No maxima occur at any of the compositions which correspond to the intermetallic compounds In_2Bi, In_5Bi_3 and InBi. For InBi, which is metallic in contrast to other semiconducting III-V compounds, a relative decrease in specific volume by 2.9% is found. The experimental density data for Bi-concentrations up to 50 at.% may be expressed in an additive fashion by attributing a mean atomic volume of 33.8 $\mathring{A}^3$ to the bismuth atom instead of the conventional value of 35.4 $\mathring{A}^3$. The bismuth atom, therefore, acts in the alloys with a density it would have at room temperature in its supercooled liquid state.

*Work supported by NASA Contract NAS8-27809 with Marshall Space Flight Center.

Paper submitted for publication in the Journal of the Less-Common Metals.

INTRODUCTION

The density as a macroscopic property of materials is essentially determined by atomic parameters such as crystal structure, lattice spacing and atomic mass. In a binary alloy system with continuous solid solubility, the density changes smoothly with the amount of the second component (Vegard's rule); however, this behavior is no longer necessarily the case when the formation of a compound occurs [1]. The rearrangement of the atoms in a different structure and the correlated change of the electronic bonds results in a volume expansion or contraction relative to the constituents. Whereas the fomation of compounds between transition and non-transition elements normally results in a volume decrease, the semiconducting III-V compounds like InP, InAs, InSb are characterized by large increases in volume [2]. As a rule, there exists a distinct proportionality between the decrease in interatomic distances, the change of specific volume and the heats of reaction in compound formation [1,3]. The use of ΔV data to derive changes in entropy and enthalpy in liquid alloy systems has been demonstrated by Predel and Eman [3].

We have investigated the behavior of the density in the In-Bi alloy system which contains several stable and metastable phases [4,5]. Constitution diagram [4,5,6] and crystal structures [7,8,9] have been investigated by several authors so that we are able to exactly correlate the experimental densities with the phase status of the alloy. Of special interest was the III-V compound InBi because it is not a semiconductor and exhibits metallic character [10]. The density of liquid In-Bi alloys has been investigated recently [3,11] and a volume increase upon alloying has been reported. This volume expansion is exactly the trend one would expect for a semiconducting alloy system.

Sample Preparation and Measuring Techniques

Polycrystalline samples of various compositions $In_{1-x}Bi_x$ were prepared from high purity (99.999%) indium and bismuth pellets. The corresponding compositions were weighed and the material was melted in a pyrex beaker under silicone oil on a hot plate. Ingots were cast in a cylindrically-shaped split graphite mold and afterwards sectioned into two or three pieces with a mass of approximately 3 grams each. The density of the sections at 24 °C was determined by the buoyancy technique using distilled water. Corrections were applied for the weight of the mounting wire and for the temperature dependent density of the distilled water. The density of two sample halves never differed by more than 0.3%. Such an error can be attributed to inhomogeneities in the material and to micro-voids rather than to the accuracy (0.1%) of the density determination itself.

Debye-Scherrer X-ray data were taken from selected single phase alloys in order to compare the experimental densities with those obtained from the dimensions of the unit cell. Samples consisting of two phases were annealed at room temperature for several months and could be considered to be in structural equilibrium. This fact had been verified by measuring the time dependence of the electrical resistivity on specially prepared wires [12]. The density measurements are part of a broader effort to characterize multiphase materials by their electric and superconducting properties and are described elsewhere [13].

Results and Discussion

The average value of the densities obtained from the two halves of a sample are plotted in Figure 1 as a function of the bismuth concentration up to 50 at.%. It can be seen that the density of the alloys increases smoothly with the Bi-content and that the occurrence of the intermetallic compounds In_2Bi, In_5Bi_3, and InBi apparently does not influence this behavior within the accuracy of the measurements. In order to increase the sensitivity of the scale in Fig. 1, the data for the following samples with high Bi concentrations have been omitted: $In_{0.6}Bi_{0.4}$, $In_{0.1}Bi_{0.9}$, and Bi, whose densities are: 9.18, 9.65, and 9.80 g/cm^3, respectively. With the exception of Bi, these samples are two-phase, consisting of InBi and Bi in corresponding proportions.

Since five single phase regions occur in the alloying system, the experimentally obtained densities of these materials may be compared with the density calculated from X-ray data of the unit cell. The results of this computation using lattice parameters from our own measurements and various other sources are given in Table 1. The agreement of the densities in all cases is excellent and nowhere deviates by more than 0.6%. It also reflects the expected low concentration of vacancies in these alloys [14].

The change in the specific volume upon compound formation can be calculated from the experimental densities as [3]

$$\Delta V = V_a - \Sigma V_i \qquad (1)$$

where V_a and V_i are the specific volume of the alloy and of each of the components respectively. ΔV values obtained from X-ray data of single phase materials are also listed in Table 1. It may be noted that for all three compounds which are stable at room temperature, a volume contraction upon alloying is observed. The change in specific volume is largest for InBi with -0.54 cm^3/g-atom or equivalent to a shrinkage of 2.9%.

The change in specific volume for the single and multiphase alloys is given in Fig. 2. Irregardless of the phase status of the alloy, ΔV seems to decrease proportionally to the Bi concentration up to 50 at.% Bi. The small deviations of the experimental data from linearity in the two-phase region In_5Bi_3 - InBi are probably caused by microcracks in the samples which develop upon thermal cycling of InBi. Some samples had been cooled to 4.2 K at least once for superconductivity measurements prior to the density determination. It has been shown by Lal et al. [20] that the thermal expansion coefficient of InBi single crystals is highly anisotropic and that irreversible changes in morphology can occur by thermal cycling. For this reason, it seems adequate that the X-ray density of 8.99 g/cm^3 is a reliable value [17] for InBi.

Also shown in Fig. 2 are the ΔV values for liquid In-Bi alloys at 300 °C taken from reference [11]. The volume expansion upon alloying is contrary to the solid alloys and indicates a tendency for repulsive forces in the liquid state. This volume expansion of the liquid alloys which is also observed for the systems In-Pb, In-Zn and Pb-Zn is attributed to an excess in entropy and enthalpy upon mixing [11].

The obvious proportionality of ΔV with the Bi concentration in solid alloys may lead to the conclusion that the Bi atom in the alloys acts with a constant specific volume which is different from that in its elemental form. A mean atomic volume of In and Bi for the compounds can be calculated from the specific volumes. Applying the same procedure to the two-phase alloys, a pseudo-atomic volume is obtained. The mean atomic volumes thus computed for all alloys are plotted in Fig. 3 as a function of the Bi concentration. It can be seen that up to a concentration of 50 at.%, the mean atomic volume increases linearly for single-phase and two-phase alloys. At 50 at.%, the line shows a distinct break. Extrapolating the data to pure bismuth leads to a mean atomic volume of 33.8 Å^3 which corresponds to a density of 10.27 g/cm^3. This density, however, is by 4.8% larger than the density of elemental Bi which has a mean atomic volume of 35.4 Å^3. Could it be possible that the Bi acts in the alloys as if it were associated with a different phase?

Bismuth is known to exhibit several high-pressure modifications [21,24] whose crystal structures are of controversial nature [21,22,23]. It is also found that these Bi modifications are metallic and become superconducting at 3.9 K, 7.1 K, and 8.3 K for BiII, BiIII, and BiV, respectively [21]. The first modification of BiI/BiII occurs at 25.6 kbar. If BiII were to be stable at room temperature and ambient pressure, it should have a density of 10.86 g/cm^3 when using the data of Bridgman [24] for extrapolation. This value is rather high for our considerations.

However, BiI expands upon freezing and has a 3.3% higher density in its liquid state at the melting temperature. Extrapolating the density of liquid Bi to room temperature in a linear fashion using the data of Predel and Emam [11] results in a value of 10.35 g/cm^3 for supercooled Bi at 20 °C. This value corresponds to a mean atomic volume of 33.53 $Å^3$ which compares rather favorably with the density in which Bi acts in the alloys. We can, therefore, hypothesize that the Bi is associated in solid In-Bi alloys with a mean atomic volume which is rather close to that for liquid Bi. Since the influence of bismuth on the total density of the alloys is purely additive regardless of compound formation, the densities of In-Bi alloys up to 50 at.% may be expressed by the relationship

$$\rho = (1-f)\,\rho(In) + f\rho(Bi) \qquad (2)$$

where f is the volume fraction of bismuth in the alloy. Again, a value for $\rho(Bi) = 10.27\ g/cm^3$ has to be chosen in order to fit the data. As can be shown, Eq. (2) gives the experimental densities with an error of less than 0.5%. Above a concentration of 50 at.%, in the two-phase region InBi-Bi, the elemental bismuth acts with a density of 9.80 g/cm^3. The high pressure In-Bi phase which was shown (22,23) to exist in the concentration range between 55 and 80 at.% Bi under a hydrostatic pressure of 25 kbar would probably also be located on the extrapolated line of Fig. 3 when it were stable at ambient pressure.

It is of interest to investigate with which atomic volume the Bi is represented in other binary alloy systems with non-transition elements. If this were a general behavior, systems with the occurrence of solid solutions or compounds should extrapolate to a similar atomic volume. Unfortunately, most of the alloy systems of Bi with the non-transition elements are either insoluble or eutectic in nature with very restricted solubilities [25]. The available mean atomic volumes from the literature are also plotted in Figure 3.

The only closely related alloy system is found in the Tl-Bi phase diagram which shows an extraordinarily large solubility of Bi in Tl and the formation of the intermetallic phase $TlBi_2$. Using the published lattice constants [26] to calculate the mean atomic volume for the alloys, a density for Bi of 10.27 g/cm^3 can be derived. However, the available X-ray data are most inaccurate and not plentiful enough to support this conclusion. Also given in Figure 3 are the atomic volumes of the Sn-Bi system [27] which has a very restricted Bi-solubility of only 13.1 at.% and is, therefore, difficult to extrapolate. In addition, data of Pb-Bi are given [28,29] and they do extrapolate to an even smaller atomic volume for Bi. It has been noted by Klement [29], however, that a possible polymorphism of Pb may be present in these alloys. According to the lattice parameters of the solid solution system Sb-Bi [30], the mean atomic volume changes linearly as expected between 35.38 $\mathring{A}^3$ for Bi and 30.54 $\mathring{A}^3$ for Sb. It can be concluded that for all available binary systems with the exception of Sb-Bi, the atomic volume for Bi extrapolates to a value which is always smaller than that measured for Bi in its elemental form.

SUMMARY

We have shown that the density in the alloy system In-Bi varies smoothly between the values of the terminal elements. No peaks in the specific volume are observed at compositions corresponding to the compounds In_2Bi, In_5Bi_3 and InBi. However, a volume contraction does take place upon compound formation. The density data can be explained in an additive fashion, attributing a mean atomic volume of 33.8 $Å^3$ to bismuth. This value represents the atomic volume of Bi in its liquid state at room temperature. The same atomic volume could be found in Tl-Bi alloys, however, more accurate lattice parameters are needed to support the statement.

ACKNOWLEDGEMENTS

The valuable assistance of Mr. T. Stuhlinger and Mr. W. Betowt with the measurements and data reduction is gratefully acknowledged. This investigation was sponsored by contract with NASA/Marshall Space Flight Center and we thank Dr. L. L. Lacy for his encouraging comments during the course of the work.

REFERENCES

1. O. Kubaschewski and E. LL. Evans "Metallurgical Thermochemistry," Pergamon Press, N. Y. 1958 p. 205.

2. N. N. Sirota in "Semiconductors and Semimetals" (R. K. Willardson and A. C. Beer, eds.) p. 127. Academic Press, New York, 1968.

3. B. Predel and A. Emam: J. Less-Common Metals 18, 358 (1969).

4. B. C. Giessen, M. Morris, and N. J. Grant: Trans. Met. Soc. AIME 239, 883 (1967).

5. O. H. Henry and E. L. Badwick: Trans. AIME 171, 389 (1947).

6. E. A. Peretti and S. C. Carapella: Trans. Am. Soc. Metals 41, 947 (1949).

7. E. S. Makarov: Soviet Phys. Cryst. 3, 3 (1958). Data from Ref 25.

8. R. Wang, B. C. Giessen, and N. J. Grant: Zeitschr. Kristallographie 128, 244 (1969).

9. W. P. Binnie: Acta Cryst. 9, 686 (1956).

10. H. Bruns and G. Lautz: Wissenschaftl. Abhandlungen 6, 47 (1954).

11. B. Predel und A. Emam: Th rmochimica Acta 7, 1 (1973).

12. G. H. Otto: Bull. Am. Phys. Soc., Series II, 18, 253 (19?3).

13. L. L. Lacy and G. H. Otto: AIAA Journal 13, 219 (1975).

14. M. E. Straumanis, P. B. Rao, and W. J. James: Z. Metallkunde 62, 493 (1971).

15. Present Investigation

16. E. S. Makarov: Do dy Akad. Nauk. S. S. S. R. 59, 899 (1948). Data from Ref. 25.

17. Y. C. Akgöz, J. M. Farley, and G. A. Saunders: J. Phys. Chem. Solids 34, 141 (1973).

18. A. Jevins, M. Straumanis, K. Karlsons: Z. Physik. Chem. 40B, 347 (1938).

19. C. S. Barrett: Australian J. Phys. 13, 209 (1969).

20. R. B. Lal, J. H. Davis, and P. E. Powell: J. of Less-Common Metals 27, 367 (1972).

21. N. B. Brandt and N. I. Ginzburg: Sov. Physics Uspekhi 8, 202 (1965), also in Scientific American, Vol. 224, April 1971, p. 83.

22. D. E. Gordon and B. C. Deaton: Phys. Rev. B6, 2982 (1972)

23. V. N. Laukhin, V. K. Matyushchenkov, and A. G. Rabin'kin: Sov. Phys. Solid State 16, 183 (1974).

24. P. W. Bridgman: Proc. Am. Acad. Arts Sci. 74,21 (1940)

25. M. Hansen: "Constitution of Binary Alloys," McGraw-Hill, New York 1958.

26. A. Ölander: Z. Krist. 89, 89 (1934). Data from Ref. 25.

27. J. A. Lee and G. V. Raynor: Proc. Phys. Soc. London 67B, 737 (1954).

28. H. W. King, C. M. Russell and J. A. Hulbert: Phys. Letters 20, 600 (1966).

29. W. Klement: J. Chem. Phys. 38, 298 (1963).

30. P. Chucka and C. S. Barrett: Acta Cryst. 15, 865 (1962).

Table 1: Lattice data and densities for single phase In-Bi alloys at 24 °C

Phase	Structure	Atoms per Unit Cell	Lattice Parameter (Å)		Ref.	X-ray Density (g/cm^3)	Exp. Density (g/cm^3)	$\Delta V^{\S}$ (X-ray) (cm^3/g-atom)
In	tetragonal	4	a=4.5993	c=4.9507	14	7.280	7.28	0
			a=4.600	c=4.948	15	7.282		-0.007
In_2Bi	hexagonal	6	a=5.496	c=6.579	7	8.461	8.45	-0.343
			a=5.500	c=6.575	15	8.454		-0.328
In_5Bi_3	tetragonal	4	a=8.544	c=12.68	8	8.616	8.61	-0.429
InBi	tetragonal	2	a=5.000	c=4.773	9	9.009	8.95	-0.578
			a=5.015	c=4.781	16	8.949		-0.440
			a=5.004†	c=4.775†	17	8.991		-0.542
Bi	rhombohedral	2	a=4.746	α=57°14.2'	18	9.805	9.80	0
			a=4.5459+	c=11.8623+	19			

+Dimensions for a hexagonal setting containing six atoms

§Based on ρ(In) = 7.28 g/cm³ and ρ(Bi) = 9.80 g/cm³. $\Delta V = V - \Sigma V_i$

†Single crystal data

FIGURE CAPTIONS

Figure 1: The density of In-Bi alloys up to a Bi-concentration of 50 at.%. A representative error bar is given for the eutectic composition. The dashed line is a linear interpolation between the densities of In and Bi.

Figure 2: Excessive volume of In-Bi alloys. Experimental data points are for the individual samples. The curve for T = 300 °C is taken from Ref. [11].

Figure 3: Mean atomic volumes of binary bismuth alloys with non-transition elements. Besides In-Bi, the data are computed from the following sources: Tl-Bi (26), Sn-Bi (27), Pb-Bi (28,29), and Sb-Bi (30).

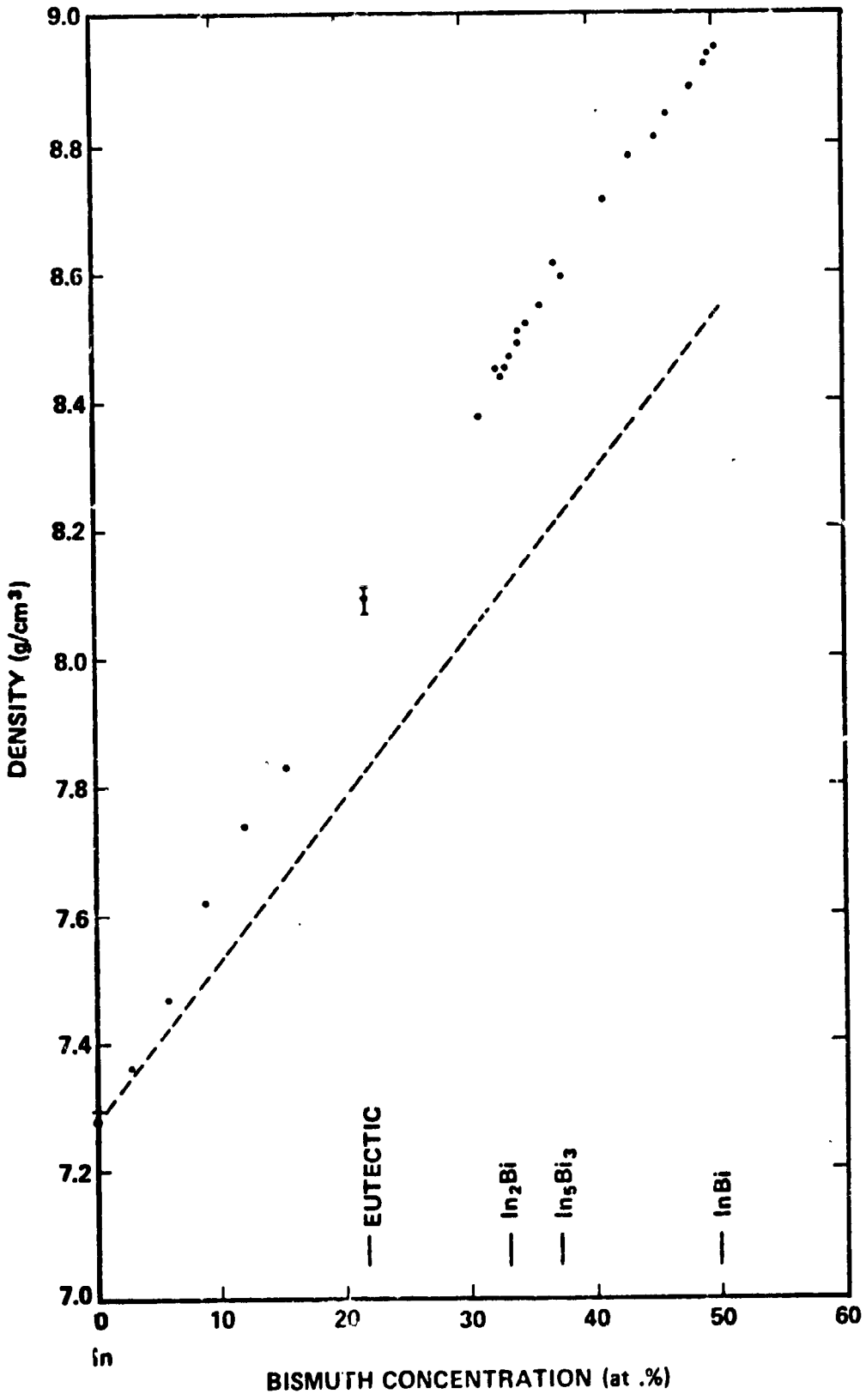
9.0
8.8
8.6
8.4
8.2
8.0
7.8
7.6
7.4
7.2
7.0
DENSITY (g/cm³)
0
10
20
30
40
50
60
In
BISMUTH CONCENTRATION (at .%)
EUTECTIC
In2Bi
In5Bi3
InBi

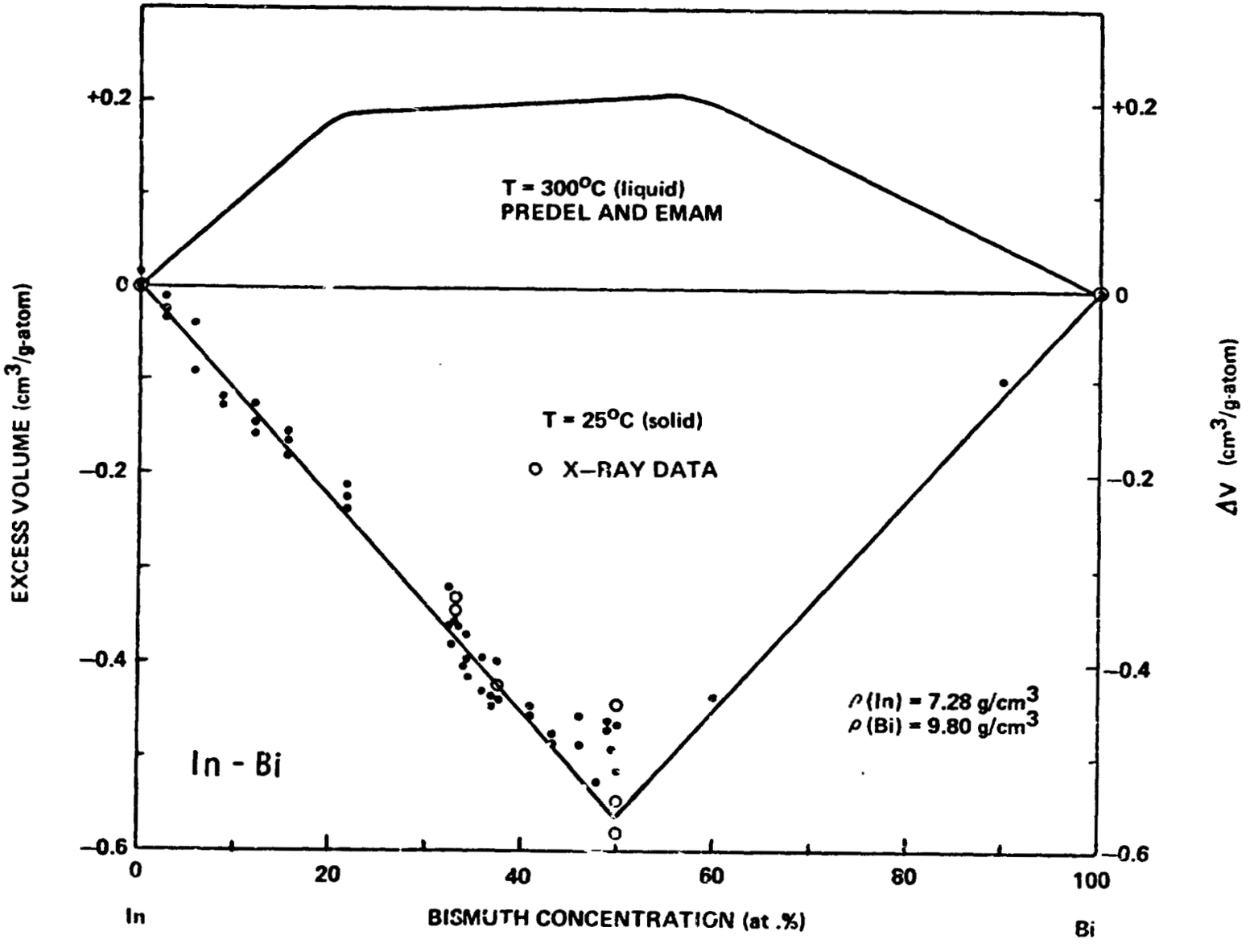
+0.2
0
−0.2
−0.4
−0.6
T = 300°C (liquid)
PREDEL AND EMAM
T = 25°C (solid)
o X–RAY DATA
ρ (In) = 7.28 g/cm3
ρ (Bi) = 9.80 g/cm3
In - Bi
EXCESS VOLUME (cm3/g-atom)
ΔV (cm3/g-atom)
0
20
40
60
80
100
In
BISMUTH CONCENTRATION (at .%)
Bi

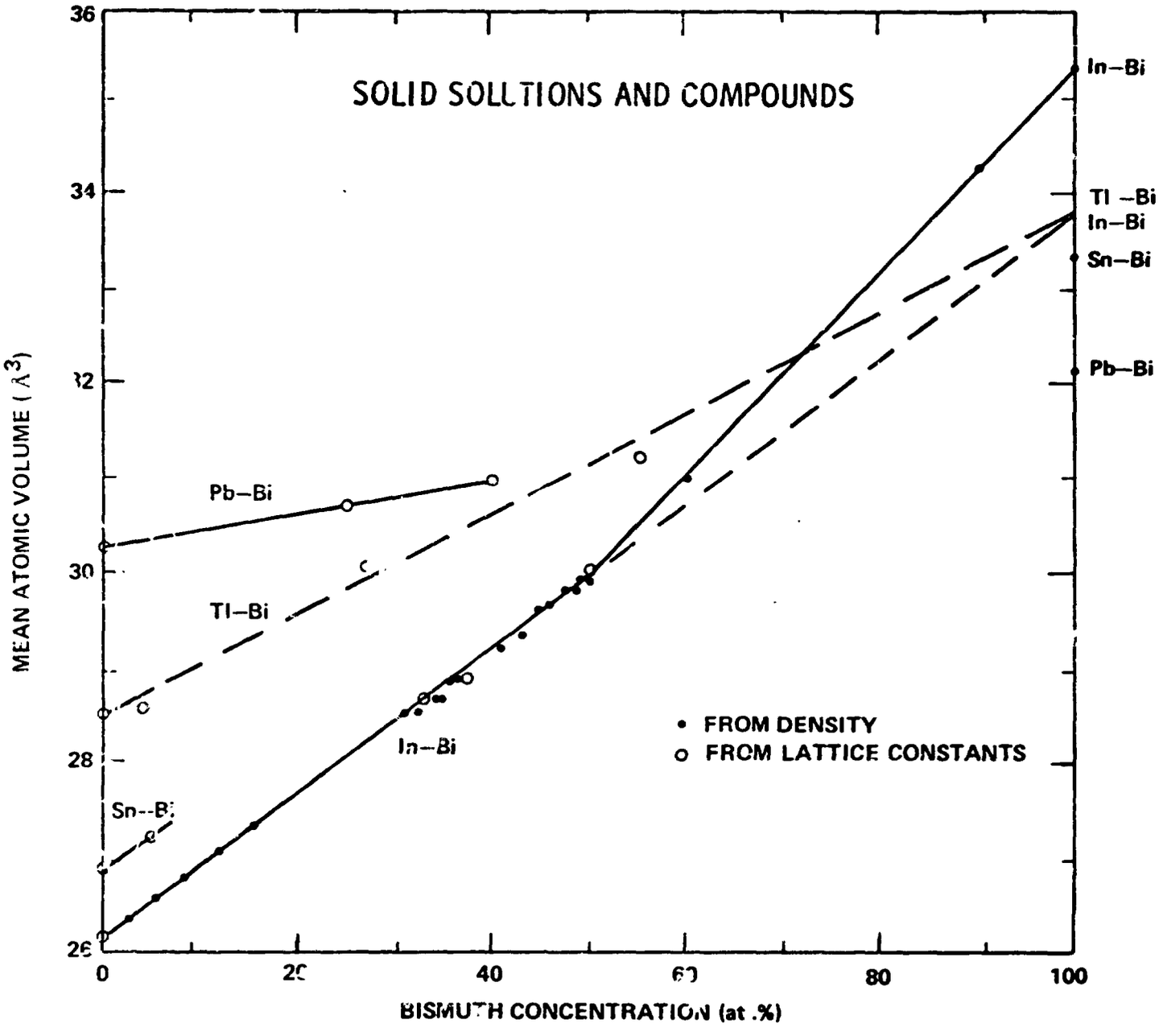
SOLID SOLUTIONS AND COMPOUNDS
MEAN ATOMIC VOLUME (Å³)
BISMUTH CONCENTRATION (at.%)
36
34
32
30
28
26
0
20
40
60
80
100
In–Bi
Tl –Bi
In–Bi
Sn–Bi
Pb–Bi
Pb–Bi
Tl–Bi
In–Bi
Sn–Bi
• FROM DENSITY
o FROM LATTICE CONSTANTS

APPENDIX B

Abstract Submitted
for the 1972 Meeting of the
Southeastern Section of the American Physical Society
November 16-18, 1972

Time Dependent Resistivity of In-Bi Eutectic.*†
GUENTHER H. OTTO, The University of Alabama in Hutsville.--
Upon cooling of a solid In-Bi eutectic (66.3 w.%) sample, the compound In_2Bi (β-phase) will be precipitated from the supersaturated α-In phase which leads to a time-dependent resistivity. We have measured the change in resistivity in In-Bi eutectic wires as a function of time after a change of temperature was introduced. The sample resistivity for this isothermal process can be correlated with the nucleation and growth of the participating phases. The kinetics of precipitation leading to the equilibrium composition will be discussed.

*Submitted by PALMER N. PETERS
†Work supported by NASA Contract No. NAS8-27809

Abstract published in the Bulletin of the American Physical Society, Series II, 18, 253 (1973).

C. 2

APPENDIX C

THE PRECIPITATION OF In_2Bi FROM SUPERSATURATED α-PHASE*

Guenther H. Otto
Department of Physics
The University of Alabama in Huntsville
Huntsville, Alabama

Indium, having a face centered tetragonal lattice, forms a substitutional solid solution (α-phase) with bismuth where the maximum solubility is strongly temperature dependent. At temperatures below the solubility limit, the α-phase becomes metastable, and the Bi content in the solid solution can be reduced only by incoherent precipitation of the intermetallic compound In_2Bi.

We have followed the course of the isothermal precipitation of the second phase by resistivity measurement on a polycrystalline indium wire containing 8.8 at.% (15 w.%) bismuth. The characteristic temperature at which the solubility limit is reached for this composition was found to be 52 °C. The sample, with the electrical contacts attached, was annealed above the characteristic temperature until a stable resistivity reading was reached and then repeatedly quenched into a temperature-regulated water bath of different temperatures. The observed time-dependent decrease in resistivity is caused by the nucleation and growth of the In_2Bi phase. Plotting the fractional change of the measured resistivity $(\rho_0 - \rho)/(\rho_0 - \rho_\infty) \equiv \Delta\rho$ as a function of time, t, (with ρ_0 and ρ_∞ being the resistivity at $t = 0$ and $t = \infty$, respectively) gives sigmoidal curves in which $\Delta\rho$ increases slowly at first, then much more rapidly, and finally slowly again. However, all curves can be linearized up to $\Delta\rho = 0.5$ utilizing the relation $\Delta\rho = 1 - \exp(-bt^n)$, which was first proposed by Avrami. For this expression, b is a measure for the reaction velocity, whereas n is governed by the geometry of the growing particles. For the material investigated, the value of n varied between four and one, where the latter is obtained at a decomposition temperature of 0 °C.

* Supported by NASA-Marshall Space Flight Center

Abstract published in the Journal of the Alabama Academy of Science: 44, 200 (1973)

APPENDIX 'D'

Journal of the Less-Common Metals, 32 (1973) 355–364

SHOCK WAVE SYNTHESIS AND CHARACTERIZATION OF Nb_3Sn

G. H. OTTO* and U. ROY**

The University of Alabama in Huntsville, Huntsville, Ala. 35807 (U.S.A.)

O. Y. REECE

Marshall Space Flight Center, National Aeronautics and Space Administration, Huntsville, Ala. 35812 (U.S.A.)

(Received March 5, 1973)

SUMMARY

The synthesis of Nb_3Sn, a hard superconductor, has been accomplished by the use of a converging shock wave arrangement. The irreversible phase formation for stoichiometric and non-stoichiometric powder mixtures was studied by changing the shock wave intensity. Evidence of compound formation was obtained by quantitative metallography, microhardness, X-ray diffraction, and superconductivity measurements. It is concluded that tin, due to its high compressibility and low specific heat, acts as the main source of heat while the use of powder materials favours ready achievement of the reaction temperature. The same procedure, when applied to the formation of the isostructural Nb_3Al phase, resulted in $NbAl_3$ instead.

INTRODUCTION

In the past 25 years, great strides have been made in the peaceful uses of high power chemical explosives, once of purely military significance. Materials technologies such as explosive forming, -bonding, and -metal powder compaction have been introduced. Furthermore, the investigation of shock effects in solids has proved to be a useful tool in solid state research[1]. This paper describes the use of shock waves in the synthesis of intermetallic compounds. A brief account of the technique has been published elsewhere[2]. The chemical reaction is herein activated by the energy of a converging shock wave. The attributes of the technique are that it is relatively simple, that the process is completed in a span of micro-seconds, and that the sample is recovered in a practically pressure–temperature quenched state. Its transient nature affords an opportunity to freeze-in metastable or non-equilibrium phases.

The shock wave synthesis of Nb_3Sn, a high field superconductor, was undertaken for several reasons. This compound is of commercial interest because of its

* Supported by NASA Contract with Marshall Space Flight Center.

** Present Address: 2411 Fantasia Circle, Huntsville, Ala. 35805 (U.S.A.).

applicability in magnets, generators, or frictionless bearings. The characterization techniques for this compound are well developed. Equilibrium techniques such as casting, sintering, diffusion, sputtering, and vapor deposition are mainly used to fabricate this compound. According to the phase diagram[3], Nb_3Sn is formed by a peritectic reaction at 1980°C. Its high brittleness and the associated fabrication difficulties, however, limit its usefulness.

The main objective of this work was to investigate the compound formation by shock waves and to understand the underlying reaction mechanism.

EXPERIMENTAL DESCRIPTION

Fine grain powders (−325 mesh) of niobium (99.9%) and tin (99.99%) were used as the starting materials. The powders were weighed to correspond to the chemical composition $Nb_{1-x}Sn_x$ where x was varied between 0.2 and 0.67. Mechanically mixed composite powders were packed in a copper tube of 6.2 mm o.d. and 0.8 mm wall thickness. A number of specimen tubes were evacuated to a pressure of 1×10^{-6} Torr and were sealed under vacuum by electron-beam welding. The samples with their ends either crimped or e.b. welded were inserted centrally into separate but identical cylindrical containers packed with nitroguanidine explosive of varying densities. Figure 1 shows the arrangement in schematic fashion. In order to ensure a homogeneous shock wave formation across the entire sample length (10 cm), the top end of the sample and the detonator were kept 5 cm apart. The shock initiation was accomplished with an electrical detonator and tetryl booster cap positioned centrally on top of the container. A cone-shaped converging shock wave focussed on the symmetry axis of the set-up travels the entire length of the sample. As the ductile copper jacket collapses, the powdered material is subjected to an extensive compaction. Due to the chosen geometry, an increasing pressure

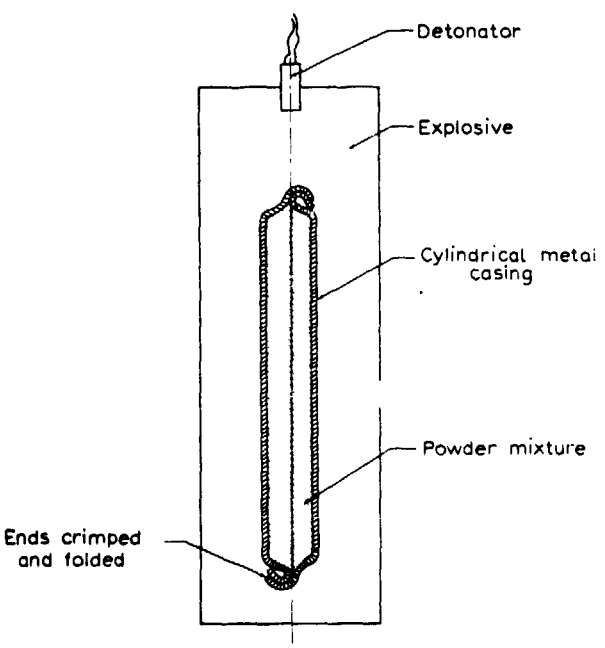

Fig. 1. Schematic representation of the converging shock wave technique.

is generated toward the center of the sample. The locally achieved relative compaction and pressure determine the new state of energy on the Hugoniot curve. This state is also associated with a higher temperature. The magnitude of the temperature increase depends primarily on specific heat and compressibility; small specific heat and large compressibility favor the achievement of high temperatures. Due to the high porosity of the powder mixtures, which results in a larger compressibility, an additional temperature increase is obtained[4]. In this work, the resultant shock pressure, and hence the temperature level in the sample, was further controlled by changing the density of the explosive charge.

RESULTS

It should be pointed out that we were mainly concerned with the residual shock effects, *i.e.*, the irreversible phase formation from its constituents. Only qualitative arguments will be presented as to the reaction mechanism during the transient state. Evidence of phase formation was studied by quantitative metallography, microhardness, X-ray diffraction, and measurements of the superconducting transition temperatures. The results are presented systematically, the variable parameters being the explosive charge or the chemical composition.

Stoichiometric powder composition (3Nb: 1Sn)

The polished cross sections of the shocked samples were anodized to establish a visual phase separation by different interference colors. According to Picklesimer[5], the colors for the intermetallic phases in the system Nb–Sn range from light blue for elemental niobium to red-brown for $NbSn_2$. The intermetallic compound, Nb_3Sn, is represented by a dark blue color. The micrographs in Fig. 2(a) and (b) are black-and-white reproductions of color photographs from a longitudinal and a

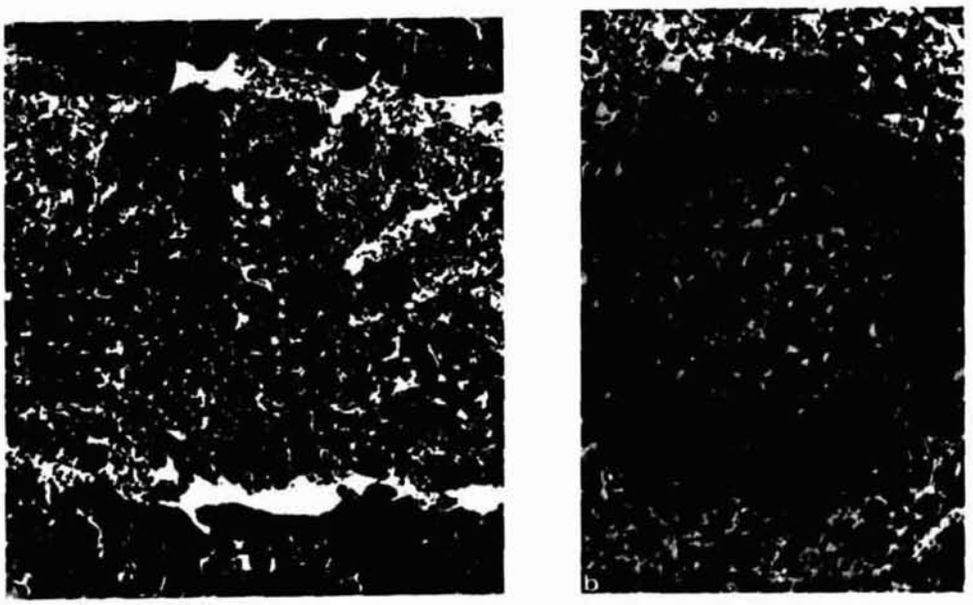

Fig. 2. Section of a 3Nb: 1Sn powder mixture explosively shocked with a charge density of 0.55 g/cm^3. (a) Longitudinal section (× 60). (b) Transverse section (× 60).

transverse cross section of a sample submitted to a charge density of 0.55 g/cm^3. A distinct zone of compound formation is observed in the core of the sample. The diameter of this reaction zone for a given charge density is uniform throughout the entire specimen length, as represented in Fig. 2(a). Investigation of samples submitted to progressively increasing charge density showed that a reaction zone appears only after a critical load is exceeded. Thereafter the diameter of the reaction zone increases as the shock pressure, and thereby the conserved energy of the shock wave increase. From observations of anodized specimens, an average diameter of the reaction zone has been plotted against the charge density in Fig. 3.

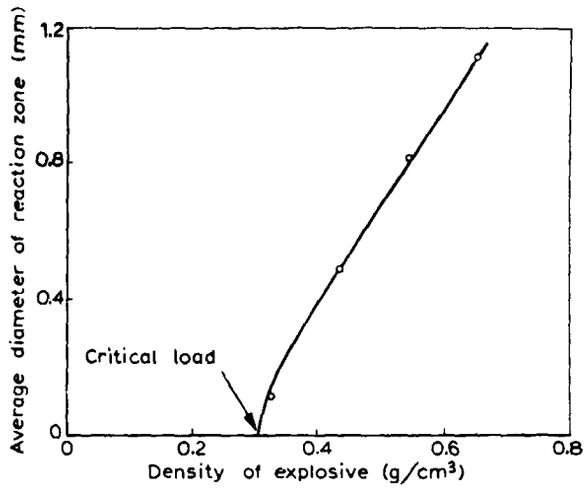

Fig. 3. Average diameter of the reaction zone from shocked 3Nb:1Sn powders as a function of charge density.

The reaction zone consists predominantly of the Nb_3Sn phase with some particles of unreacted tin and niobium. No evidence for the formation of Nb_6Sn_5 or $NbSn_2$, which are unstable[3] above 930°C, was found. The newly formed Nb_3Sn compound consists of interconnected particles of approximately 5 μm in diameter. The degree of interparticle network formation is strongly dependent on explosive load and initial tin content

Microhardness measurements were performed on a number of samples with a load of 50 g. The average hardness values in DPH are 140, 230, and 540 kp/mm^2 for niobium particles outside the reaction zone, inside the reaction zone, and the Nb_3Sn phase, respectively. The almost fourfold increase in microhardness for the reaction product is evidently due to the formation of the compound.

Since the transition temperature, T_c, of the equilibrium Nb_3Sn phase is 18.0 K, which is much higher than those of Nb ($T_c = 9.3$ K) and Sn ($T_c = 3.7$ K), superconductivity measurements provided a sensitive means of detecting Nb_3Sn phase formation. Resistivity as well as a.c. inductive methods were used to measure the transitions to superconductivity. Figure 4 shows normalized resistive transition curves of stoichiometric powder mixtures subjected to increasing shock pressures. On samples submitted to sub-critical loads, and thereby exhibiting no reaction zone, only the transition of the niobium is observed. The T_c of the shocked niobium is lowered by 0.9 K compared with the unshocked powder. Once the critical load

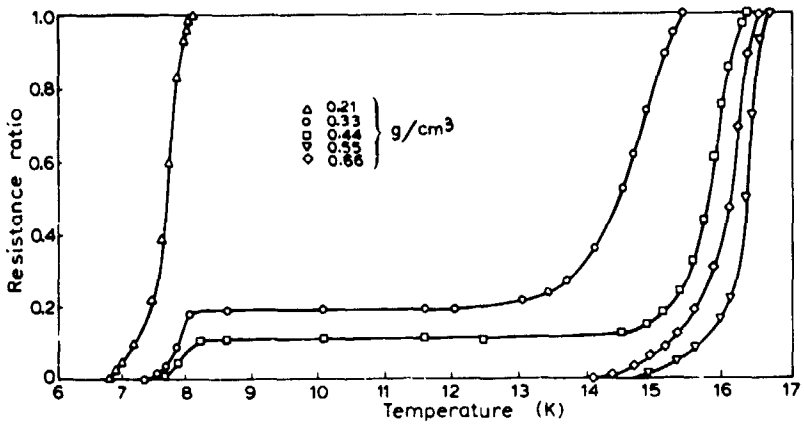

Fig. 4. Superconducting transition curves of shocked 3Nb:1Sn powders subjected to different charge densities.

is exceeded, the transition temperature is rapidly attained to a maximum of 16.4 K with an onset-temperature to superconductivity of 16.7 K. The samples shocked with non-optimum conditions show only partially connected Nb_3Sn particles, allowing no continuous path for the supercurrent, and therefore the transition for the unreacted niobium is also observed.

The X-ray diffraction patterns of powders taken from different cross-sections of the specimen again confirmed the formation of Nb_3Sn. The lattice parameter for the $A15$ phase was calculated to be 5.287 ± 0.003 Å, which is in good agreement with published data[6]. The (110) reflection, which is most order-sensitive in this structure[7], could not be detected. This indicates that the compound is formed in a partially disordered state wherein the Nb sites in the lattice are occupied by Sn atoms and *vice versa.*

The transition temperature measurement was repeated on samples that were vacuum sealed prior to the shocking process. Practically no difference in T_c was observed on samples that contained air pockets and those sealed under vacuum.

Off-stoichiometric powder composition

From the results of the previous section the optimum charge density needed for the formation of Nb_3Sn is inferred to be 0.5 g/cm^3. This experimental parameter was now kept constant so that the same shock pressure was applied on the copper jacket from sample to sample, whereas the composition of the composite powder was deliberately varied. The average diameter of the reaction area is plotted against the tin content in Fig. 5 which shows that the increase in tin content markedly expands the reaction zone. Microscopic examination of the anodized samples revealed the formation of the Nb_3Sn phase in the core. However, with increase in the tin content, the interconnection of the Nb_3Sn particles became less frequent and finally the individual particles were completely separated, resulting in the disappearance of the network formation. Figure 6 shows that T_c is essentially independent of the composition change up to 40 at.% tin. With higher Sn content, the Nb_3Sn lattice becomes unstable, associated with a rapid drop in the transition temperature. This behavior is in agreement with T_c measurements on as-cast samples, as reported by Kunz and Saur[8].

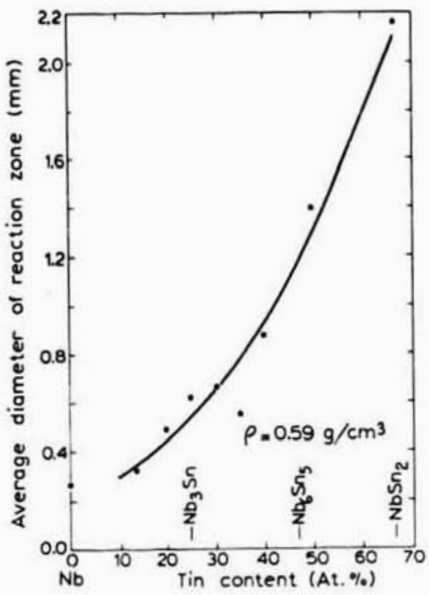

Fig. 5. Average diameter of the reaction zone against tin content.

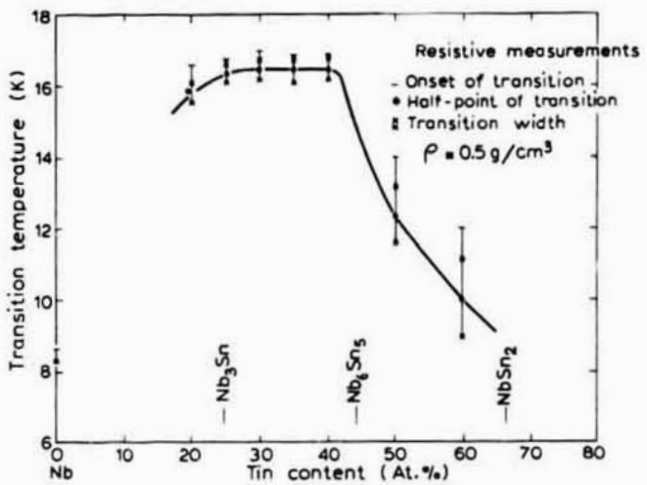

Fig. 6. Transition temperatures of samples in dependence of tin content.

Shock compaction of ternary composite powders

An attempt was made to synthesize the isostructural high T_c compound Nb_3Al by the same technique starting from a stoichiometric powder mixture. A

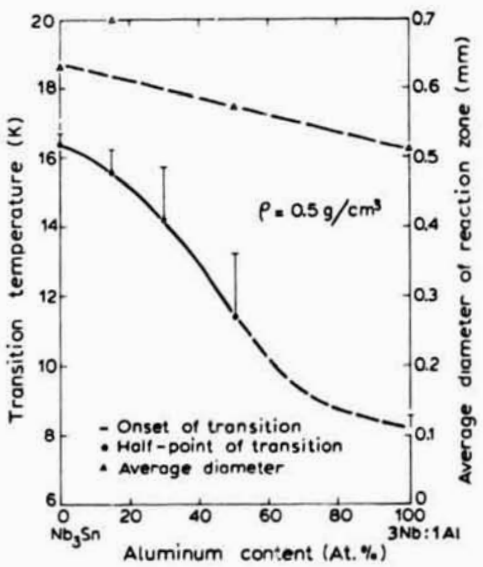

Fig. 7. Section of the reaction zone of a 3Nb:1Al powder mixture shocked with a charge density of 0.5 g/cm³. Reproduction of a color photograph from an anodized surface. (× 100)

Fig. 8. Transition temperatures as well as the average diameters of reaction zone in $Nb_3(Sn_{1-x}Al_x)$ samples.

reaction zone with uniform microstructure yielding an average microhardness of 500 kp/mm^2 in comparison to a reading of 200 kp/mm^2 outside this area was observed. A black-and-white reproduction of a color photomicrograph obtained on an anodized specimen is shown in Fig. 7 and demonstrates the presence of at least one new phase. The T_c measurements, on the other hand, gave a value of 8.4 K which can be attributed to the transition temperature of the shocked niobium itself. The Debye–Scherrer X-ray data of the core material revealed no Nb_3Al with the $A15$ structure. Using the characteristic data published by Brauer[9], all reflection lines could however be indexed to the intermetallic compound $NbAl_3$ with body-centered tetragonal structure and a melting temperature[10] of 1605°C.

In order to resolve this question, an approach involving a ternary powder composition was adopted, the Sn atoms being gradually substituted by Al atoms in the compound Nb_3Sn—a phase which readily forms by shock waves. The initial powder composition corresponded to the formula $Nb_3(Sn_{1-x}Al_x)$. Figure 8 is a plot of T_c and the average diameter of the reaction zone against the Al content in Nb_3Sn. The experimental conditions were adjusted to keep the shock parameters unchanged and optimum in regard to the formation of Nb_3Sn. The extent of the reaction zone does not display any appreciable dependence on the degree of Sn substitution. The transition temperature decreases markedly as the Al content in the sample increases —an effect which is also observed on cast specimens[11]. However, no rise in T_c occurs as the composition of Nb_3Al is approached. This might be caused by the severe quenching rate which suppresses the formation of the $A15$ lattice.

DISCUSSION

Our results show that the technique leads to the formation of a bulk quantity of the Nb_3Sn phase, the yield under optimum shock conditions being as high as 80% within the reaction zone. Since the shock-synthesized Nb_3Sn was formed under high pressure during the time interval in which the shock wave passed through the reaction zone, some properties are expected to be different from those of Nb_3Sn prepared under equilibrium conditions. The lattice parameter of $a=5.287$ Å is somewhat smaller than that reported[6,12] for stoichiometric Nb_3Sn of 5.290 Å. This difference can be accounted for by the fact that the shock-synthesized compound is slightly off-stoichiometric composition though still within the range of homogeneity.

The transition temperature of the shock-synthesized Nb_3Sn is lower by 1.3 K than that reported[8] for cast and subsequently annealed material. This reduction in T_c may be caused by the severe quenching the compound experiences after passage of the shock wave. A similar reduction in T_c has been observed by Matthias *et al.*[13] on splat cooled Nb_3Sn (cooling rate 10^6 deg/s). The process of quenching freezes-in the high degree of atomic disorder which is present at the temperature of formation. The degree of disorder is such that Nb sites in the $A15$ lattice are occupied by Sn atoms and *vice versa*, which shows up in the missing order-sensitive (110) X-ray reflection as well as in the reduction of the superconducting transition temperature. The degree of atomic order could be subsequently improved by annealing of the shocked material at temperatures around 800°C; however, the additional formation of Nb_3Sn from unreacted Nb and Sn by a diffusion process cannot then be avoided.

The temperature pulse induced in a material by a shock wave is specified in the following way: when a shock wave travels through a solid material, the matter is severely compressed (in an isentropic process) and the atoms are accelerated in the direction of the velocity vector of the shock wave. The local pressure, and the relative compaction of the material thereby generated, determine the new state of internal energy on the Hugoniot equation of state curve and the resultant temperature[14]. After the passage of the shock wave the pressure is released to ambient conditions by an adiabatic expansion. Since the entropy in this process is not conserved there will be residual heat left in the material. It is generally impossible to measure the temperature of the material behind the shock wave, but this quantity can be calculated for a number of elements for which the Hugoniot equation of state has been measured[15].

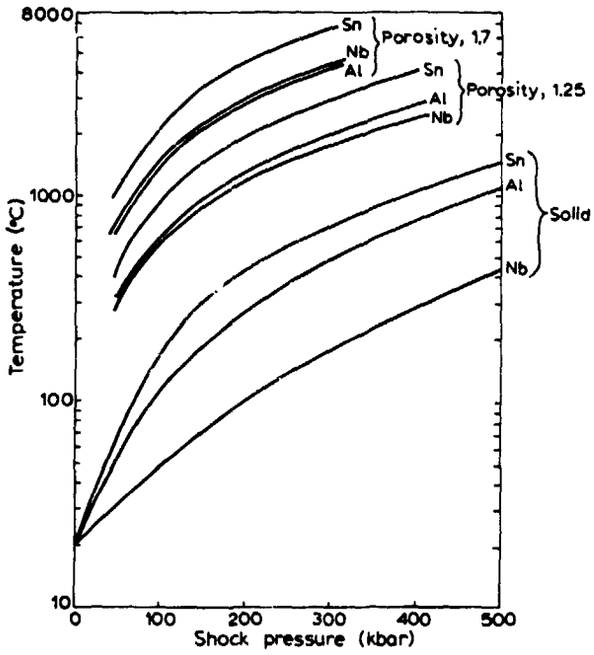

Fig. 9. Calculated temperature-pressure diagram for bulk and porous metals (after McQueen *et al.*[15]).

Figure 9 shows calculated temperatures for bulk Nb, Sn, and Al along the Hugoniot curve during compression, published by McQueen and co-workers[15,16]. It is seen that, for the same pressure, the temperature increase for tin is considerably higher than that for niobium, because of the higher compressibility and lower specific heat of Sn compared with Nb. We infer that, in order to initiate the reaction of the components, the necessary temperature is generated by the compaction of tin rather than of niobium. If, on the other hand, porous materials are used, the compressibility is considerably higher, and the same temperature is readily achieved under a lower shock pressure. This is demonstrated by the curves for materials of different porosities shown in Fig. 9. The temperatures are calculated for a porosity of 40% and 20%, which is a representative range for the used powders. The additional temperature increase of the shocked, porous material over the

shocked, non-porous material is assumed[4] to be proportional to the locally achieved pressure and to the difference in the initial specific volume of the porous and non-porous materials.

The diameter of the reaction zone is found to depend on the charge density. It reflects that the detonation pressure at the explosive–sample (copper) interface can be varied by packing the explosive with different densities. The diameter of the reaction zone also depends on the tin content (Fig. 5), while the charge density and the shock wave configuration were kept constant. This is caused by the dissipation of the heat in the varying amount of niobium. If the amount of tin is gradually replaced by aluminum under the same experimental conditions, the temperature distribution in the sample during passage of the shock wave is only slightly changed and the average diameter of the reaction area decreases slightly as shown in Fig. 8.

The shock pressure at the nitroguanidine/copper interface is estimated[17] to lie between 200 and 250 kbar, depending on the packing density of the explosive. The cone-shaped converging shock wave used here compensates for all losses in its energy which may be caused by reflection at the various interfaces or by the process of melting after entering the sample. It is therefore assumed that the reaction of the two components occurs only when the required temperature for the peritectic reaction is reached. At these pressures the tin will be in a molten state (225 kbar being the incipient melting pressure[18]) whereas the niobium is still solid. Under these conditions the Nb will be dissolved in liquid tin and as the peritectic temperature is reached the solid Nb_3Sn phase forms, with its subsequent rapid build-up. This reaction mechanism is supported by the observation that the unreacted Nb particles are surrounded by the Nb_3Sn phase which shows a tendency to break away from the niobium and form a granular, interconnected particle network. The transient nature of the process precludes the formation of α-Nb solid solution which would require a sluggish solid state diffusion. At higher than stoichiometric tin content, the Nb_3Sn phase again forms but then becomes increasingly isolated through the medium of unreacted and excess tin.

The Nb_3Al phase should also form by a peritectic reaction[10] at 1960°C but the phase diagram in this case (above 1000°C) is much more complex than that of Nb–Sn due to the presence of two more intermetallic phases. In addition, it can be expected that Al does not melt at shock pressures between 200 and 300 kbar, for which process a shock pressure in excess of 600 kbar is needed[19]. The X-ray data show that the process of shock wave synthesis in this case evidently favors the formation of the $NbAl_3$ phase over the intended Nb_3Al phase. The cause may again be the high quenching rate of the shock wave synthesizing process.

ACKNOWLEDGEMENTS

We would like to thank Dr. E. W. Urban and Dr. L. L. Lacy for their encouragement and for comments on the manuscript. Part of the results were obtained while one of the authors (G.H.O.) held a National Academy of Sciences Fellowship.

REFERENCES

1 D. G. Doran and R. K. Linde, in F. Seitz and D. Turnbull (eds.), *Solid State Physics*, Academic Press, New York, 1966, Vol. 19, p. 230.

2 G. Otto, O. Y. Reece and U. Roy, *Appl. Phys. Letters*, 18 (1971) 418.
3 J. H. N. van Vucht, D. J. van Oojen and H. A. C. M. Bruning, *Philips Res. Repts.*, 20 (1965) 136.
4 T. J. Ahrens, W. H. Gust and F. B. Royce, *J. Appl. Phys.*, 39 (1968) 4610.
5 M. L. Picklesimer, *ORNL Rept. 2296*, 1957; *Microscope*, 15 (1967) 472.
6 J. J. Hanak, K. Strater and G. W. Cullen, *RCA Rev.*, 25 (1964) 342.
7 E. C. van Reuth and R. M. Waterstrat, *Acta Cryst.*, B24 (1968) 186.
8 W. Kunz and E. Saur, *Z. Physik*, 189 (1966) 401.
9 G. Brauer, *Z. Anorg. Allgem. Chem.*, 242 (1939) 1; *Naturwiss.*, 26 (1938) 710.
10 C. E. Lundin and A. S. Yamamoto, *Trans. AIME*, 236 (1966) 863.
11 G. Otto, *Z. Physik*, 215 (1968) 323.
12 L. J. Vieland, *RCA Rev.*, 25 (1964) 366.
13 B. T. Matthias, T. H. Geballe, R. H. Willens, E. Corenzwit and G. W. Hull, *Phys. Rev.*, 139 (1965) A1501.
14 J. M. Walsh and R. H. Christian, *Phys. Rev.*, 97 (1955) 1544.
15 R. G. McQueen, S. P. Marsh, J. W. Taylor, J. N. Fritz and W. J. Carter, in R. Kinslow (ed.), *High Velocity Impact Phenomena*, Academic Press, New York, 1970, p. 293.
16 R. G. McQueen and S. P. Marsh, *J. Appl. Phys.*, 31 (1960) 1253.
17 A. S. Bahrani and B. Crossland, *Metals and Mater.*, 1 (1968) 41.
18 M. H. Rice, R. G. McQueen and J. M. Walsh, in F. Seitz and D. Turnbull (eds.), *Solid State Physics*, Academic Press, New York, 1958, Vol. 6, p. 60.
19 J. W. Gehring, in R. Kinslow (ed.), *High Velocity Impact Phenomena*, Academic Press, New York, 1970, p. 105.